PhD Program in Translational and Molecular Medicine

DIMET

(XXXI cycle, academic year 2017/2018)

University of Milano-Bicocca
School of Medicine and Surgery

Neonatal combination therapy approaches, based on hematopoietic stem cell transplantation (HSCT) and enzyme replacement therapy (ERT), in a mouse model of Mucopolysaccharidosis type I (MPS-I)

Coordinator: Prof. Andrea Biondi
Tutor: Dr. Marta Serafini

Ludovica Santi
Matr. 773276

AAVs	Adeno-associated vectors
aBMT	Adult bone marrow transplantation
ACK	Ammonium chloride-potassium
ADA-SCID	Adenosine deaminase severe combined immunodeficiency
APC	Allophycocyanin
aUCBT	Adult umbilical cord blood transplantation
BA	Bone area
BBB	Blood brain barrier
BFU-E	Burst-forming unit-erythroid
BM	Bone marrow
BMC	Bone marrow cell
BMD	Bone mineral density
BMT	Bone marrow transplantation
BSA	Bovine serum albumine
CFC	Colony forming cell
CFU-G	Colony-forming unit-granulocyte
CFU-GEMM	Colony-forming unit-granulocyte, erythroid, macrophage, megakaryocyte
CFU-GM	Colony-forming unit-granulocyte, macrophage
CFU-M	Colony-forming unit-macrophage
CNS	Central nervous system
CHO	Chinese hamster ovary
CLEAR	Coordinated lysosomal expression and regulation
CS	Chondroitin sulphate
CT	Computed tomography
CTL	Cytotoxic T lymphocyte
Ct.Th	Cortical thickness
DBS	Dried blood spot
ΔDiHS-0S	2-acetamido-2-deoxy-4-O-(4-deoxy-α-L-threo-hex-4-enopyranosyluronic acid) -D- glucose
ΔDiHS-NS	2-deoxy-2-sulfamino-4-O-(4-deoxy-α-L-threo-hex-4-enopyranosyluronic acid)-D- glucose

ΔDi-4S	2-acetamido-2-deoxy-4-O-(4-deoxy-α-L threohex-4-enopyranosyluronic acid)-4-O-sulfo-D-glucose
DNA	Deoxyribonucleic acid
DS	Dermatan sulphate
ELISA	Enzyme-linked immunosorbent assay
EMA	European Medicines Agency
ERT	Enzyme replacement therapy
FITC	Fluorescein isothiocyanate
GAG	Glycosaminoglycan
GFAP	Glial fibrillary acid protein
GM	Ganglioside
GT	Gene therapy
GVHD	Graft versus host disease
HA	Hyaluronic acid
hi-nBMT	Highly engrafted-neonatal bone marrow transplantation
hi-nBMT+ERT	Highly engrafted-neonatal bone marrow transplantation + enzyme replacement therapy
HLA	Human leukocyte antigen
HPP-CFC	High proliferative potential-colony-forming cells
HS	Heparan sulphate
HSCs	Hematopoietic stem cells
HSCT	Hematopoietic stem cell transplantation
Iba-1	Ionized calcium binding adaptor molecule 1
IDUA	Alpha-L-iduronidase
IEM	Inborn errors of metabolism
IgG	Immunoglobulin G
IP	Intraperitoneal
IV	Intravenous
Kb	Kilobase
kDa	KiloDalton
KS	Keratan sulphate
LAMP	Lysosomal associated membrane protein

LC-MS/MS	Liquid chromatography-tandem mass spectrometry
LPS	Lipopolysaccharide
LSDs	Lysosmal storage diseases
LSK	$Lin^{-}Sca1^{+}c\text{-}kit^{+}$
LVs	Lentiviral vectors
MA	Medullary area
MMPs	Matrix metalloproteinases
MPSs	Mucopolisaccharidoses
MPS-I	Mucopolysaccharidosis type I
MPS-I-H	Hurler syndrome
MPS-I-H/S	Hurler/Scheie syndrome
MPS-I-S	Scheie syndrome
MPS II	Mucopolysaccharidosis type II (Hunter syndrome)
MPS III	Mucopolysaccharidosis type III (San Filippo syndrome)
MPS IV	Mucopolysaccharidosis type IV (Morquio syndrome)
MPS VI	Mucopolysaccharidosis type VI (Maroteaux-Lamy syndrome)
MPS VII	Mucopolysaccharidosis type VII (Sly syndrome)
MPS IX	Mucopolysaccharidosis type IX (Natowicz syndrome)
M6P	Mannose-6-phosphate
M6PR	Mannose-6-phosphate receptor
nBMT	Neonatal bone marrow transplantation
nBMT+ERT	Neonatal bone marrow transplantation + enzyme replacement therapy
NBS	Newborn screening system
NSG	NOD scid gamma
nUCBT	Neonatal umbilical cord blood transplantation
nUCBT-hi	Neonatal umbilical cord blood transplantation, highly engrafted

nUCBT-lo	Neonatal umbilical cord blood transplantation, low engrafted
OPD	O-phenylenediamine dihydrochloride
PB	Peripheral blood
PBS	Dulbecco's phosphate-buffered saline
PCT	Pharmacological chaperone therapy
PE	Phycoerythrin
PerCP	Peridinin chlorphyll protein
RER	Rough endoplasmic reticulum
rhIDUA	Recombinant human alpha-L-iduronidase
RUSP	Recommended uniform screening panel
SD	Standard deviation
siRNA	Small interfering RNA
SRT	Substrate reduction therapy
TA	Total area
TFEB	Transcription factor EB
TRAP	Tartare resistant acid phosphatase
TUNEL	Terminal deoxynucleotidyl transferase dUTP nick end labeling
UCB	Umbilical cord blood
UCBT	Umbilical cord blood transplantation
VAMP2	Vescicle associated membrane protein
WT	Wild-type

TABLE OF CONTENTS

CHAPTER 1

GENERAL INTRODUCTION

1. MUCOPOLYSACCHARIDOSIS TYPE I DISEASE

1.1 Lysosomal storage diseases

Lysosmal storage diseases (LSDs) are a group of inherited metabolic disorders caused by mutations in genes that alter lysosomal homeostasis, such as lysosomal hydrolases, membrane proteins and transporters, that result in the accumulation of undegraded molecules in different tissues and organs[1]. Nowadays, 58 LSDs are known and they are classified, according to the nature of the accumulated substrate, in four main subgroups: mucopolysaccharidoses, glycolipidoses, mucolipidoses and glycoproteinoses[2]. Although each disease is extremely rare, their overall frequency is high, 1 in 8000 live births[3]. Most of them are autosomal recessive disorders, except for Hunter syndrome, Fabry disease and Danon disease, which show an X-linked recessive inheritance[4].

The clinical phenotypes of LSDs are really complex and heterogeneous, depending on the specific mutation, the degree of protein function and the stored material. Although age of onset, symptoms, affected organs and life expectancy may vary from patient to patient, LSDs are multisystemic diseases characterized by a chronic progressive course, abnormalities of multiple tissues and organs such as nervous system, bone, cartilage, and viscera[5].

Lysosomes are ubiquitous acid organelles that are involved in the

degradation of cellular substrates. Their main characteristic is an acid internal pH (4.5-5.0) that is fundamental for the enzymatic breakdown of molecules including proteins, glycogen, glycosaminoglycans (GAGs), and sphyngolipids[6]. This catabolic role is performed by over 60 soluble enzymes, mainly acid hydrolases within these cell organelle. Lysosomal enzymes are synthetized in the rough endoplasmic reticulum (RER) and then modified in the *cis* Golgi compartment, by adding a mannose-6-phosphate (M6P) residue, that act as targeting signal, allowing the segregation of lysosomal hydrolases from other proteins[7]. In the *trans* Golgi network, lysosomal hydrolases are first recognized by the M6P receptor (M6PR), gathered into clathrin-coated vescicles, and then, after having budded from the Golgi, they fuse with late endosomes. The acidic pH of the organelles is responsible for the dissociation of the enzyme-receptor complexes: the hydrolases are released as soluble active enzymes, while the M6PR is recycled to the Golgi apparatus[8]. Nevertheless, 5-20% of lysosomal hydrolases may escape this trafficking and are directed to the cell surface in order to be secreted. Anyway, since M6PRs are localized to the plasma membrane too, they are able to recapture the escaped enzyme that can reach the lysosomes via endocytosis[8].

Lysosomal enzymes perform the catabolism of substrates by a stepwise activity, in which the previous hydrolase is essential for the next degradation step. In fact, if one step fails, the degradation process stops, resulting in the accumulation of materials[9]. The storage materials, due to the enzyme deficiency, is the first cause of lysosomal dysfunction that generally leads to other secondary cellular responses, until cell death. Other cellular pathways, connected to the primary

lysosomal engulfment, have been recognized, such as oxidative stress, inflammation, defective Ca^{2+} homeostasis, endoplasmic reticulum stress, autophagy block and others[3,10]. In recent years, it has been shown that autophagy is markedly reduced in LSDs. As lysosomes play a fundamental role in all three autophagic processes (macroautophagy, microautophagy and chaperone-mediated autophagy), lysosomal engulfment inhibits the fusion between autophagosomes and lysosomes; it results in the autophagy block, affecting cell architecture and function, and leading cells to apopotosis[11]. In particular it has been demonstrated that the autophagic pathway is highly controlled by the transcription factor EB (TFEB) which regulates a series of genes belonging to the coordinated lysosomal expression and regulation (CLEAR) network. Indeed, TFEB signalling pathway impairment has been associated in the pathogenesis of LSDs[12].

1.2 Mucopolysaccharidoses

Mucopolisaccharidoses (MPSs) are a group of LSDs, characterized by the deficient activity of a specific lysosomal enzyme involved in the catabolism of glycosaminoglycans (GAGs). Nowadays, 11 types of MPSs have been known, which give rise to seven distinct forms of MPS, such as MPS I (Hurler, Hurler-Scheie and Scheie syndrome), MPS II (Hunter syndrome), MPS III (San Filippo syndrome, with four subtypes, A, B, C and D), MPS IV (Morquio syndrome, with two subtypes, A and B), MPS VI (Maroteaux-Lamy syndrome), MPS VII (Sly syndrome), and MPS IX (Natowicz syndrome)[13]. Regarding the hereditary transmission, MPSs are autosomal recessive diseases,

except for MPS II which is inherited in a X-linked recessive manner[14].

GAGs are long, negatively charged, unbranched polysaccharides, which consist of a repeated disaccharide unit of an amino sugar, glucosamine or galactosamine and uronic acid or galactose[15]. The majority of them are characterized by a high rate of sulphation and in fact GAGs are divided into two main categories: sulphated, which include dermatan sulphate (DS), heparan sulphate (HS), keratan sulphate (KS), chondroitin sulphate (CS) and heparin, and non-sulphated, which include hyaluronic acid (HA)[16]. Except HA, GAGs are able to link core proteins to form larger complexes, best known as proteoglycans. GAGs are one of the main component of the extracellular matrix of connective tissues, and they can be found in skin, blood vessels, cartilage and bone[13]. GAGs are involved in a wide range of cellular functions, and their role is linked to their ability to bind water and to their elastic properties. As they are located at the plasma membrane too, they are able to bind and modulate growth factors and cytokines, regulating cell adhesion and migration; they have been implicated in other cellular processes and, among them, proliferation, apoptosis, angiogenesis and autophagy, and recently it has been demonstrated their involvement during embryogenesis and development[16,17]. As GAGs are frequently renewed, a failure of the degradation process, due to lysosomal enzyme deficiency, leads to GAGs accumulation and consequently to perturbation of cellular homeostasis. Although the precise pathogenesis is still not completely known, GAGs storage is the first consequence of the genetic alteration, representing the initial pathogenic event, that results in the

activation of secondary downstream pathogenic cascades[18]. The degree of breakdown impairment varies from patient to patient and determines the clinical phenotype. Indeed, MPSs show a progressive course which varies from severe forms, characterized by early onset and rapid progression, to attenuated forms[19]. GAGs storage itself is thought to be the main cause of lysosomal and, consequently, organ enlargement that characterizes these diseases. MPSs are multisystemic disorders and the most common manifestations are hepatosplenomegaly, mental retardation, short stature, coarsened facial features, and a series of muscoloskeletal manifestations, known as "dysostosis multiplex". The skeletal deformities are due to GAGs accumulation in joint capsules, ligaments, tendons, in the growth plate and in the articular cartilage. Furthermore it has been shown that DS, one of the accumulated GAGs, presents similarities with bacterial lipopolysaccharide (LPS), triggering inflammatory responses[14].

1.3 Mucopolysaccharidosis type I (MPS-I)

Mucopolysaccharidosis type I (MPS-I) is a chronic and multisystemic disorder that affects approximately 1 in 100.000 births, being one of the most frequent LSDs[20]. It shows an autosomal recessive pattern of inheritance and it is caused by mutations in the gene that encodes for the alpha-L-iduronidase (IDUA) enzyme. This lysosomal enzyme is involved in the catabolism of the GAGs heparan and dermatan sulphate, and its absence or low activity leads to GAGs accumulation and consequently to cellular and organ dysfunction[21]. Since MPS-I shows a high clinical heterogeneity, it has been classified in three different phenotypes based on the severity of the disease. Hurler

syndrome, the most severe and predominant form (MPS-I-H), Hurler/Scheie syndrome (MPS-I-H/S), the intermediate form, and Scheie syndrome (MPS-I-S), the most attenuated one. In general, it is considered severe when the onset of symptoms is before 1 year of age and mental retardation appears before 3 years; otherwise the mild form is characterized by the onset of symptoms after 5 years of age, normal life-span and by the absence of mental retardation[22].

1.4 Discovery of MPS-I

Although the first description of a MPS-I affected patient was made by Berkhan in 1907, Melnhard von Pfaundler and Gertrud Hurler made a more precise clinical description of two affected patients, named Hurler-Pfaundler syndrome, currently known as Hurler syndrome or MPS-I. It was also referred to as "Gargoylism", due to the coarse facial features of patients[23]. In 1952 the term mucopolysaccharidosis was introduced by Brante, relying on chemical analysis[24]. In 1962, an attenuated phenotype was described by Harold Scheie, called Scheie syndrome after him[25]. And a few years later, in 1968, Fratantoni *et al*. demontrated the cross correction mechanism by co-colturing Hurler and Hunter fibroblasts. For the first time they speculated the presence of the "Hurler corrective factor"[26], later recognized also for both Scheie and Hurler syndrome.

1.5 Molecular bases of MPS-I

IDUA is an ubiquitous lysosomal enzyme required for the breakdown of HS and DS, removing, by hydrolysis, the terminal iduronic acid residues. It is a 74 kDa polypeptide composed of 653 amino acids[23].

The *IDUA* gene has been localised, by Scott *et al*. in 1990, to chromosome 4p16.3, approximately 1100kb from the telomere. It is composed of 14 exons with a total length of 19kb[27]. So far over 200 pathogenic variants have been recognized, and the majority of them are missense, nonsense, deletions, insertions and splice site mutations. Currently genotype-phenotype correlation is difficult to define due to the high heterogeneity of the disease[22]. Patients with the most severe form of MPS-I have generally mutations on both alleles that inhibit the production and the functionality of the enzyme; among Caucasians, the W402X and Q70X nonsense mutations are associated with the severe clinical phenotype among homozygotes. On the other hand, patients with the attenuated form have at least one missense mutation, which however enables for some residual enzyme activity. Furthermore, non-pathogenic variants, best known as polymorphisms, have been recognized in non-affected people; these variants may influence and modify the severity of the disease if combined with a pathogenic MSP-I mutation[28].

1.6 Clinical manifestations

Although accumulation of HS and DS in lysosomes and in the extracellular matrix, known as primary GAG storage, is the main cause of homeostasis perturbation in MPS-I, it has been found that tissue and organ dysfunction are also mediated by alterations of secondary pathways. The precise relationship between GAGs accumulation and clinical symptoms is not completely understood, even though the molecular defect is well characterized[29]. High clinical heterogeneity, one of the main feature of MPS-I, reflects mutational

heterogeneity. In fact MPS-I is a chronic and progressive multisystemic disorder characterized by a wide range of signs and symptoms[28]. In general, MPS-I patients do not display major defects at birth, but symptoms appear early in childhood, especially for severe forms. If untreated, life expectancy is really reduced: death occurs before the first decade of life[30].

Cognitive impairment and neurodegeneration are hallmarks of severe MPS-I. Even though cognitive development is not altered during the first months of age, mental retardation and delay occur within the second year of life. MPS-I patients have reduced language skills, due not only to cognitive impairment, but also to enlarged tongue and hearing loss[28]. Communicating hydrocephalus, cervical spinal cord compression and cervical instability are other frequent symptoms among MPS-I patients[31].

Respiratory and cardiac manifestations are frequently observed. For what concern the first symptoms, upper airway disease and respiratory insufficiency are really common, and mostly due to obstructive sleep apnea, restrictive lung disease and asthma[28]. Cardiac disease consists of arrhythmia, myocardial thickening, valvular disease, hypertension and coronary artery disease. Indeed cardiovascular abnormalities are a frequent cause of early death in MPS-I severe patients[32]. Corneal clouding and retinal degeneration are responsible for loss of vision; ophthalmic complications, including acute blindness may occur[33]. Otolaryngological manifestations are other typical symptoms. Tonsillectomy and adenoidectomy are the direct consequences of chronic rhinitis and ear infections[28]. Organomegaly, especially hepatosplenomegaly, causing inguinal and umbilical hernias, is really

frequent. In addition to these features, musculoskeletal abnormalities are the main hallmark, not only of MPS-I, but of each different type of MPSs. Although the precise biological mechanism is still not completely known, accumulated GAGs in connective tissues are thought to be the main responsible for this kind of manifestations[14]. *Dysostosis multiplex* is the term used to portray the progressive skeletal abnormalities, typical of MPSs (*Figure 1*). Ossification abnormalities, GAGs accumulation into joints, ligaments and tendons and lack of skeletal remodelling are at the base of skeletal dysplasia[34]. Furthermore, similarities between dermatan sulphate and lipopolysaccharide (LPS) trigger inflammation processes through activation of LPS signalling pathway[35], and osteoclasts dysfunction, mostly due to inhibition of cathepsin K activity[36], contribute to the skeletal defects. From a clinical point of view, patients develop a progressive skeletal disease, and in particular short stature, dorsal gibbus, genu valgum, hip dysplasia, joint stiffness, irregular metaphysis, narrow epiphysis, contractures, macrocephaly, carpal tunnel syndrome, and dental problems[14,31]. Osteopenia, microfractures and artropathy progressively lead to generalized pain and impaired movements[28].

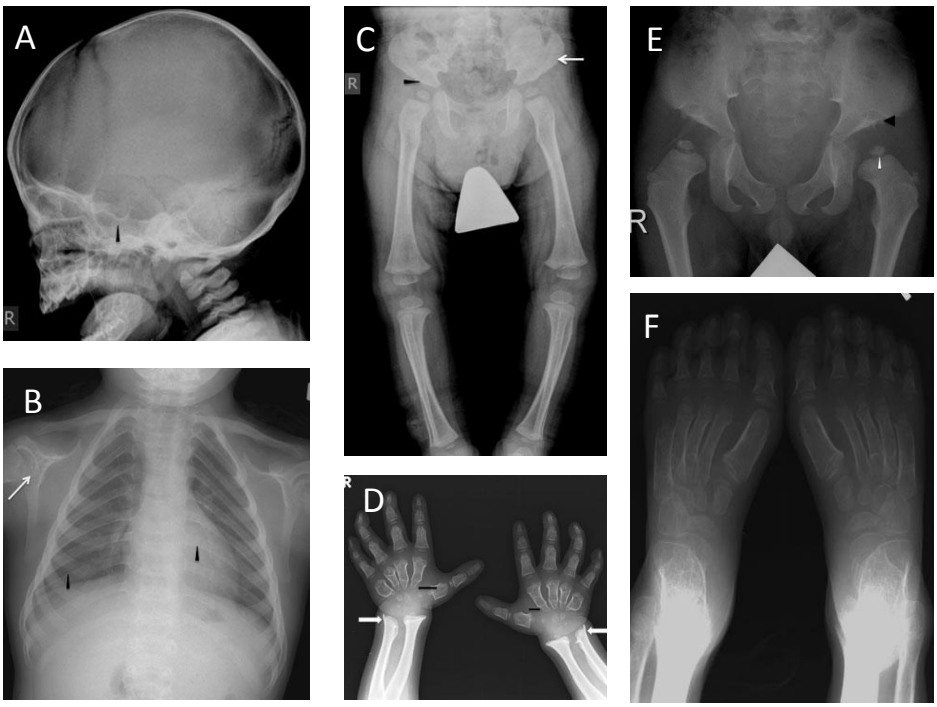

Figure 1. Dysostosis multiplex ***A)*** *Macrocephaly.* ***B)*** *Thick ribs (black arrows) and hypoplastic genoids fossae (white arrow).* ***C)*** *Flattening of acetabula (arrowhead).* ***D)*** *Short and wide metacarpals (black arrows) and Madelung's deformity (white arrows).* ***E)*** *Bilateral flared iliac wings, flattened acetabular roofs and dysplastic femoral epiphysies* ***F)*** *Calcaneovalgus deformities of feet*[37].

1.7 Diagnosis of MPS-I

Due to the high clinical heterogeneity of MPSs, diagnosis could result extremely challenging. In fact symptoms severity, age of onset and disease progression can really vary from patient to patient and can result in diagnostic delay[38]. Furthermore, many MPS-I patients do not

show specific signs and symptoms at birth, and some patients with attenuated forms can remain undiagnosed for years. The initial suspect of MPS-I derives from clinical signs and symptoms, such as respiratory infections, coarse facial features, enlarged tongue and hernias[39]. As MPS-I is a progressive disorder, that worsens over time, an early and precise diagnosis is essential to avoid irreversible damages and to optimize treatment outcomes. Measurement of urinary GAGs levels is the first and most common diagnostic procedure for MPS-I. It is a sensitive but nonspecific test, as false-negative results may occur[30]. Primary storage material can be measured in other biological fluids, such as serum, plasma and cerebral spinal fluid[38]. α-L-iduronidase activity is then measured in patient' fibroblasts, leucocytes, plasma or serum, in order to assess enzyme catalytic activity and patients expected clinical phenotype[40]. Biochemical analysis are followed by molecular tests, required to establish a definitive diagnosis. *IDUA* gene sequencing assess patient's mutation(s) and sometimes it may allow a prediction of the phenotype[30].

As a substantial delay between age of onset (6 months) and initial treatment (17 months) has been demonstrated, it is necessary to develop newborn screening systems (NBSs) that allow an early diagnosis and, as a consequence, an early treatment[41]. In fact it has been demonstrated, in a mouse model of MPS-I, that treatment in neonatal period significantly reduced signs and symptoms before they appear, showing that an early intervention is associated with a better clinical outcome[42]. Indeed in 2016 the US Secretary of Health and Human Services added MPS-I to the recommended uniform screening

panel (RUSP) for newborn screening[20]. Nowadays NBSs are recognized as preventive public health programs that may significantly reduce disease severity. In recent years, dried blood spot (DBS) technique has been introduced, replacing fibroblasts culture, leukocytes and biological fluids[43]. A few drops of blood are collected from newborns' heel, put on a filter paper, and allowed to dry. The first method relies on measuring the enzymatic activity of the deficient enzyme: 4-methyhylumbeliferyl-α-L-iduronide is used as a substrate, and fluorescence of the enzyme product 4-methylumbelliferone is measured[44]. One of the main limits is that other NBSs for LSDs yield the same product at the end of the enzyme reaction and consequently multiplexing is not feasible; furthermore, this assay is not able to differentiate pseudodeficiency from true positive patients[45]. The second method measures GAGs content on DBSs by using liquid chromatography-tandem mass spectrometry (LC-MS/MS) systems, considered a highly sensitive, specific and inexpensive assay[46]. Prenatal diagnosis is also feasible through measurement of GAGs content in amniotic fluid during pregnancy. It is considered a useful, fast and cost-effective diagnostic assay[47].

2. TREATMENT OF MUCOPOLYSACCHARIDOSIS TYPE I

It is widely accepted that an early diagnosis and, more importantly, an early treatment is fundamental for MPS-I patients outcome. Due to the progressive nature of the disease, an early treatment aims to prevent disease worsening and organ damages that could be irreversible with time. The clinical success depends on different factors, such as severity of disease phenotype, symptoms onset, degree of disease progression[30]. The age at which treatment is performed is an important predictor for prognosis. MPS-I patients management, in terms of diagnosis, treatment and follow up, requires supportive care and a multidisciplinary clinical team. In recent years, thanks to a better understanding of disease pathogenesis and to the availability of specific treatments, patient's lifespan and quality of life strongly improved[48]. Nevertheless, despite the increasing clinical success, patients may develop burden of disease and complications, that often require surgical interventions[49]. These includes hernia repair, adenotonsillectomy, carpal tunnel release, heart valve replacement, decompression of cervical spine cord, ventriculoperitoneal shunt and orthopaedic procedures. Because of susceptibility of respiratory infection, cardiac disease, skeletal impairment, MPS-I patients are at high risk for complications during anaesthetic and surgical procedures[48].

Nowadays, enzyme replacement therapy (ERT) and hematopoietic stem cell transplantation (HSCT) are the standard of care for MPS-I patients. Providing the missing enzyme is the rationale for both treatments: in the case of ERT it is supplied by intravenous injection, and in the case of HSCT it is supplied by transplanted cells. In both

cases, the cross correction mechanism, described by Fratantoni and Neufeld in 1968, lies at the basis of the therapeutic approaches[48].

2.1 Enzyme replacement therapy

ERT is a disease-specific treatment aimed to stop disease progression by reducing and/or preventing GAGs accumulation. It consists in the periodic intravenous injection of the missing enzyme.

The discovery of the cross correction mechanism was a crucial finding in the development of ERT. Indeed the diffusible factor, nowadays identified as α-L-iduronidase, can be uptaken through endocytosis by affected cells which are able to recognize the M6P-tag of lysosomal enzymes[23]. The first potential clinical use of ERT was in 1994 thanks to Kakkis *et al*. They managed to produce and purify a variant of human alpha-L-iduronidase in the Chinese hamster ovary (CHO) cell line, by recombinant DNA technology[50]. Studies in the canine model of MPS-I, after weekly infusion of the missing enzyme, demonstrated a significant reduction of GAGs accumulation in many organs, such as liver and spleen, but no improvement in brain, myocardium and cartilage[51]. Following the promising results on efficacy and safety of ERT of the Phase I/II clinical trial[52], 45 patients were enrolled in an international, multi-centre, randomised, double-blind, placebo-controlled Phase III clinical trial[23]. Indeed in 2003, recombinant human alpha-L-iduronidase (laronidase, Aldurazyme®, Genzyme/Biomarin) was approved for the treatment of MPS-I patients in USA and in Europe. The recommended dose is 0.58 mg/kg body weight, and it is dispersed in isotonic saline and infused over 2-4 hours, once a week[48].

The overall findings of clinical trials showed promising results in terms of efficacy, beyond safety. Weekly alpha-L-iduronidase infusions lead to improvement in joint mobility and airway functions, and a significant reduction of hepatosplenomegaly and urinary GAGs excretion[53]. Nevertheless, current ERT has some limitations due to the fact that it is not always effective for all clinical symptoms. First of all, it has not shown neurocognitive benefits if administered intravenously, as the recombinant enzyme is not able to cross the blood brain barrier (BBB). Indeed, although ERT has been approved for MPS-I, it is recommended only for attenuated forms, with no neurocognitive involvement[30,49]. In order to bypass this barrier, alternative delivery strategies have been tested. Intranasal and intrathecal administration, in animal models, showed an increase in α-L-iduronidase activity with a reduction of GAGs in the central nervous system (CNS)[54,55]. Improvement and correction of skeletal deformities are another main limit of ERT approach, as established dysostosis multiplex remains stable with no amelioration. In fact the recombinant enzyme hardly spread through poorly vascularized tissues, such as bone, and it seems to have accessibility issues to reach chondrocytes through the molecular structure of the matrix[13]. Cardiac valvular disease and airway disease do not normalize with ERT treatment, as once these alterations begun, they may not be reversible[53]. With regard to adverse effects after ERT, MPS-I patients may develop infusion-related hypersensitivity reactions, such as flushing, fever, headache and rash, that may be controlled by slowing the infusion rate and administering antipyretic and/or steroids[30]. Furthermore, mostly MPS-I patients receiving ERT develop IgG anti-

drug antibodies, as the recombinant protein is seen as foreign. Although the significance of immune response is unclear and it may not seem to influence the clinical efficacy of ERT, it must be taken into consideration when evaluating the outcome[56,30]. Finally as ERT is a chronic treatment that requires infusions over a lifetime, it strongly impairs patients' quality of life.

2.2 Hematopoietic stem cell transplantation

Hematopoietic stem cell transplantation (HSCT) has been proposed as a treatment for patients with inherited metabolic disorders. The first HSCT was performed in a patient with MPS-I in 1980. Hobbs *et al*. reported an increase in IDUA activity, reduction in urinary GAGs excretion and improvement in terms of hepatosplenomegaly and airway disease after HSCT[57]. Since then, more than 500 HSCT have been performed for MPS-I patients, making it the most frequently transplanted LSD[58]. Nowadays HSCT is considered the first-choice therapy for MPS-I-H, and recently it is increasingly recommended for MPS-I-H/S patients with neurological manifestations[49].

The efficacy of HSCT relies on the cross-correction mechanism; it depends on migration, homing and engraftment of donor derived cells (*Figure 2*). Indeed, engrafted donor cells represent a constant source of the missing enzyme. Furthermore, it is widely recognized that cells from the hematopoietic compartment can differentiate, secrete the functional enzyme and correct non-hematological organs. For example donor-derived macrophages can become Kupffer cells in the liver, alveolar macrophages in the lungs and microglial cells in the brain. In

fact donor cells are able to pass the BBB, allowing the delivery of the enzyme into the CNS[59].

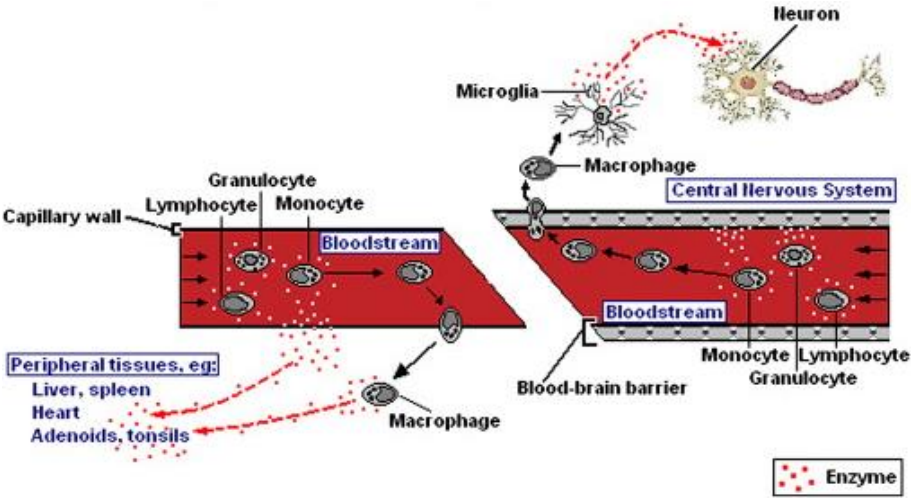

Figure 2. Enzyme delivery to peripheral tissues and central nervous system after HSCT[60].

With respect to the hematopoietic stem cells sources, although bone marrow was historically the first source of hematopoietic stem cells (HSCs) employed for HSCT, recently umbilical cord blood (UCB) seems to guarantee better results[61]. In fact, as UCB shows a reduced incidence of graft versus host disease (GVHD), a greater degree of human leukocyte antigen (HLA)-mismatch, rapid availability, and higher level of donor chimerism, it has become the preferred stem cells source[59,61]. Furthermore, it has been shown that UCB contains a small percentage of mesenchymal stem cells that can differentiate into healthy chondrocytes, able to replace the affected ones[62].

HSCT strongly improves the general clinical condition and quality of life of MPS-I patients. In particular, restoration of IDUA activity in organs and the consequent reduction of GAGs accumulation lead to a

decreased hepatosplenomegaly, amelioration of upper respiratory symptoms, preservation of cardiac function, stabilization or improvement in corneal clouding and joint mobility[63]. Furthermore, HSCT may stabilize neurocognitive development and adaptive skills[64]. However HSCT has a greater efficacy if it is performed early in childhood. Early treatment has become one of the crucial issues in MPS-I[39]. In general, the effectiveness of the clinical outcome depends on multiple factors, as the time at which HSCT is performed, patient's clinical status, type of donor, the engraftment rate achieved[28]. Nevertheless, even after a successful HSCT, disease-related problems may occur. Certain abnormalities, such as corneal clouding, valvular dysfunction, delayed or precocious puberty are not corrected after treatment. Moreover, HSCT does not seem to reverse any neurocognitive defects after they have already occurred, and cognitive abilites continue to decline[30]. And then, muscoloskeletal and orthopedic problems still deteriorate and impact patient'quality of life. Possible explanations of the correction failure could be a limited penetration of the functional enzyme into poorly vascularized tissues, and/or the irreversibility of some lesions at the time of transplantation[39]. Indeed the persistent dysostosis multiplex often requires surgical interventions, such as hemiepiphysiodesis for bilateral medial proximal tibia and thoraco-lumbar spinal fusion[62]. Besides the limitations related to the symptoms, HSCT presents limits related to the transplantation procedure itself. Transplant-related morbidity and mortality, due to GVHD, infections and other complications, are factors that must be taken into account. Boelens *et al*. showed a 15% of mortality rate after transplantation and only 56%

of patients survived and had a successful engraftment chimerism[65]. Furthermore, a toxic ablative conditioning regimen is required in order to remove patient's own stem cell compartment and to allow a donor engraftment[48].

2.3 HSCT in combination with ERT

The risk/benefit ratio for HSCT or ERT must be evaluated every time and for each patient, depending on age, disease severity, CNS involvement. As a significant residual disease burden after a successful HSCT may occur, ERT has been proposed as a supportive/adjuvant treatment in addition to HSCT[49]. Both peri-transplant and post-transplant ERT have been considered to counteract the manifestations that affect patients after HSCT, as the combination therapy could enhance the clinical outcome. An increasing number of MPS-I patients receive ERT in the pre-transplant period, as beneficial effects have been reported. ERT administration before HSCT does not negatively impact donor cell engraftment and GVHD, so in general it is considered a safe procedure[66,67]. Moreover, a reduced morbidity and mortality are associated with the ability of ERT to decrease GAGs accumulation in organs, for instance limiting upper airway obstruction and improving cardiorespiratory capacity. Peri-transplant ERT may facilitate donor cell engraftment through GAGs clearance of the bone marrow niche, generating a more permissive environment[66]. Now it is widley accepted that ERT should be initiated as soon as possible, or anyway during the period between diagnosis and HSCT, to enhance the probability of a succesfull transplantation[48].

With regard to post-transplant ERT, it has been performed in order to

solve disease manifestations after HSCT. Currently, the use of laronidase in patients that underwent HSCT is under investigation, as theoretically, donor engrafted cells should provide the missing enzyme[48,49]. However post-transplant ERT may be beneficial and effective, as suggested by Valayannopoulos *et al*. in one case report. Despite high level of donor chimerism and IDUA activity, a 14-years old patient developed respiratory failure, almost 11 years after HSCT. Weekly laronidase infusions led to an improvement of his respiratory functions and quality of life[68]. In murine models, it has been shown an increased permeability of the BBB after the conditioning regimen such as radiation or chemotherapy. So ERT administration, after transplantation, could determine an enhanced penetration of the enzyme into the CNS[69]. Further studies will clarify and demonstrate the possible positive impact of ERT administration after a successful HSCT.

2.4 Early treatments

It is widely accepted that precocious treatment for MPS-I, but in general for LSDs, is crucial in order to achieve a good clinical outcome and to avoid long-term pathological manifestations. Higher long-term clinical outcome has been demonstrated when ERT and/or HSCT are performed early in childhood[39]. Several studies, in different animal models, demonstrated an improved outcome if ERT was administrated at birth. In mouse models of MPS-I and MPS-IVA, neonatal ERT has a greater efficacy in reducing and preventing heart valves and bone abnormalities, as compared to adult mice[70,71]. Similar findings have been obtained in large animal models, such as canine

and feline models[72,73]. Moreover sibling cases of MPS-I patients provide evidence that early ERT led to a better clinical outcome, preventing and delaying the onset of signs and symptoms[74].

Likewise, HSCT performed at an early stage of life, shows significant improvement in neurocognitive development and skeletal lesions. It has been demonstrated in a mouse model of MPS-I that neonatal HSCT was able to restore IDUA activity, rescuing bone abnormalities[42,61]. Evidences of clinical benefits come also from the retrospective analysis, that portrays superior long-term clinical outcome when HSCT is performed early in life. In fact, age at which the transplantation is performed is considered an important predictor for better outcomes[75].

2.5 Gene therapy

Gene therapy (GT) is considered a promising and hopeful clinical approach for LSDs, able to correct the genetic defect. It consists in delivering the copy of the missing gene, by viral or nonviral vectors. LSDs appear to be ideal candidates for GT, first of all because they are monogenic disorders, and secondly because it is not necessary to transduce all patient's cells[76]. In fact, thanks to the cross-correction mechanism, a small number of gene-corrected cells may secrete the functional enzyme that can be uptaken by untransduced affected cells. Furthermore, it has been proven that only a small increase of the enzymatic activity is sufficient for clinical improvement[77]. GT could be considered a valid therapeutic option, especially when currently available treatments (HSCT and/or ERT) fail to fully correct disease phenotype[78]. Although HSCT is the first-choice therapy, it is still

associated with morbidity and mortality issues, and as donors are often heterozygous siblings, the amount of the secreted enzyme could be insufficient to correct patient's abnormalities. Moreover GT allows a long-term gene expression, overcoming ERT periodic infusions[79,80]. GT approaches can be divided into two main classes: *in vivo* and *ex vivo* GT. *In vivo* GT consists in the administration of a gene transfer vector directly into the bloodstream or into a tissue. It has been demonstrated that adeno-associated vectors (AAVs) and lentiviral vectors (LVs) could provide a successful delivery. Several studies, with different animal models, showed an improved clinical phenotype after *in vivo* GT, especially in neonatal period[81,82]. Nevertheless, immune response, and in particular cytotoxic T lymphocyte (CTL) response, may inhibit the therapeutic effect[83,84]. In order to better treat the CNS manifestations of LSDs, other administration routes to deliver gene therapy vectors have been proposed with the aim of bypassing the BBB issue. AAVs have been employed in different animal models to correct neuropathology of different MPSs. Intracranial, intracerebroventricular and intrathecal infusions determined a markedly improvement not only of histological and biochemical anomalies, but also of neurocognitive functions[85,86,87].

The *ex vivo* GT approach consists in the infusion of autologous target cells, that have been previously modified. It implies collection and isolation of patient's cells, gene correction in order to express the therapeutic gene, and reinfusion into the patient[88]. Various cell types have been considered as target cells for *ex vivo* GT, but HSCs remain the most attractive and promising tool thanks to their ability to

regenerate, persist long term, migrate and differentiate[78]. Also in the case of *ex vivo* GT, the main purpose is to obtain a long-term engraftment with a consequent production of the enzyme able to cross-correct affected cells. Transplantation of autologous modified HSCs showed two key advantages over HSCT: genetically engineered cells allow supra-physiological levels of the missing gene, and the use of autologous cells reduces morbidity and mortality issues, associated to GVHD[89]. One of the first demonstration of effective *ex vivo* GT in MPSs was made by Wolfe *et al*., by transducing retroviral vector expressing β-glucuronidase in a MPS VII mouse model[90]. In recent years LVs are seen the main actors of the *ex vivo* GT approaches. With regard to MPS-I, Visigalli *et al.* efficiently transduced murine BM HSCs with a LV encoding the IDUA gene. They achieved correction of neurologic and skeletal abnormalities, considered critical manifestations for MPS-I[79]. In order to support the application of LV HSC gene therapy in MPS-I patients, biosafety studies in terms of toxicology and biodistribution were conducted[91]. In 2016 the first ex vivo GT approach was approved by the European Medicines Agency (EMA) for ADA-severe combined immunodeficiency (ADA-SCID) patients. It consists in transplantation of autologous CD34+ transduced to express adenosine deaminase (ADA) for patients with no suitable matched donor[92]. Although e*x vivo* GT has a great potential to benefit LSDs and other storage disorders, representing a viable method to deliver the missing enzyme to multiple tissues, some issues still remain. Major concerns are viral vector safety and the possibility of the immune system to limit the effectiveness of the treatment. Furthermore, it is still unknown if supra-physiological

levels of the transduced enzyme may have harmful effects[76,93].

2.6 Small molecules therapy

Recently, small molecules therapy is an emerging and promising therapeutic approach for LSD patients. A better comprehension of the pathological mechanism and molecular basis of LSDs have led to the development of alternative strategies. These emerging therapies are under investigation and the possibility to combine several therapeutic approaches must be taken into account. Among them, pharmacological chaperone therapy (PCT), substrate reduction therapy (SRT) and non-sense suppression therapy are currently under developing.

PCT aims to stabilize misfolded proteins, and in this case misfolded lysosomal enzymes. In fact, in some cases, LSDs are caused by missense mutations that lead to an abnormal conformation of the enzymes. Aberrant enzymes are then recognized by the endoplasmic reticulum which provides their degradation. Pharmacological chaperons are able to interact with misfolded enzymes, rescuing the enzymatic activity by correcting their conformation[94]. The oral administration route, the non-immunogenic property and the ability to reach the CNS are some of the advantages compared to ERT[76].

The aim of SRT is to inhibit specific steps of substrate biosynthesis in order to balance the equilibrium between their catabolism and synthesis. Reducing GAGs synthesis means reducing their accumulation, so this treatment can be administrated only in patients

with residual enzyme activity[95]. Genistein (5, 7-dihydroxy-3-[4-hydroxyphenyl]-4H-1-benzopyran-4-one) and Rhodamine B ([9-(2-carboxyphenyl)-6-diethylamino-3- xanthenylidene]-diethylammonium chloride) are specific chemical compounds able to inhibit GAGs synthesis and to determine improvements of some clinical aspects, such as learning ability, thanks to their ability of cross the BBB[96,97]. Another possible way to interfere with substrate biosynthesis is by silencing genes encoding for GAG synthetases. Small interfering RNA (siRNA) procedure represents a specific strategy to reduce GAGs accumulation that could be potentially considered to treat MPS patients with CNS involvement[98].

Nonsense suppression therapy is a strategy aimed to treat diseases caused by nonsense mutations that give rise to a premature stop codon. It determines the generation of a truncated protein that cannot be functional. This therapy allows the translational machinery to generate a full-length protein, by ignoring the stop codon. Compounds such as gentamicin and NB84 are able to restore functional IDUA activity in a mouse model of MPS-I, with clinical benefits in terms of urine GAGs excretion and GAGs accumulation into multiple tissues[99,100]. As nonsense mutations are very common among MPS-I patients, it is reasonable to consider these drugs as a therapeutic option.

3. ANIMAL MODELS FOR MUCOPOLYSACCHARIDOSIS TYPE I

3.1 Murine models

Animal models are considered a powerful tool to study the pathobiology and mechanisms of diseases, but also to test the safety and efficacy of treatment approaches. With respect to MPS-I, several animal models have been developed or naturally occurred. Among them, feline, canine and murine model have been employed to better understand the pathophysiology of this metabolic disease[101,102,103]. Gene knockout and gene knock in technology represent valid strategies that strongly contributed to understand gene function. Regarding murine models, both immunocompetent and immunodeficient mouse models have been developed. The first immunocompetent MPS-I mouse model was generated by Lorne A. Clarke *et al.* in 1997. Authors disrupted the *Idua* gene with an interruption construct, because of the presence of the overlapping gene *Sat-1*. Chimeric mice were mated with C57BL/6 animals, and a colony of $Idua^{+/+}$, $Idua^{+/-}$ and $Idua^{-/-}$ (MPS-I) was established. MPS-I mice exhibited a lacked expression of IDUA mRNA and an absent acitivty of the enzyme in tissues, with an increased excrection of urinary GAGs (3-fold more than $Idua^{+/+}$ mice). Although at birth $Idua^{-/-}$ mice do not show any differences, by 4 weeks of age progressive dysmorphism becomes evident. Coarse face, broadened cranium, broadened paws are some of features that characterized MPS-I mice. Radiographs show dysostosis multiplex, thickned ribs and zygomatic arches that worsen with time (*Figure 3*). Abnormal lysosomal storage can be found in cortex, liver, spleen, kidney and

bone. Nevertheless in the first 20 weeks of life no difference in mortality is observed, indicating an attenuated phenotype as compared to humans [103].

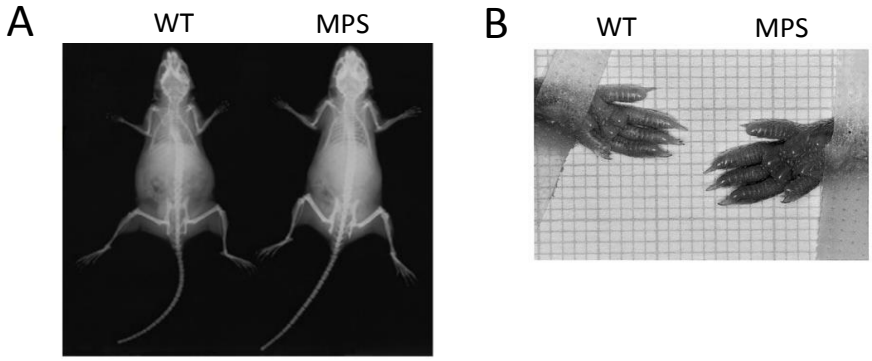

Figure 3. ***A)*** *Full body radiographs of 15-weeks-aged mice show general thickening of the bones.* ***B)*** *Photograph of hind paws, showing broadness and thickness of the digits*[103]

Other immunocompetent MPS-I mouse model have been generated and characterized, both with knock out[104,105] and knock in technology, for instance by introducing the *Idua*-W392X targeting construct[106]. The resulted phenotype of these animals is similar to the one obtained by Clarke, with an increased GAGs accumulation in several organs, increased bone mineral density (BMD), limitation in joint mobility and decreased performance in behavioural tests. Ragarding the knock in mouse model, it faithfully represents the most common mutation founded in MPS-I-H patients, and it can be used to test specific therapeutic approaches, such as nonsense suppression strategy[106]. More recently, an immunodeficient MPS-I mouse model has been generated by Garcia-Rivera *et al.* in 2007. Based on NOD/SCID

background, this model less likely develops immune reactions in case of IDUA enzyme injection or transplantation of human cells[107]. As this model presents disadvantages, such as development of thymic lymphomas and short life-span, a novel immunodeficient model, based on NOD/SCID/IL2Rγ (NSG) background, has been generated. This model shows classical MPS-I features, absent IDUA activity, GAGs storage in organs and neurological manifestations, and furthermore it is tumor-free and its half-life is longer than 1 year[108].

3.2 Skeletal and neurological disease in MPS-I mice

Skeletal abnormalities related to MPS-I are well recognized and reported, but their causes, from a molecular and cellular point of view, are still poorly understood. GAGs storage represents the primary pathological defect, triggering several secondary effects, that lead to tissue and organ damage and dysfunction[109]. Studies using the MPS-I mouse model reveal that skeletal abnormalities arise from disordered bone remodeling, endochondral and intramembranous ossification[29,36]. It has been demonstrated that accumulated HS and DS inhibit the activity of cathepsin K, a protease involved in the endochondral ossification process. It is highly expressed by osteoclasts and it normally degrades type II collagen, being responsible for bone resorption during the normal development of long bones. Collagenolytic activity impairment of cathepsin K may contribute to disease abnormalities, as it determines a decreased cartilage resorption by osteoclasts[36]. Other studies showed an impaired osteoclastogenesis in MPS-I mice with an increased bone mass phenotype, that is evident in older animals and not present in young mice. Indeed it is reasonable

that skeletal abnormalities are the consequences of altered bone remodelling rather than impaired skeletal development[110]. Moreover, alterations in the OPG/RANK/RANKL pathway have been reported in MPS-I mesenchymal stem cells too[111]. A progressive joint disease, due to inflammatory cytokines and inflammatory cells, increased expression of matrix metalloproteinases (MMPs) and collagen depletion, has been demonstrated in MPS-I mice[112,105]. Synovial fluid has been proposed as a biomarker source for MPS-I patients who undergo orthopedic procedures, as GAGs and inflammatory molecules may be monitored to evaluate the state of bone and joint disease[109].

Neurological abnormalities are generally associated with the most severe form of MPS-I, but their etiology is still unclear. Several works demonstrated accumulation of GAGs in Purkinje cells in the cerebellum and in glial cells in the cortex, but secondary storage has been reported too. Total ganglioside content, and in particular GM2 and GM3 gangliosides, is markedly increased in the whole brain of MPS-I mice[113,114]. Alterations in several proteins levels have been demonstrated, such as an increased expression of lysosomal associated membrane protein (LAMP) that is associated with a larger lysosomal compartment size[104,115]. Moreover, a reduced expression of proteins involved in synaptic plasticity have been reported, and among them, vescicle associated membrane protein (VAMP2) and Homer-1, compared to WT brains[116]. Overexpression of glial fibrillary acid protein (GFAP) is linked to a high level of inflammation, suggesting that a neuroinflammmatory process could be responsible for neuronal abnormalities. Furthermore, evaluating apoptosis, by TUNEL assay or by ubiquitin quantification, no differences have been reported between

WT and MPS-I mice hippocampus, suggesting that neuronal dysfunction is not due to cell death, but rather to neuroinflammation and/or alterations in synaptic plasticity[115,117]. These neurological alterations determine a decreased performance in behavioral tests. Indeed, MPS-I mice showed a less exploratory behavior in the open-field test, with a reduced number of crossing, velocity and distance walked[118]. Hypoactivity was also confirmed by other studies which demonstrated a reduced initial activity and adaptation in a novel environment[119], and a decrease in grip strength and a decreased performance in the rotarod test, which measures learning and balance[105].

3.3 Treatment approaches in murine models

In the last years, several treatment strategies have been tested in murine models of MPSs. Different novel cellular and gene therapy approaches, also in combination with ERT, have been proposed especially early in life, as it is widely accepted that a precocious treatment is crucial to obtain a favourable prognosis, due to the progressive nature of the disease[39]. It has been demonstrated that the administration of ERT started at birth is associated with a better outcome in MPS-IVA and MPS-I mice. Regarding the Morquio A mouse model, Tomatsu *et al*. showed that newborn ERT was able to partially correct bone pathology, that is generally hard to revert due to the poorly vascularized tissue during adulthood[71]. In another study, Baldo *et al*. compared the ERT treatment started at birth and at 2 months in a mouse model of MPS-I. Even though GAGs levels were significantly reduced after both treatments, α-L-iduronidase

administrated early in life had a better outcome in correcting heart valves and aorta[70]. Furthermore, mice treated at birth developed less anti-IDUA-IgG antibodies, in agreement with the immune tolerance observed in newborn MPS-I dogs[72].

With regard to transplantation approaches, Pievani *et al*. and Azario *et al.* proposed neonatal HSCT in MPS-I mice as a new therapeutic option, both with bone marrow and umbilical cord blood stem cell sources. Transplantation at birth determined a restoration of α-L-iduronidase activity with a consequent reduction of GAGs levels in visceral organs and prevention of skeletal dysplasia. In fact, radiographs, micro-CT and histology performed on bones showed an amelioration of the skeletal phenotype[42,61].

Combination therapies approaches have been tested in adult mouse models. Administration of ERT and BMT in *Idua*-deficient mice determined a normalization of histomorphometric parameters of bone remodelling[110]. Moreover in MPS-II mice, ERT in combination with BMT had an additive effect in reducing GAGs levels in visceral organs, such as heart, kidney and lung[120].

In MPS mouse model, the gene-correction strategy has mainly been performed on hematopoietic cells. Cells, generally derived from BM, are transduced and transplanted into recipients animals. HSC gene therapy has demonstrated high therapeutic efficacy in ameliorating disease abnormalities in a mouse model of MPS-I. Neurologic and skeletal defects, that are generally hard to target, were completely corrected after lentiviral based gene therapy[79]. HSC gene therapy, both with lentivirally and retrovirally bone marrow cells, has a therapeutic effect on brain manifestations also on MPS-II and MPS-

IIIB mice[121,122]. Not only BM cells were employed as a cell source, but in other studies neural stem cells and mesenchymal stromal cells have been transduced for gene therapy approaches in MPS-VII mice[123,124].

4. SCOPE OF THE THESIS

The aim of my PhD project was to deeply investigate the therapeutic effect of hematopoietic stem cell transplantation (HSCT) and enzyme replacement therapy (ERT), administered at birth, in the MPS-I mouse model.

- In the first part, we compared the combination therapy approach, based on HSCT and ERT, over the therapies administered alone, in the immunocompetent murine model of MPS-I. Therapies were administered at birth, considering the importance of developing therapeutic options at an early stage of life. We demontrated that all three treatments under investigation, individually or in combination, were able to significantly decrease GAGs storage in visceral organs, but they had a differential effect with respect to bone lesions and a limited effect on brain manifestations.

- In the second part, we studied the efficacy of UCB transplantation (UCBT) in MPS-I mice at neonatal age. First of all, we characterized murine UCB cells and then we demonstrated the efficacy of UCBT in restoring IDUA activity and reducing GAGs storage in organs and in plasma, and in ameliorating skeletal manifestations.

REFERENCES

1. Platt, F. M., Boland, B. & van der Spoel, A. C. Lysosomal storage disorders: The cellular impact of lysosomal dysfunction. *J Cell Biol.* 199:723–734 (2012).
2. Alroy, J., Garganta, C. & Wiederschain, G. Secondary biochemical and morphological consequences in lysosomal storage diseases. *Biochem.* 79:619–636 (2014).
3. Parenti, G., Pignata, C., Vajro, P. & Salerno, M. New strategies for the treatment of lysosomal storage diseases (Review). *Int J Mol Med.* 31:11–20 (2013).
4. James, R. A., Singh-Grewal, D., Lee, S.-J., McGill, J. & Adib, N. Lysosomal storage disorders: A review of the musculoskeletal features. *J Paediatr. Child Health.* 52:262–271 (2016).
5. Parenti, G., Andria, G. & Ballabio, A. Lysosomal Storage Diseases: From Pathophysiology to Therapy. *Annu Rev Med.* 66:471–486 (2015).
6. Lieberman, A. P. *et al.* Autophagy in lysosomal storage disorders. *Autophagy.* 8:719–730 (2012).
7. Coutinho, M. F., Prata, M. J. & Alves, S. Mannose-6-phosphate pathway : A review on its role in lysosomal function and dysfunction. *Mol Genet Metab.* 105: 42–550 (2012).
8. Solomon, M. & Muro, S. Lysosomal enzyme replacement therapies: Historical development, clinical outcomes, and future perspectives. *Adv Drug Deliv Rev.* 118:109–134 (2017).
9. Ellinwood, N. M., Vite, C. H. & Haskins, M. E. Gene therapy for lysosomal storage diseases: the lessons and promise of animal models. *J Gene Med.* 6:481–506 (2004).
10. Segatori, L. Impairment of Homeostasis in Lysosomal Storage Disorders *International Union of Biochemistry and Molecular Biology.* 66:472–477 (2014)
11. Settembre, C. *et al.* A block of autophagy in lysosomal storage disorders. *Human Molecula Genetics.* 17:119–129 (2008).
12. Sardiello, M. Transcription factor EB: from master coordinator of lysosomal pathways to candidate therapeutic target in degenerative storage diseases. *Ann N Y Acad Sci*. 1371:3–14 (2017).
13. Oussoren, E., Brands, M.M. M. G., Ruijter, G. J. G., Ploeg, A. T. Van Der & Reuser, A.J.J. Bone, joint and tooth development in mucopolysaccharidoses: Relevance to therapeutic options. *BBA - Mol Basis Dis.* 1812:1542–1556 (2011).
14. Aldenhoven, M., Sakkers, R. J. B., Boelens, J., Koning, T. J. De & Wulffraat, N. M. Musculoskeletal manifestations of lysosomal storage disorders. *Ann Rheum Dis.* 68:1659–1665 (2009).

15. Khan, S. A., Mason, R. W., Giugliani, R., Orii, K. & Fukao, T. Glycosaminoglycans analysis in blood and urine of patients with mucopolysaccharidosis. *Molecular Genetics and Metabolism.* 125:44-52 (2018).
16. De Pasquale, V. *et al.* Targeting Heparan Sulfate Proteoglycans as a Novel Therapeutic Strategy for Mucopolysaccharidoses. *Molecular Therapy: Methods & Clinical Development.*10:8–16 (2018).
17. Poulain, F. E. & Yost, H. J. Heparan sulfate proteoglycans: a sugar code for vertebrate development? *Development.* 142:3456–3467 (2015).
18. Heard, J. M., Bruy, J. & Roy, E. Storage problems in lysosomal diseases. *Biochemical Society Transactions.* 38:1442–1447 (2010).
19. Clarke, L. A. The mucopolysaccharidoses: a success of molecular medicine. *Expert Rev Mol Med.* 10:1–18 (2008).
20. Grosse, S. D., Lam, W. K. K., Wiggins, L. D. & Kemper, A. R. Cognitive outcomes and age of detection of severe mucopolysaccharidosis type 1. *Genet Med.* 19:975-982 (2017).
21. De Ru, M. H. *et al.* Capturing phenotypic heterogeneity in MPS I: results of an international consensus procedure. *Orphanet J Rare Dis.* 7:22 (2012).
22. Terlato, N. J. & Cox, G. F. Can mucopolysaccharidosis type I disease severity be predicted based on a patient's genotype? A comprehensive review of the literature. *Genet Med.* 5:286–294 (2003).
23. Brooks, D. A. Alpha-L-iduronidase and enzyme replacement therapy for mucopolysaccharidosis I. *Expert Opin Biol Ther.* 2:967–76 (2002).
24. Brante, G. Gargoylism-A Mucopolysaccharidosis. *Scand J Clin Lab Invest.* (1952).
25. Scheie, H. G., Hambrick, G. W. & Barness, L. A. A Newly Recognized Forme Fruste of Hurler's Disease (Gargoylism). *Am J Ophthalmol.* 53:753–769 (1962).
26. Fratantoni, J., Hall, C. & Neufeld, E. Hurler and Hunter Syndromes: Mutual Correction of the Defect in Cultured Fibroblasts. *Science.* 162:570-572 (1968).
27. Scott, H. S. *et al.* Chromosomal Localization of the Human a-L-iduronidase (IDUA) to 4p16.3. *Am J Hum Genet.* 47:802–807 (1990).
28. Muenzer, J., Wraith, J. E. & Clarke, L. A. Mucopolysaccharidosis I : Management and Treatment Guidelines. *Pediatrics.* 123:19-29 (2009).
29. Clarke, L. A. Pathogenesis of skeletal and connective tissue involvement in the mucopolysaccharidoses: glycosaminoglycan storage is merely the instigator. *Rheumatology (Oxford).* 5:13–18 (2011).
30. Muenzer, J. Overview of the mucopolysaccharidoses. *Rheumatology (Oxford.)* 50 Suppl 5:v4-12 (2011).
31. Wang, R. Y., Bodamer, O. A. & Watson, M. S. Lysosomal storage diseases: Diagnostic confirmation and management of presymptomatic individuals. *Genetics in Medicine* 13:457–484 (2011).

32. Rigante, D. & Segni, G. Cardiac Structural Involvement in Mucopolysaccharidoses. *Cardiology*. 98:18–20 (2002).
33. Ashworth, J., Biswas, S., Wraith, E. & Lloyd, I. The ocular features of the mucopolysaccaridoses. *Eye*. 20:553–563 (2006).
34. Xing, M., Parker, E., Moreno De Luca, A., Harmouche, E. & Terk, M. Radiological and clinical characterization of the lysosomal storage disorders: non-lipid disorders. *British Institute of Radiology*. 1–14 (2014).
35. Simonaro, C. M., Haskins, M. E. & Schuchman, E. H. Articular Chondrocytes from Animals with a Dermatan Sulfate Storage Disease Undergo a High Rate of Apoptosis and Release Nitric Oxide and Inflammatory Cytokines: A Possible Mechanism Underlying Degenerative Joint Disease in the Mucopolysaccharidoses. *Laboratory Investigation*. 81:1319–1328 (2001).
36. Wilson, S. *et al.* Glycosaminoglycan-Mediated Loss of Cathepsin K Collagenolytic Activity in MPS I Contributes to Osteoclast and Growth Plate Abnormalities. *Am J Pathol.* 175:2053–2062 (2009).
37. Rasalkar, D. *et al.* Pictorial review of mucopolysaccharidosis with emphasis on MRI features of brain and spine. *Br J Radiol.* 84:469–477 (2011).
38. Clarke, L. A., Winchester, B., Giugliani, R., Tylki-szyma, A. & Amartino, H. Biomarkers for the mucopolysaccharidoses: Discovery and clinical utility. *Mol Genet Metab.* 106:395–402 (2012).
39. Tomatsu, S. *et al.* Neonatal cellular and gene therapies for mucopolysaccharidoses: the earlier the better? *J Inherit Metab Dis*. 39:189–202 (2016).
40. Ashton, L. J. *et al.* Immunoquantification and Enzyme Kinetics of a-L-lduronidase in Cultured Fibroblasts from Normal Controls and Mucopolysaccharidosis Type I Patients. *Am J Hum Genet.* 50:787–794 (1992).
41. D'Aco, K., Underhill, L. & Rangachari, L. Diagnosis and treatment trends in mucopolysaccharidosis I: findings from the MPS I Registry. *Eur J Pediatr*. 171:911–919 (2012).
42. Pievani, A. *et al.* Neonatal bone marrow transplantation prevents bone pathology in a mouse model of mucopolysaccharidosis type I. *Blood.* 125:1662–1672 (2015).
43. Verma, J., Thomas, D. C., Kasper, D. C., Sharma, S. & Puri, R. D. Inherited Metabolic Disorders: Efficacy of Enzyme Assays on Dried Blood Spots for the Diagnosis of Lysosomal Storage Disorders. *JIMD Rep*. 31:15-27 (2017)
44. Chamoles, N. A., Blanco, M. & Gaggioli, D. Diagnosis of α-L-Iduronidase Deficiency in Dried Blood Spots on Filter Paper: The Possibility of Newborn Diagnosis. *Clin Chem.* 47:780–781 (2001).
45. Nakamura, K., Hattori, K. & Endo, F. Newborn Screening for Lysosomal Storage Disorders. *Am J Med Genet C Semin Med Genet.* 157:63–71 (2011).

46. Tomatsu, S., Montaño, A. M., Oguma, T. & Dung, V. C. Dermatan sulfate and heparan sulfate as a biomarker for mucopolysaccharidosis I. *J Inherit Metab Dis.* 33:141-150 (2010).
47. Akella, R. R. D. & Kadali, S. Amniotic fluid glycosaminoglycans in the prenatal diagnosis of mucopolysaccharidoses-A useful biomarker. *Clin Chim Acta*. 460:63–66 (2016).
48. Valayannopoulos, V. & Wijburg, F. A. Therapy for the mucopolysaccharidoses. *Rheumatology (Oxford). 5:*49–59 (2011).
49. Parini, R. *et al.* Open issues in Mucopolysaccharidosis type I-Hurler. *Orphanet J Rare Dis.* 12:112 (2017).
50. Kakkis, E. D., Matynia, A., Jonas, A. J. & Neufeld, E. F. Overexpression of the Human Lysosomal Enzyme α-L-iduronidase in Chinese Hamster Ovary Cells. *Protein Expr Purif.* 5:225-232 (1994).
51. Shull, R. M. *et al.* Enzyme replacement in a canine model of Hurler syndrome. *Proc Natl Acad Sci.* 91:12937–12941 (2006).
52. Kakkis, E. D. *et al.* Enzyme-replacement therapy in Mucopolysaccharidosis I. *N Engl J Med.* 344:182–188 (2001).
53. Muenzer, J. Early initiation of enzyme replacement therapy for the mucopolysaccharidoses. *Mol Genet Metab.* 111:63–72 (2014).
54. Wolf, D. A. *et al.* Lysosomal enzyme can bypass the blood – brain barrier and reach the CNS following intranasal administration. *Mol Genet Metab* 106:131–134 (2012).
55. Kakkis, E. *et al.* Intrathecal enzyme replacement therapy reduces lysosomal storage in the brain and meninges of the canine model of MPS I. *Mol Genet Metab.* 83:163–174 (2004).
56. Laraway, S. *et al.* Outcomes of Long-Term Treatment with Laronidase in Patients with Mucopolysaccharidosis Type I. *J Pediatr.* 178:219-226.e211 (2016).
57. Hobbs, J. R. *et al.* Reversal of Clinical Features of Hurler 's Disease and Biochemical Improvement after Treatment by Bone Marrow Transplantation. *J Inher Metab Dis.* 1:59–60 (1982).
58. Boelens, J. J. *et al.* Outcomes of transplantation using various hematopoietic cell sources in children with Hurler syndrome after myeloablative conditioning Outcomes of transplantation using various hematopoietic cell sources in children with Hurler syndrome after myeloablative conditioning. *Blood. 121:*3981–3987 (2013).
59. Prasad, V. K. & Kurtzberg, J. Cord blood and bone marrow transplantation in inherited metabolic diseases: scientific basis, current status and future directions. *Br J Haematol. 148:*356–372 (2009).
60. Aldenhoven, M., Boelens, J. & Koning, T. J. De. The Clinical Outcome of Hurler Syndrome after Stem Cell Transplantation. *Biol Blood Marrow Transplant.* 14:485–498 (2008).
61. Azario, I. *et al.* Neonatal umbilical cord blood transplantation halts skeletal

disease progression in the murine model of MPS-I. *Sci Rep*. 7:9473 (2017).
62. Yasuda, E. *et al.* Long-term follow-up of post hematopoietic stem cell transplantation for Hurler syndrome: Clinical, biochemical, and pathological improvements. *Molecular Genetics and Metabolism Reports*. 2:65–76 (2015).
63. Prasad, V. K. & Kurtzberg, J. Transplant Outcomes in Mucopolysaccharidoses. *Semin Hematol.* 47:59–69 (2010).
64. Kunin-Batson, A. *et al.* Long-Term Cognitive and Functional Outcomes in Children with Mucopolysaccharidosis (MPS)-IH (Hurler Syndrome) Treated with Hematopoietic Cell Transplantation. *JIMD Rep*. 29:95-102 (2016).
65. Boelens, J. J. *et al.* Outcomes of hematopoietic stem cell transplantation for Hurler ' s syndrome in Europe: a risk factor analysis for graft failure. *Bone Marrow Transplantation.* 40:225–233 (2007).
66. Tolar, J. *et al.* Combination of enzyme replacement and hematopoietic stem cell transplantation as therapy for Hurler syndrome. *Bone Marrow Transplantation.* 41:531–535 (2008).
67. Eisengart, J. B. *et al.* Enzyme replacement is associated with better cognitive outcomes after transplant in Hurler syndrome. *J Pediatr*. 162:375–380 (2014).
68. Valayannopoulos, V. *et al*. Laronidase for Cardiopulmonary Disease in Hurler Syndrome 12 Years After Bone Marrow Transplantation. *Pediatrics*. 126:e1242 (2015).
69. Kennedy, B. D. W. & Abkowitz, J. L. Kinetics of Central Nervous System Microglial and Macrophage Engraftment: Analysis Using a Transgenic Bone Marrow Transplantation Model. *Blood*. 90:986–993 (2018).
70. Baldo, G. *et al.* Enzyme replacement therapy started at birth improves outcome in dif fi cult-to-treat organs in mucopolysaccharidosis I mice. *Molecular Genetics and Metabolism.* 109:33–40 (2013).
71. Tomatsu, S. *et al.* Enzyme replacement therapy in newborn mucopolysaccharidosis IVA mice: early treatment rescus bone lesions? *Mol Genet Metab*. 114:195–202 (2016).
72. Dierenfeld, A. *et al.* Replacing the Enzyme α-L-iduronidase at Birth Ameliorates Symptoms in the Brain and Peripehery of Dogs with Mucopolysaccharidosis type I. *Sci Transl Med.* 2: 60ra89 (2011).
73. Crawley, A. C. *et al.* Enzyme Replacement Therapy from Birth in a Feline Model of Mucopolysaccharidosis Type VI. *J Clin Invest.* 99:651–662
74. Gabrielli, A. O., Clarke, L. A., Bruni, S. & Coppa, G. V. Enzyme-Replacement Therapy in a 5-Month-Old Boy With Attenuated Presymptomatic MPS I : 5-Year Follow-up. *Pediatrics*. 125:e183 (2015).
75. Aldenhoven, M. *et al.* Long-term outcome f hurler syndrome after HCT: an international multicenter study. *Blood.* 125: 2164-2172 (2018).
76. Parenti, G., Pignata, C., Vajro, P. & Salerno, M. New strategies for the treatment of lysosomal storage diseases (Review). *Int J Mol Med.* 31:11–20

(2013).
77. Haskins, M. E. Gene Therapy for Lysosomal Storage Diseases (LSDs) in Large Animal Models. *ILAR J*. 50:112–121 (2012).
78. Biffi, A. Gene therapy for lysosomal storage disorders: a good start. *Hum Mol Genet*. 25:65–75 (2016).
79. Visigalli, I. *et al.* Gene therapy augments the efficacy of hematopoietic cell transplantation and fully corrects mucopolysaccharidosis type I phenotype in the mouse model. *Blood*. 116:5130–5139 (2013).
80. Macauley, S. L. Combination Therapies for Lysosomal Storafe Diseases: A Complex Answer to a Simple Problem. *Pediatr Endocrinol Rev*. 13:639–648 (2017).
81. Kobayashi, H. *et al.* Neonatal Gene Therapy of MPS I Mice by Intravenous Injection of a Lentiviral Vector. *Molecular Therapy*. 11:776–789 (2005).
82. Mango, R. L. *et al.* Neonatal retroviral vector-mediated hepatic gene therapy reduces bone, joint, and cartilage disease in mucopolysaccharidosis VII mice and dogs. *Molecular Genetics and Metabolism*, 82:4–19 (2004).
83. Ponder, K. P. *et al.* Mucopolysaccharidosis I Cats Mount a Cytotoxic T Lymphocyte Response after Neonatal Gene Therapy That Can Be Blocked with CTLA4-Ig. *Molecular Therapy.* 14:5–13 (2006).
84. Ma, X. *et al.* Improvements in Mucopolysaccharidosis I Mice After Adult Retroviral Vector – mediated Gene Therapy with Immunomodulation. *Molecular Therapy.* 15:889–902 (2007).
85. Cressant, A. *et al.* Improved Behavior and Neuropathology in the Mouse Model of Sanfilippo Type IIIB Disease after Adeno-Associated Virus-Mediated Gene Transfer in the Striatum. *The Journal of Neuroscience. 24:*10229–10239 (2004).
86. Fraldi, A. *et al.* Functional correction of CNS lesions in an MPS-IIIA mouse model by intracerebral AAV-mediated delivery of sulfamidase and SUMF1 genes. *Human Molecular Genetics.* 16:2693–2702 (2007).
87. Hinderer, C. *et al.* Intrathecal Gene Therapy Corrects CNS Pathology in a Feline Model of Mucopolysaccharidosis I. *The American Society of Gene & Cell Therapy.* 22:2018–2027 (2018).
88. Penati, R., Fumagalli, F., Calbi, V., Bernardo, M. E. & Aiuti, A. Gene therapy for lysosomal storage disorders: recent advances for metachromatic leukodystrophy and mucopolysaccaridosis I. *J Inherit Metab Dis. 40:*543–554 (2017).
89. Biffi, A. Hematopoietic Stem Cell Gene Therapy for Storage Disease : Current and New Indications. *Molecular Therapy*. 25:1155–1162 (2017).
90. Wolfe, J. H. *et al.* Reversal of pathology in murne mucopolysaccharidosis type VII by somatic cell gene transfer. *Nature.* 360 (1992).
91. Visigalli, I. *et al.* Preclinical testing of the safety and tolerability of LV-mediated above normal alpha-L-iduronidase expression in murine and human hematopoietic cells using toxicology and biodistribution GLP

studies. *Hum Gene Ther. 27:813-829*

92. Stirnadel-Farrant, H. *et al.* Gene therapy in rare diseases: the benefits and challenges of developing a patient- centric registry for Strimvelis in ADA-SCID. *Orphanet Journal of Rare Diseases.* 13:49 (2018).
93. Byrne, B. J., Falk, D. J., Cle, N. & Mah, C. S. Gene Therapy Approaches for Lysosomal Storage Disease: Next-Generation Treatment. *Human Gene Therapy*. 23:808–815 (2012).
94. Wyatt, K. *et al.* The effectiveness and cost of enzyme replacement and substrate reduction therapies: a longitudinal cohort study of people with lysosomal storage disorders. *Health Technology Assessment.* 16 (2012).
95. Derrick-Roberts, A. L. K., Marais, W. & Byers, S. Rhodamine B and 2-acetamido-1 , 3 , 6-tri-O-acetyl-4-deoxy-4- fl uoro- D -glucopyranose (F-GlcNAc) inhibit chondroitin / dermatan and keratan sulphate synthesis by different mechanisms in bovine chondrocytes. *Mol Genet Metab.* 106:214–220 (2012).
96. Derrick-Roberts, A. L. K., Jackson, M. R., Pyragius, C. E. & Byers, S. Substrate Deprivation Therapy to Reduce Glycosaminoglycan Synthesis Improves Aspects of Neurological and Skeletal Pathology in MPS I Mice. *Diseases*. 5 (2017).
97. Kloska, A., Jakóbkiewicz-banecka, J., Narajczyk, M. & Banecka-majkutewicz, Z. Effects of flavonoids on glycosaminoglycan synthesis : implications for substrate reduction therapy in Sanfilippo disease and other mucopolysaccharidoses. *Metab Brain Dis.* 26:1–8 (2011).
98. Dziedzic, D., Wegrzyn, G. & Jakobkiewicz-Banecka, J. Impairment of glycosaminoglycan synthesis in mucopolysaccharidosis type IIIA cells by using siRNA: a potential therapeutic approach for Sanfilippo disease. *European journal of Human Genetics.* 18:200–205 (2010).
99. Gunn, G. *et al.* Long-term Nonsense Suppression Therapy Moderates MPS I-H Disease Progression. *Mol Genet Metab.* 111:374–381 (2015).
100. Wang, D. *et al.* The Designer Aminoglycoside NB84 Significantly Reduces Glycosaminoglycan Accumulation Associated with MPS i-H in the Idua-W392X Mouse. *Mol Genet metab.* 105:116–125 (2013).
101. Haskins, M. E., Aguirre, G. D., Jezyk, P. F., Desnick, R. J. & Patterson, D. F. The Pathology of the Feline Mucopolysaccharidosis I. *AJP*. 27–36 (1983).
102. Shull, R. M., Munger, R. J., Hall, C. W., Constantopoulos, G. & Neufeld, E. F. Canine α-L-Iduronidase Deficiency A Model of Mucopolysaccharidosis I. *AJP*. 244–248 (1982).
103. Clarke, L. A. *et al.* Murine mucopolysaccharidosis type I: targeted disruption of the murine α - L -iduronidase gene. *Hum Mol Genet.* 6:503–511 (1997).
104. Ohmi, K. *et al.* Activated microglia in cortex of mouse models of mucopolysaccharidoses I and IIIB. *Proc Natl Acad Sci USA.* 4:1902-1907

(2003).
105. Kim, C. *et al.* Decreased performance in IDUA knockout mouse mimic limitations of joint function and locomotion in patients with Hurler syndrome. *Orphanet J Rare Dis.*10:121 (2015).
106. Wang, D. *et al.* Characterization of an MPS I-H Knock-In Mouse that Carries a Nonsense Mutation Analogous to the Huma IDUA-W402X Mutation. *Mol Genet Metab.* 99:62–71 (2011).
107. Garcia-Rivera, M. F. *et al.* Characterization of an immunodeficient mouse model of mucopolysaccharidosis type I suitable for preclinical testing of human stem cell and gene therapy. *Brain Res Bull.* 74:429–438 (2008).
108. Mendez, D. C. *et al.* A novel, long-lived, and highly engraftable immunodeficient mouse model of mucopolysaccharidosis type I. *Mol Ther Methods Clin Dev. 2:14068* (2015).
109. Simonaro, C. M., Angelo, M. D., Haskins, M. E. & Schuchman, E. H. Mechanism of Glycosaminoglycan-Mediated Bone and Joint Disease Implications for the Mucopolysaccharidoses and Other. *Am J Pathol.* 172:112–122 (2008).
110. Kuehn, S. C. *et al.* Impaired bone remodeling and its correction by combination therapy in a mouse model of mucopolysaccharidosis-I. *Human Molecular Genetics.* 24:7075–7086 (2015).
111. Gatto, F. *et al.* Hurler Disease Bone Marrow Stromal Cells Exhibit Altered Ability to Support Osteoclast Formation. *Stem Cells Dev*. 21:1466–1477 (2012).
112. De Oliveira, P.G. *et al.* Characterization of joint disease in mucopolysaccharidosis type I mice. *Int J Exp Pathol. 94:*305–311 (2013).
113. Russell, C. *et al.* Murine MPS I: insights into the pathogenesis of Hurler syndrome. *Clin Genet. 53:*349–361 (1998).
114. Heinecke, K. A., Peacock, B. N., Blaza, B. R., Tolar, J. & Seyfried, T. N. Lipid Composition of Whole Brain and Cerebellum in Hurler Syndrome (MPS IH) Mice. *Neurochem Res*. 36:1669–1676 (2011).
115. Baldo, G. *et al.* Shotgun proteomics reveals possible mechanisms for cognitive impairment in Mucopolysaccharidosis I mice. *Mol Genet Metab.* 114:138–145 (2015).
116. Wilkinson, F. L. *et al.* Neuropathology in Mouse Models of Mucopolysaccharidosis Type I , IIIA and IIIB. *PLoS One.* 7:e35787 (2012).
117. Baldo, G. *et al.* Evidence of a progressive motor dysfunction in Mucopolysaccharidosis type I mice. *Behav Brain Res.* 233:169–175 (2013).
118. Pasqualim, G., Baldo, G., Carvalho, T. G. De & Maria, A. Effects of Enzyme Replacement Therapy Started Late in a Murine Model of Mucopolysaccharidosis Type I. *PLoS One.10:e0117271* (2015).
119. Baldo, G., Wozniak, D. F., Ohlemiller, K. K., Zhang, Y. & Ponder, K. P. Retroviral Vector-mediated Gene Therapy to Mucopolysaccharidosis I mice Improves Sensorimoto Impairments and Other Behavior Deficits. *J Inherit*

Metab Dis. 36:499–512 (2014).

120. Akiyama, K. *et al.* Enzyme augmentation therapy enhances the therapeutic ef fi cacy of bone marrow transplantation in mucopolysaccharidosis type II mice. *Molecular Genetics and Metabolism.* 111:139–146 (2014).
121. Wakabayashi, T. *et al.* Hematopoietic Stem Cell Gene Therapy Corrects Neuropathic Phenotype in Murine Model of Mucopolysaccharidosis Type II. *Human Gene Therapy.* 26:1–10 (2015).
122. Zheng, Y. *et al.* Retrovirally transduced bone marrow has a therapeutic effect on brain in the mouse model of mucopolysaccharidosis IIIB. *Mol Genet Metab.* 82:286–295 (2004).
123. Meng, X. *et al.* Brain Transplantation of Genetically Engineered Human Neural Stem Cells Globally Corrects Brain Lesions in the Mucopolysaccharidosis Type VII Mouse. *J Neurosci Res.* 74:266–277 (2003).
124. Meyerrose, T. E. *et al.* Lentiviral-Transduced Human Mesenchymal Stem Cells Persistently Express Therapeutic Levels of Enzyme in a Xenotransplantation Model of Human Disease. *Stem Cells.* 26:1713–1722 (2009).

CHAPTER 2

Neonatal combination therapy approach in MPS-I mouse model: would it be even better?

Ludovica Santi[a], Giada De Ponti[a], Giorgia Dina[b], Alice Pievani[a], Alessandro Corsi[c], Kazuki Sawamoto[d], Laura Antolini[e], Silvia Gregori[f], Andrea Annoni[f], Andrea Biondi[g], Angelo Quattrini[b], Shunji Tomatsu[d], Marta Serafini[a]

[a] Centro Ricerca M. Tettamanti, Department of Pediatrics, University of Milano-Bicocca, Monza, 20900, Italy

[b] Experimental Neuropathology Unit, INSPE, Division of Neuroscience, IRCCS Ospedale San Raffaele, Milano, Italy

[c] Department of Molecular Medicine, Sapienza University, Rome, 00161, Italy

[d] Department of Biomedical Research, Alfred I. duPont Hospital for Children, Wilmington, DE, 19803, USA

[e] Centro di Biostatistica per l'epidemiologia clinica, Department of Health Sciences, University of Milano-Bicocca, Monza, 20900, Italy

[f] San Raffaele Telethon Institute for Gene Therapy, IRCCS San Raffaele Scientific Institute, Milan, Italy.

[g] Department of Pediatrics, University of Milano-Bicocca, Monza, 20900, Italy

ABSTRACT

Mucopolysaccharidosis type I (MPS-I) is a lysosomal storage disorder due to deficiency in the alpha-L-iduronidase enzyme, resulting in the progressive accumulation of glycosaminoglycans (GAGs) in multiple organs and the consequent multiorgan dysfunction. Hematopoietic stem cell transplantation (HSCT) and enzyme replacement therapy (ERT) are the currently available therapies for MPS-I patients. Despite their effectiveness in correcting most clinical manifestations, muscoloskeletal abnormalities and neurocognitive defects still impact quality of life of treated patients. It is widely accepted that an early intervention may be crucial to obtain a better outcome.

On the basis of these observations, we tested the therapeutic efficacy of HSCT and ERT, alone or in combination, administered at birth, in a MPS-I mouse model.

We demonstrated that all three treatments were able to prevent biochemical and pathological manifestations of the disease in visceral organs, and, in particular, the combination therapy had a better outcome in difficult-to-treat organs, such as kidney and heart. Of note, transplant procedure can halt the production of antibodies specific for the recombinant enzyme that could reduce ERT efficacy. Regarding the severe skeletal disease, we observed a differential effect in reduction of bone disease, with a significant better correction in transplanted mice, in the presence of ERT or not. Otherwise in the brain, all the treatments provided a moderate decrease of inflammation without an evident metabolic correction.

Our findings demonstrated that most manifestations of MPS-I can be prevented by a neonatal treatment based on a combination of HSCT and ERT, promoting the idea of an early intervention supported by the development of newborn screening programs.

INTRODUCTION

Mucopolysaccharidosis type I (MPS-I), an inherited metabolic disorder, is caused by mutations of *IDUA* gene encoding the lysosomal enzyme α-L-iduronidase involved in the catabolism of glycosaminoglycans (GAGs) heparan and dermatan sulphate[1]. IDUA activity impairment leads to accumulation of GAGs in tissues, resulting in progressive multi-organ dysfunction and a wide range of clinical manifestations, including upper airway obstruction, cardiomyopathy, central nervous system (CNS) anomalies and skeletal deformities, known as *dysostosis multiplex*[2].

Allogeneic hematopoietic stem cell transplantation (HSCT) and enzyme replacement therapy (ERT) are the currently available treatments for MPS-I patients, both of which provide the missing enzyme. Although weekly human recombinant α-L-iduronidase (laronidase, Aldurazyme®, Genzyme) infusions reduce GAGs storage and ameliorate some clinical aspects[3], ERT treatment does not completely correct bone, cardiac valve disease, corneal clouding[4] and CNS disease, as it is unable to cross the blood-brain barrier (BBB)[5]. Nowadays, HSCT is considerd the first-choice therapy for the most severe form of MPS-I (Hurler syndrome) with neurocognitive impairment, restoring IDUA levels by various cell types including microglial cells infiltrating in the CNS[6]. Nevertheless, despite the clinical success of HSCT in ameliorating multiorgan morbidity, patients may develop an important disease burden. Muscoloskeletal abnormalities still impact transplanted patient's quality of life, probably due to a limited penetration of the enzyme into poorly

vascularized tissues and/or to the irreversibility of some lesions at the time of transplantation[7-8]. Furthermore, HSCT does not seem to correct any neurocognitive defects after they have already occurred but only halts their progression[9].

It is widely accepted that a precocious treatment is fundamental to achieve a good clinical outcome. Evidences, coming from experimental data on animal models, show a higher degree of anomalies corrections when treatment is performed early in life, both for ERT[10-11] and for HSCT[12-13]. Clinical data also confirm the need of an early intervention[14-15] that is clearly evident in affected siblings cases treated at different ages[16].

Considering that neither ERT nor HSCT is resolvent on clinical manifestations, in particular on orthopedic alterations, non-progressive mental retardation and valve deformities[17-6], an approach consisting on the combination of both therapies could be a possible strategy to further improve patients outcome[18]. Peri-transplant ERT administration from diagnosis to engraftment has been demonstrated to be effective in stabilizing the clinical conditions of patients in pre-transplant phase[19], and post-transplant ERT seems to reduce the residual disease burden[20]. ERT in combination with HSCT does not negatively affect the engraftment[21] and HSCT seems to attenuate the formation of neutralizing allo-antibodies against recombinant IDUA[22]. Regarding the bone disease, it has been demostrated that HSCT dramatically increased osteoclastogenesis in MPS-I mice whereas bone remodeling was fully normalized by a combination therapy[23]. To better elucidate the effectiveness of the combination therapy over the single ERT and HSCT therapies in refractory organs, we used the

immunocompetent murine model of MPS-I, which recapitulates disease manifestations seen in MPS-IH patients, in particular at the bone level[24-25]. We performed a systematic comparison of the three treatment approaches administered starting from the neonatal period, considering the importance of exploring therapeutic options at an early stage of life. Indeed, the clinical outcome could be improved if it might be possible to prevent rather than correct disease manifestations[7]. In the present study, to investigate treatments efficacy, we evaluated IDUA enzyme activity, GAGs accumulation and presence of vacuoles in visceral organs and plasma, we performed radiographs to measure the extent of the skeletal phenotype correction, and examined the neurological outcome.

RESULTS

Treatments tolerability and donor cell engraftment

Newborn WT and MPS-I mice were treated according to the schematic representation and timeline, shown in *Figure 1A.* In particular, the three treatment groups were: (1) mice receiving transplant of normal CD45.1^{+} donor cells (neonatal bone marrow transplantation group, hereafter named nBMT group; n = 25 WT mice, n = 17 MPS-I mice), (2) mice receiving enzyme replacement therapy (hereafter named ERT group; n = 10 WT mice, n = 7 MPS-I mice), (3) mice receiving combination of normal CD45.1^{+} cells and ERT (nBMT+ERT group: n = 21 WT mice, n = 22 MPS-I mice). Among transplanted animals, we decided to include in our cohort only the highly engrafted mice, defined as reaching more than 50% donor cells in PB at 2 months (hi-nBMT group: n = 10 WT mice, n = 6 MPS-I mice; hi-nBMT+ERT group: n = 9 WT mice, n = 7 MPS-I mice). Untreated WT (n = 8) and MPS-I mice (n = 8) were included as control.

Low toxicity was observed in treatment groups involving nBMT. Indeed, among the nBMT and the nBMT+ERT group, 90.5% of mice (38/42) and 86% of mice (37/43), respectively, lived up to 37 weeks, as compared to the totality of ERT (17/17).

The body weight at 37 weeks of the two transplanted cohorts (median weight hi-nBMT: 17.6 g [range from 13.28 to 20.3 g]; hi-nBMT+ERT: 20 g [12.4 - 26.3 g]) was significantly lower as compared to ERT group (26.55 g [25.4 - 34.2 g]; P=0.0027 *vs* hi-nBMT, P=0.006 *vs* hi-nBMT+ERT), probably due to the conditioning

regimen-induced toxicity. Weight of mice receiving ERT was not different from untreated MPS-I mice (P=0.266) and from normal mice (P=0.435) (*Figure 1B*).

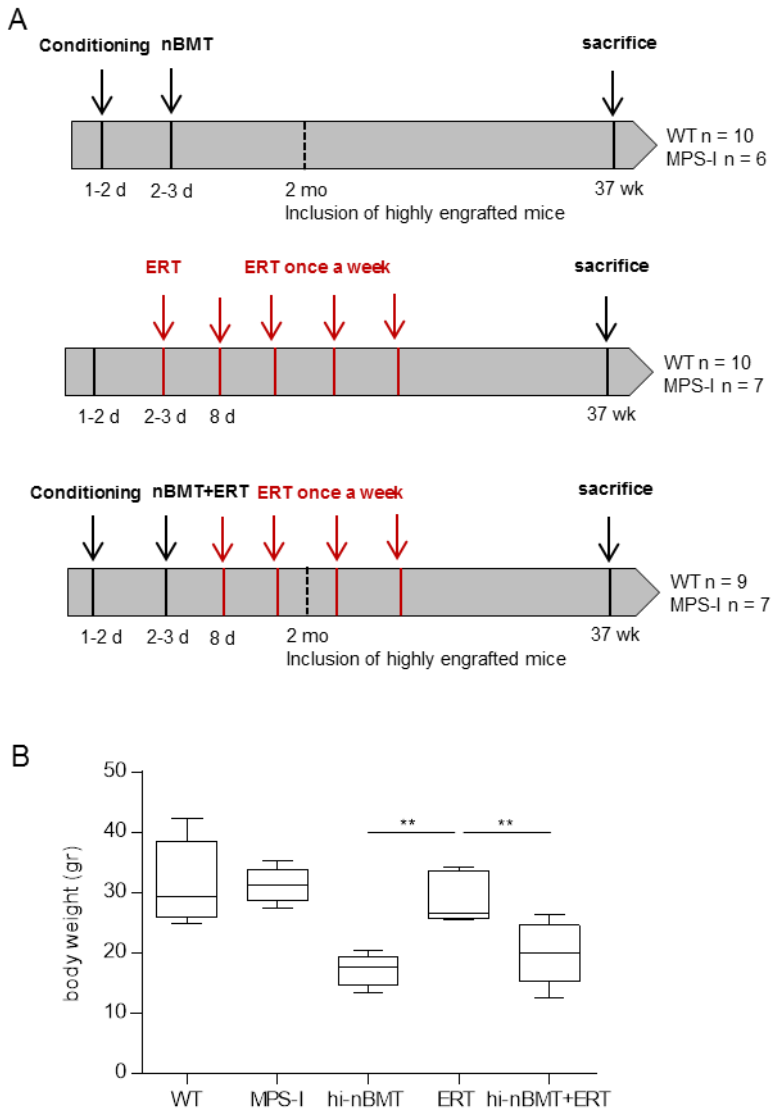

Figure 1. Tolerability of treatments. *(**A**) Schematic representation and timeline. The first group of newborn WT and MPS-I mice (nBMT) was conditioned at day 1-2 after birth with Busulfan (20mg/kg IP), and the next*

day transplanted with 2x10^6 singeneic adult WT BM cells. Engraftment evaluation was assessed by flow cytometry and only mice who reached ≥50% PB donor chimerism (namely highly engrafted, hi-nBMT) at 2 months after transplantation were included in further analyses. The second group of mice (ERT) was treated with enzyme replacement therapy (laronidase 0,58mg/kg IV) once a week from day 1-2 after birth until sacrifice. The third group of mice (nBMT+ERT) was conditioned at day 1-2 after birth, and received BM transplantation and ERT in a single injection, on the next day. ERT was continued weekly until sacrifice. Also in this case, only highly engrafted mice (hi-nBMT+ERT) were included. Number of WT and MPS-I included in each group has been reported.
***(B)** Body weight of untreated and treated mice at sacrifice. Each box plot shows the median and extends from the lowest to the highest value. **P≤0.01 by unpaired Wilcoxon test.*

First of all, we quantified short-term donor cell engraftment rate in WT and MPS-I mice belonging to the nBMT group. Chimerism in the PB was not influenced by genotype at 1 month after transplant (median engraftment in WT mice: 61.4% [range from 24.4 to 81.9%]; MPS-I: 62.1% [21.4 - 78.2%]; P=0.6116), neither at 2 months (WT: 65.9% [26.1 - 95.2%], MPS-I: 83.2% [25.4 - 94.9%]; P=0.6116).

hi-nBMT maintained a stable and sustained donor cell engraftment at 4, 6 and 9 months post transplantation, without significant differences due to the genotype (median engraftment at 4 months in WT mice: 95.25% [range from 57.4 to 96.8%], 4 months in MPS-I mice: 93.8% [88.7 - 95.9%]; P=0.3852; 6 months in WT mice: 95.75% [68 - 97.4%], 6 months in MPS-I mice: 93.1% [80.1 - 97%]; P=0.3852; 9 months in WT mice: 94.95% [68.8 - 97.2%], 9 months in MPS-I mice: 90.65% [77.3 - 97.5%]; P=0.9136) (*Figure 2A*).

Furthermore, we compared the donor engraftment levels in PB of MPS-I mice transplanted in the presence or absence of ERT. At 1 and

2 months after transplantation, no significant difference was observed between the two groups, demonstrating that ERT treatment does not interfere with transplantation outcome (median donor engraftment at 1 month in nBMT: 62.1% [range from 21.4 to 78.2%], 1 month in nBMT+ERT: 50.2% [14.3 - 88.3%]; P=0.4351; 2 months in nBMT: 83.2% [25.4 - 94.9%], 2 months in nBMT+ERT: 70.2% [13.1 - 91.4%]; P=0.3671).

Among highly engrafted MPS-I mice included in our hi-nBMT and hi-nBMT+ERT cohorts, we obtained a stable and similar donor cell engraftment, without any statistical difference, for the entire experimental period until sacrifice (P=0.2234 at 4 months; P=0.7751 at 6 months; P=0.7751 at 9 months) (*Figure 2B*).

At sacrifice, we analysed the percentage of donor engraftment in bone marrow (BM) and spleen of MPS-I mice, observing a comparable engraftment rate between hi-nBMT and hi-nBMT+ERT mice (P=0.6682 for BM; P=0.8301 for spleen). The differentiation of donor cells in lymphoid and myeloid lineages was similar both in BM and in spleen for highly engrafted MPS-I mice receiving nBMT or nBMT+ERT, indicating that ERT does not affect donor cell differentiation in hematopoietic organs (*Figure 3*). Moreover, the proportion of the long term hematopoietic stem cell population, defined as $Lin^{-}Sca1^{+}c\text{-}kit^{+}$ cells (LSK), was similarly retained in BM of both groups.

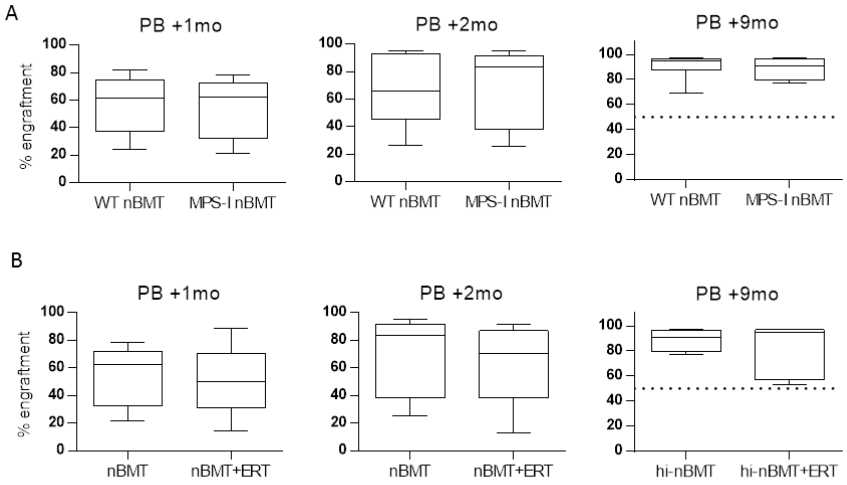

Figure 2. Engraftment of donor-derived cells*. (**A**) Donor chimerism (% CD45.1$^+$ cells) in peripheral blood (PB) of transplanted (nBMT) WT and MPS-I mice at 1 and 2 months after transplantation. Long-term donor chimerism in PB of WT and MPS-I mice highly engrafted (≥50% PB donor chimerism, hi-nBMT), assessed at sacrifice (37 weeks). (**B**) Donor cell engraftment in the PB of MPS-I mice treated with nBMT or nBMT+ERT at 1 and 2 months after transplantation. Long-term engraftment in the PB of MPS-I mice highly engrafted (hi-nBMT and hi-nBMT+ERT), analysed at sacrifice. If not indicated, P>0.05 by unpaired Wilcoxon test.*

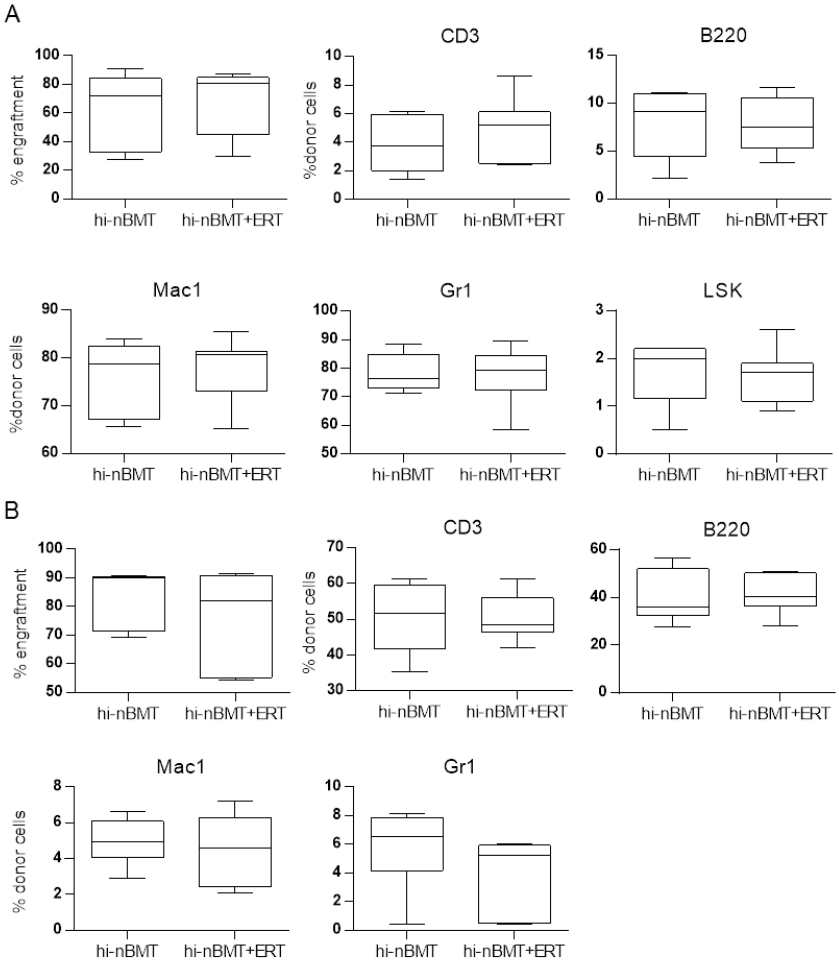

Figure 3. Donor cell engraftment in hematopoietic organs. *(**A**) Percentage of donor cell engraftment and multilineage composition in the BM of MPS-I hi-nBMT and MPS-I hi-nBMT+ERT, analysed 9 months after transplantation by flow cytometry. (**B**) Percentage of engraftment and multilineage composition in spleen of the same MPS-I treated mice. If not indicated, P>0.05 by unpaired Wilcoxon test.*

nBMT induced tolerability to immune response elicited by ERT

As the impact of the immune response after ERT treatment is currently debated, we assessed the development of IgG antibodies against the recombinant IDUA in the sera of animals under evaluation. For this purpose, blood samples were collected every month throughout the course of the study. As expected, no antibodies were detected in untreated mice and in mice that received nBMT alone (data not shown). Among the group of MPS-I mice treated with ERT, the totality of animals showed a robust antibody response to rhIDUA. In the entire cohort, the antibody levels strongly increased in the early 2 months and remained steadily high (from 5.7 µg/ml to 9.3 µg/ml) throughout the study period. Of note, 3 of 7 animals (42.8%) developed antibodies anti-rhIDUA as early as 1 month after the first administrations (*Figure 4A*).

With respect to hi-nBMT+ERT group, antibodies anti-rhIDUA could be detected only in 2 of 7 mice, starting from 1 month after the first administrations of recombinant enzyme. Antibodies concentration in the serum of these mice was comparable to mice receiving ERT alone. One mouse developed a moderate titre that increased towards the end of treatment, resulting anyway lower than ERT group (3.2 µg/ml at the end of treatment). 3 of 7 of mice (42.8%) remained tolerant to rhIDUA for the entire experimental period, while another one became tolerant only after 3 months (*Figure 4B*).

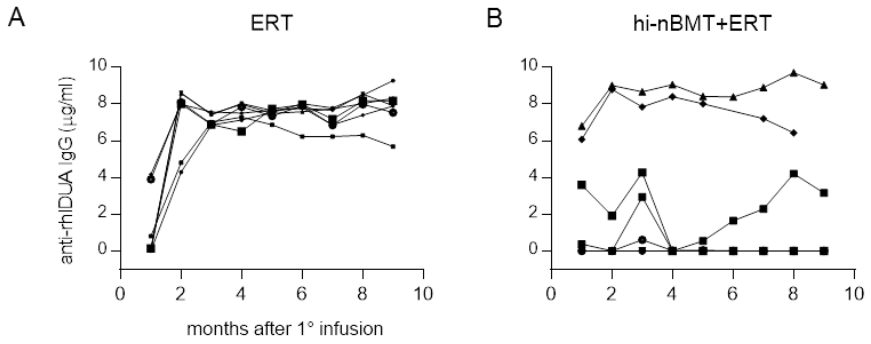

Figure 4. Anti-rhIDUA immune response*. (**A**) Anti-rhIDUA IgG concentration in the serum of MPS-I ERT mice collected every month until sacrifice. (**B**) Anti-rhIDUA IgG concentration in the serum of MPS-I hi-nBMT+ERT mice assessed every month until sacrifice. Each line represents IDUA antibody levels for an individual mouse.*

ERT, nBMT and their combination ameliorated the metabolic alterations in visceral organs of MPS-I mice

In order to investigate the effectiveness of the three approaches under evaluation, we measured IDUA activity and GAGs storage in visceral organs. IDUA activity was evaluated in the spleen, liver, kidney, lung, and heart of treated MPS-I mice and untreated controls at sacrifice. All organs homogenates from untreated MPS-I mice showed very low or absent IDUA activity, as reported in *Figure 5*. For mice that received nBMT alone, IDUA activity at 37 weeks was significantly increased in spleen (53.1 fold MPS-I), liver (7.5 fold the value in untreated MPS-I), and lung (6.8 fold MPS-I) (P=0.0019 for spleen, liver, and lung for hi-nBMT *vs* untreated MPS-I). IDUA activity in kidney and heart was slightly increased, respectively 7.95% and 4.28%, of the value in normal mice.

The IDUA activity of ERT treated mice was significantly enhanced in spleen (18 fold MPS-I, P=0.0012) and was 76.7% of that in WT mice in liver (P=0.2976 for ERT *vs* normal). Lung, kidney and heart were only partially corrected (respectively 2.46%, 10.2% and 2.47% of normal).

In mice receiving the combination of nBMT+ERT, IDUA levels were higher in lung (7.8 fold MPS-I) and kidney (2.1 fold MPS-I) and they reached values found in normal mice in spleen (99.05% of normal) and supranormal values in liver (87.8% over normal levels) (P=0.817 in spleen and P=0.203 in liver for hi-nBMT+ERT *vs* normal). Also for this treatment heart reached the 3.8% of the IDUA value in normal mice.

As a consequence of the absent IDUA activity, GAG levels in the analysed organs were significantly increased in untreated MPS-I mice respect to normal mice (P<0.001). Following the different treatments, the massive presence of GAGs was significantly reduced in all organs (*Figure 6A*). In particular, GAGs values became not statistically different from normal values in spleen, liver and lung with all treatments (P>0.05 for each organ in treated MPS-I *vs* normal). Of note, GAGs levels in kidney were normalized exclusively in hi-nBMT+ERT group (P=0.3537 for hi-nBMT+ERT *vs* normal), whereas in hi-nBMT and ERT they were reduced to values that remained respectively 1.74 and 2.7 fold of those in normal mice. In heart, GAGs levels remained modestly elevated in particular in the ERT group (1.92 fold the value in normal mice). Again, GAGs storage in heart

was significantly reduced in the hi-nBMT+ERT as compared to the hi-nBMT group (P=0.0452).
As expected, ΔDi-4S, ΔDiHS-NS, ΔDiHS-0S and mono-sulfated KS levels were significantly elevated in plasma of untreated MPS-I mice as compared to untreated WT mice (P<0.001) (*Figure 6B*). However, all three treatments under evaluation strongly reduced plasmatic GAGs levels, and in particular the nBMT+ERT treatment was the only condition able to normalize ΔDi-4S, ΔDiHS-NS and mono-sulfated KS.

Furthermore, to better investigate the degree of the metabolic correction, we analysed by histopathology the tissues of internal organs harvested at sacrifice, and in particular the cytoplasmic vacuoles, indicative of GAGs storage, were scored. As it is shown in the representative toluidine blue stained sections, untreated MPS-I mice displayed abundant storage in the spleen, liver and kidney, if compared with WT mice in which the storage was completely absent (*Figure 7A*). Following the different treatments, a complete clearance of the storage was achieved in the spleen. In hepatocytes and Kupffer cells in the liver and in glomeruli and tubules in the kidney as well, we observed a significant reduction as compared to untreated MPS-I mice, although in kidney, the combination therapy displayed a better decrease, in accordance with the biochemical assay previously shown (*Figure 7B*).

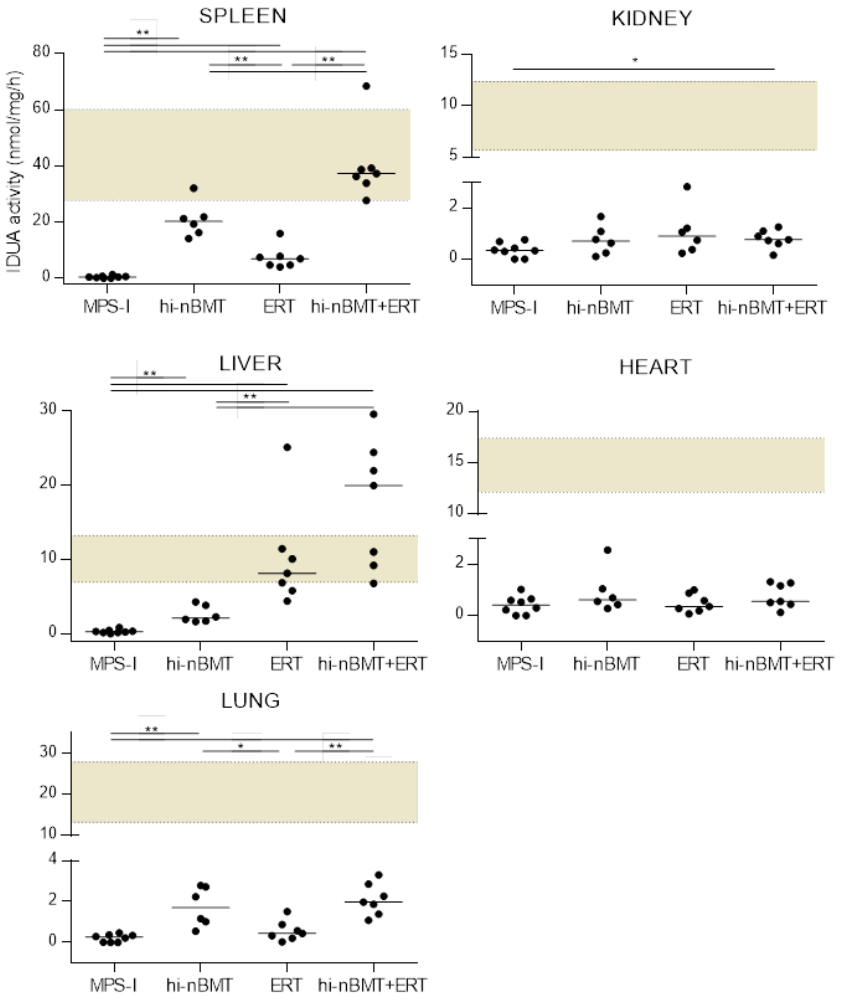

Figure 5. IDUA activity in treated mice. *IDUA activity was measured in spleen, liver, lung, kidney and heart of WT (n = 8), MPS-I (n = 8), hi-nBMT (n = 6), ERT (n = 7), hi-nBMT+ERT (n = 7) at sacrifice. Each point represents a single mouse and bar represents the median value. The brown area indicates the range (minimum and maximum) for WT mice. *P≤0.05, **P≤0.01 by unpaired Wilcoxon test.*

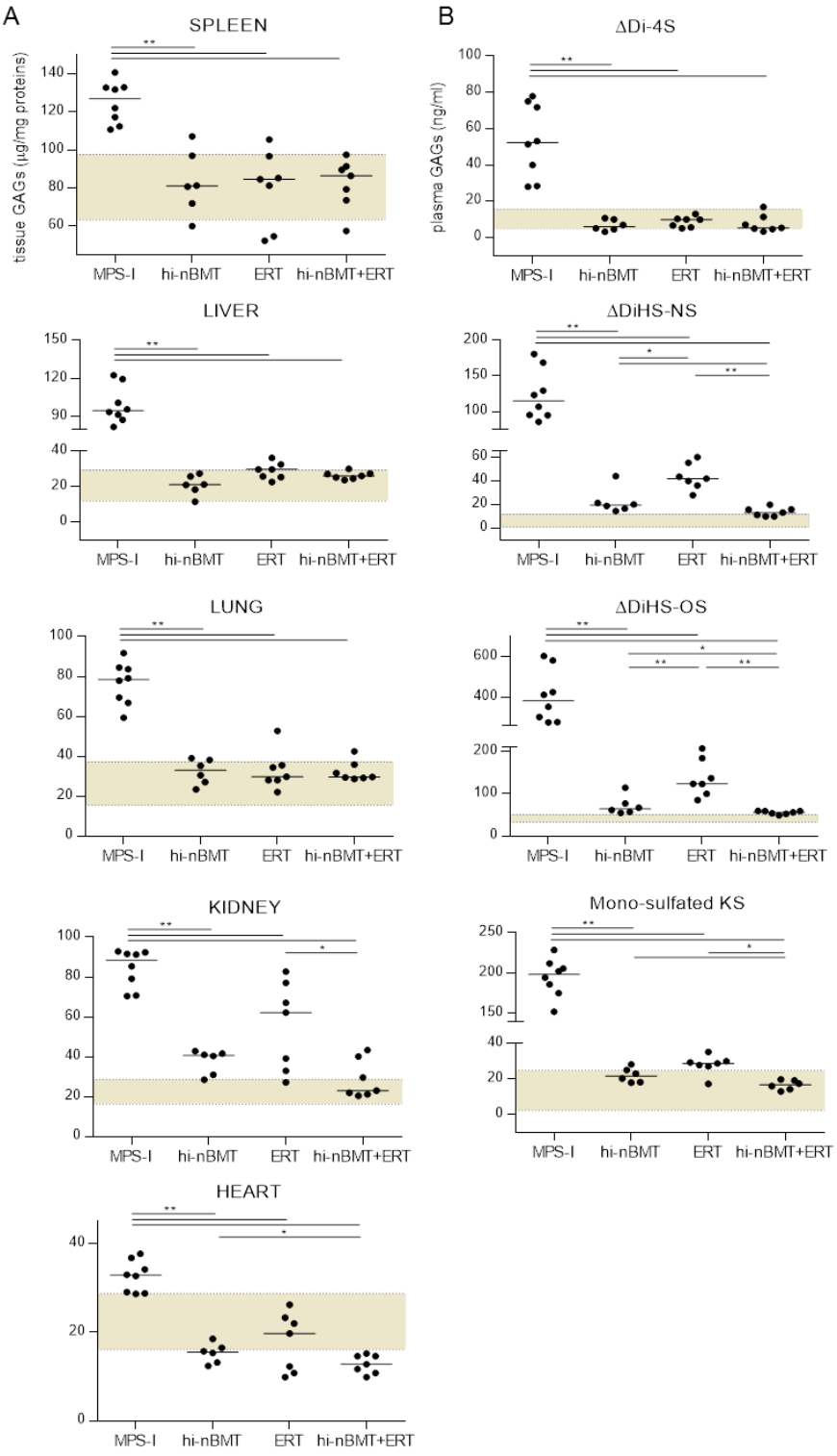
A
SPLEEN
tissue GAGs (µg/mg proteins)
MPS-I
hi-nBMT
ERT
hi-nBMT+ERT
LIVER
LUNG
KIDNEY
HEART
B
ΔDi-4S
plasma GAGs (ng/ml)
ΔDiHS-NS
ΔDiHS-OS
Mono-sulfated KS

***Figure 6. GAGs storage in treated mice**. (**A**) GAGs levels were quantified in spleen, liver, lung, kidney and heart of WT (n = 8), MPS-I (n = 8), hi-nBMT (n = 6), ERT (n = 7), hi-nBMT+ERT (n = 7) at 37 weeks of age. (**B**) Plasma levels of ΔDi-4S, ΔDiHS-NS, ΔDiHS-0S and mono-sulfated KS in the same mice at sacrifice. Each point represents a single mouse and bar represents the median value. The brown area indicates the range (minimum and maximum) for WT mice. *P≤0.05, **P≤0.01 by unpaired Wilcoxon test.*

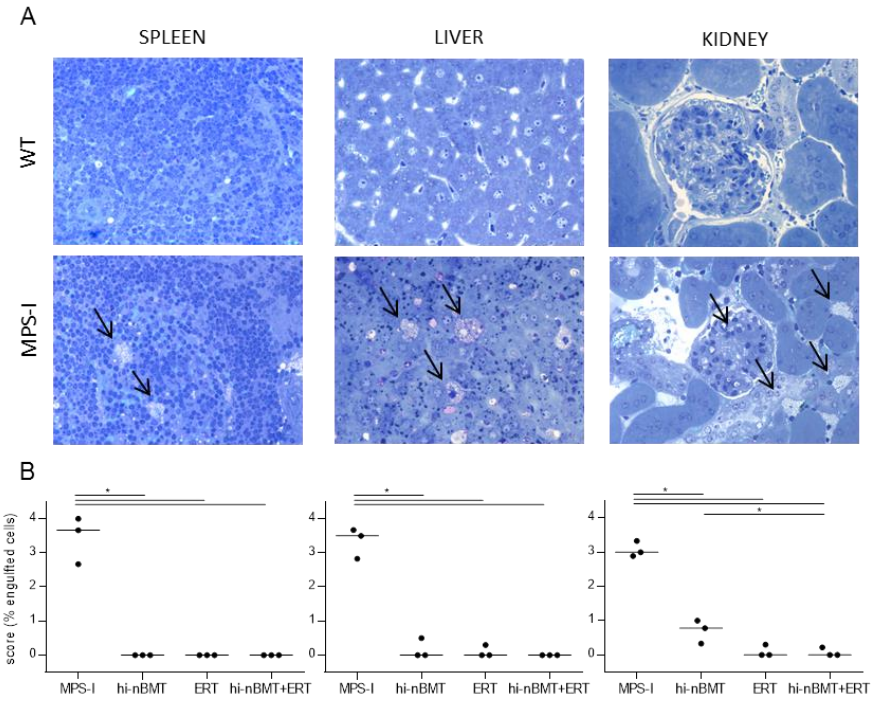

***Figure 7**. **Morphologic analysis of internal organs.** (**A**) Representative toluidine blue stained sections of spleen, liver and kidney, harvested from WT and MPS-I mice at sacrifice. Arrows indicate lysosomal storage in untreated MPS-I mice. No pathologic storage was observed in WT mice (magnification 40X). (**B**) Cell engulfment was scored in the spleen, liver and kidney of untreated and treated mice (each point represents a single mouse; 3 images per mouse were acquired) *P≤0.05 by unpaired Wilcoxon test.*

Treatments slightly improve brain alterations

To assess the efficacy of the investigated treatments in affecting MPS-I-associated lesions of the CNS, we examined the Purkinje cell layer of the cerebellum of treated and untreated mice. Density of the Purkinje cells was reduced to 88.3% of normal in untreated MPS-I mice (P=0.0209). Also ERT treated mice displayed a similar decrease of Purkinje cells, whereas hi-nBMT and hi-nBMT+ERT treated mice showed values more similar to WT mice (respectively, 95% and 97.7% of WT) (*Figure 8B*).

To better characterize the Purkinje cell layer, we performed a quantification in the histologic sections of cells presenting cytoplasmatic vacuoles. As expected, WT mice did not show any storage, whereas vacuoles were found in 33.9% of cells in untreated MPS-I mice (P=0.0139). All three treatments under evaluation were not able to efficiently reduce the percentage of vacuolated cells, as their values were close to untreated MPS-I mice (*Figure 8A, C*).

Moreover, IDUA activity in brain homogenates of MPS-I treated mice showed barely detectable levels, comparable to those found in untreated MPS-I. Indeed, a modest increase was observed after nBMT, ERT and nBMT+ERT treatment, between 3 and 6% of the IDUA levels in WT mice *(Figure 8D*).

Furthermore, we performed an immunohistochemistry staining to evaluate the level of neuroinflammation in MPS-I mice. Cerebellum sections were stained with anti-Iba-1 antibody (ionized calcium binding adaptor molecule 1) a specific marker for microglial cells[26]. Due to their change in morphology following activation, we were able to discriminate among Iba-1^{+} cells, between quiescent and activated

microglia cells, indicative of neuroinflammation. Quantitative analysis revealed a strong increase in activated microglia in MPS-I mice compared to WT mice (26.7 fold of the normal value; P=0.0209). nBMT, ERT and nBMT+ERT treatments determined a reduction of activated microglia (respectively 20.1, 18.2 and 18.5 fold of WT) although no statistical difference was observed, probably due to the small number of evaluated animals and the variation in individual mice (*Figure 8E, F).*

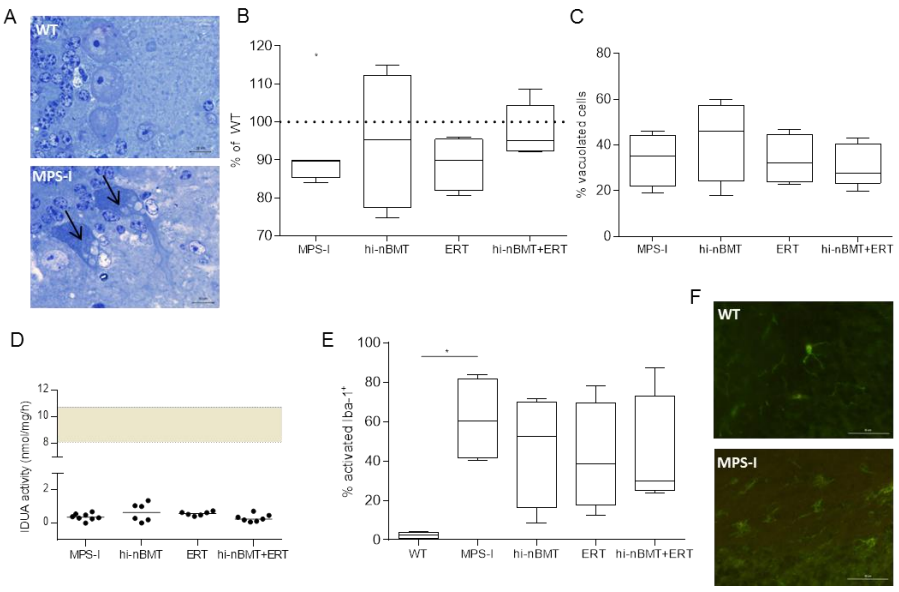

Figure 8. Brain disease markers*. (**A**) Representative images of the Purkinje cell layer of WT and MPS-I mice. Arrows showed cytoplasmatic vacuoles (magnification 100X). (**B**) Purkinje cell frequency (expressed as percentage of Purkinje cell density in WT mice) in cerebellum sections of MPS-I, hi-nBMT, ERT and hi-nBMT+ERT treated mice. (**C**) Quantification of vacuolated cells in the Purkinje cell layer of untreated and treated mice (≥20 images from 4 different animals per group were quantified). (**D**) Brain IDUA activity of WT, MPS, hi-nBMT, ERT and hi-nBMT+ERT mice. Each point represents a single mouse and bar represents the median value. The brown*

*area indicates the range (minimum and maximum) for WT mice. (**E**) Quantification of the activated cells on the total Iba-1$^+$ in cerebellum slices of WT, MPS-I, hi-BMT, ERT and hi-nBMT+ERT mice (10 images from 4 different mouse per group were quantified). (**F**) Representative images of Iba-1$^+$ cells (magnification 40X, bar: 50µm) *P≤0.05, by unpaired Wilcoxon test.*

Transplantation and combination therapy provide the same benefit in correcting bone thickening

As *dysostosis multiplex* is one of the most common treatment-resistant clinical manifestations of MPS-I patients, we focused our attention on the skeletal phenotype of mice under evaluation. At the time of sacrifice, radiographs of MPS-I mice showed marked skeletal dysplasia, and in particular a thickening of long bones compared to WT mice (femur: P=0.0012; tibia: P=0.0279; humerus: P=0.0012; radius/ulna: P=0.0018). Bone width was not significantly affected by ERT, as the analysed parameters were not different from untreated MPS-I mice, except for the femur width, in which we observed only a moderate improvement (femur: P=0.0372; tibia: P=0.7285; humerus: P=0.0641; radius/ulna: P=0.0823). As expected, nBMT treatment strongly reduced long bones thickness (femur: P=0.0019; tibia: P=0.0019; humerus: P=0.0019; radius/ulna: P=0.0019, for MPS-I *vs* hi-nBMT), and its effect was not different from the combination therapy approach (femur: P=0.3914; tibia: P=0.5677; humerus: P=0.5677; radius/ulna: P=0.8864 for hi-nBMT *vs* hi-nBMT+ERT) (*Figure 9*). Moreover, we adopted a regression model capable of elucidating a potential synergistic effect of combination therapy on MPS-I. By this analysis, we obtained the confirmation of no

differential effect of the nBMT+ERT treatment on bone thickness compared to nBMT alone (*Supplementary Figure 1*).

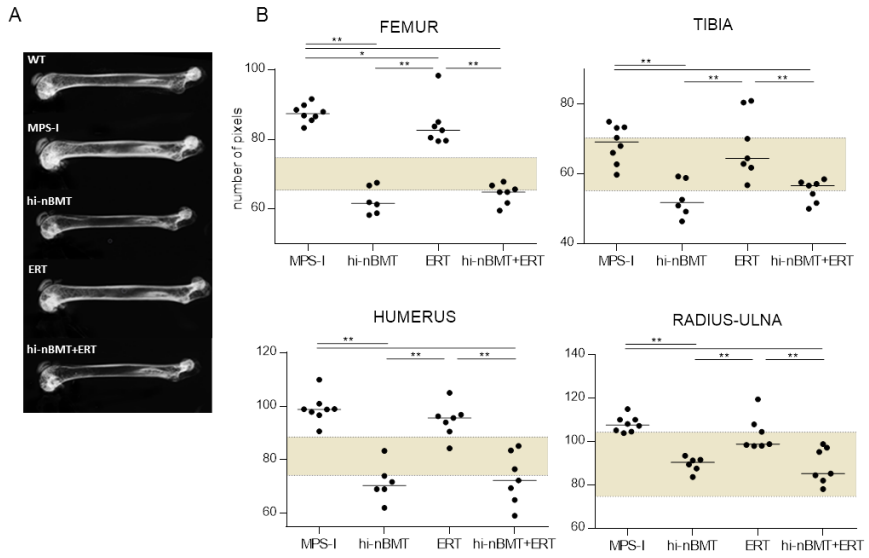

Figure 9. Skeletal outcome in treated mice. *(**A**) Representative radiographs of the femur of WT, MPS-I, ERT, hi-nBMT and hi-nBMT+ERT mice at time of sacrifice (37 weeks). (**B**) Measurements of the femur, tibia, humerus and radio-ulna width. Each point represents a single mouse and bar represents the median value. The brown area indicates the range (minimum and maximum) for WT mice. *P≤0.05, **P≤0.01 by unpaired Wilcoxon test.*

DISCUSSION

Therapeutic efficacy of the available treatments for MPS-I, HSCT and ERT, is currently well-founded[14-27]. General clinical conditions and quality of life of MPS-I patients are strongly improved after treatment, with restoration of IDUA activity and reduction of GAGs accumulation[28-4]. Nonetheless, the outcome on skeletal and brain disease could be further improved[29].

We previously demonstrated, in a mouse model of MPS-I, that the time at which treatment is performed is critical to achieve a better outcome and to prevent some pathological consequences, especially for musculoskeletal and bone pathology[7-12-13]. Indeed, when performed at neonatal age, the bone marrow transplantation corrects musculoskeletal disease in mice.

Several studies in patients with Hurler syndrome could further confim that an early treatment is associated not only with long term benefits in visceral organs and joints, but also with improved cognitive, language and motor skills[15-30]. Early diagnosis is therefore crucial for the optimal outcome of MPS-I patients.

In the last years, ERT administration has been proposed as an adjunctive treatment in combination with HSCT as it seems to have a better impact on disease status[23-31-1]. Nevertheless, there is not a general consensus as some reports recommended to treat with combination therapy only patients in a poor clinical condition[32], whereas other suggested to treat all severe MPS-I patients to decrease morbidity and mortality rate[21].

In this study, we applied the clinically available treatments, HSCT and ERT, individually or in combination during the neonatal period, identified as the best therapeutic window, to evaluate the outcome in a mouse model of MPS-I. We demonstrated that all the three treatments under evaluation (nBMT, ERT and nBMT+ERT) were able to significantly decrease GAGs storage in visceral organs, but they had a differential effect with respect to bone and to the other difficult-to-treat organs such as hearth and kidney, and a slight effect on brain abnormalities.

Among transplanted mice, no differences in the ability of donor cells to engraft in the adopted MPS-I disease model were observed, differently from the data published by Watson *et al.*, in which a donor chimerism defect was found in MPS-I mice. This may be due to the fact that they performed transplantation under limiting-dilution conditions and with a reduced-intensity conditioning[33]. Instead, after full intensity myeloablation by busulfan, we observed that nBMT resulted in a comparable chimerism between WT and MPS-I mice, in line with our previous results[12-13], suggesting that engraftment is not influenced by the genotype.

We next demonstrated that ERT administration did not impact on donor cell engraftment, as no statistical differences were observed between nBMT and nBMT+ERT groups of mice, in agreement with Tolar *et al.*[21]. Furthermore, similar multilineage donor-derived reconstitution was found in hematopoietic organs in the two groups of transplanted mice at the sacrifice.

To evaluate the outcome of MPS-I animals receiving nBMT and nBMT+ERT, we decided to include in our analyses exclusively mice

who reached ≥50% donor chimerism in PB at 2 months of age, considered as successfully engrafted mice. Indeed, in our previous study, we observed that the parameters used to evaluate the outcome of transplanted MPS-I mice (IDUA activity and GAGs levels) were not sufficiently restored in low engrafted mice (<50% PB engraftment)[13].

One of the main limitations of a therapy based on the infusion of recombinant enzyme seems to be the development of an immune response to the delivered enzyme. Clinical trials showed IgG antibody development to laronidase starting from the first months of treatment in the majority of MPS-I patients[27], but the impact of this allo-immune response on treatment outcome remains unknown. In our study, all mice treated with ERT only developed a robust antibody response starting from the first months after treatment. Antibody levels remained high and stable during the entire experimental period, although it was reported that large animal model treated at birth resulted tolerant to ERT, with no antibodies development[34]. On the other hand, only 2 of 7 mice receiving the combination therapy (nBMT+ERT) developed an immune response similar to the one observed in the ERT group. The large amount of non-immunized mice among the nBMT+ERT group could be due to the tolerogenic effect of the immunosuppressive regimen used for the conditioning or to the transplantation procedure itself. Indeed, BMT can replace the recipient immune system with that of the donor, which is naturally tolerized to IDUA, as donor cells possess normal level of the enzyme. Allogeneic HSCT seemed to have an immune tolerance induction effect also in MPS-I patients[22] and furthermore in one case report the

immunomodulatory therapy in a MPS-II patients led to a significant reduction of anti-idursulfase IgG antibody titers[35]. Nevertheless, we did not find a strong correlation between antibody concentration and GAGs level reduction in organs, although Dickson *et al.* demonstrated that the presence of antibodies anti-IDUA reduced the efficacy of the therapeutic approach in a canine MPS-I model[36]. However, we noticed that the animals with high antibody titre in the hi-nBMT+ERT group had the lowest IDUA activity in liver and heart, within their group of treatment. This phenomenon could be explained by the fact that anti-IDUA antibodies sterically impair mannose-6-phosphate binding to its receptor, resulting in the inability of the enzyme to be uptaken by the cells, particularly in organs with low levels of macrophages, such as heart[37].

With respect to biochemical parameters, although in the majority of the analyzed organs we observed only a partial increase of IDUA activity following the different treatments, it anyway resulted in a significant reduction of GAGs storage, which is an indicator of disease progression, as compared to untreated MPS-I mice. Of note, we observed in ERT and hi-nBMT+ERT treated mice a strong enhancement of IDUA activity in liver, that became comparable or superior to normal levels. The high uptake of the recombinant enzyme in the liver after ERT administration has already been noticed in tissue distribution studies in other animal models[38-39]. A complete normalization of GAGs levels was observed in liver, spleen and lung with all the three treatments proposed, with no difference among treated groups. Regarding kidney and heart, the ERT treated group had the less efficient recovery in terms of GAGs reduction in both

organs, whereas the combination treatment seemed to have an additive effect; indeed we observed a normalization in kidney, demonstrated by both the biochemical assay and the histological analysis, and a better reduction in heart, one of the most refractory organ to correct. Similarly, Akiyama *et al.* observed an additive effect in reducing GAGs accumulation in visceral organs in the MPS-II murine model, suggesting the application of the ERT treatment to already transplanted patients[40]. ERT administration beyond the transplantation period is currently under investigation, even though, theoretically, in a fully engrafted patient donor cells should provide the needed amount of the lacking enzyme[29]. However, in one case report, despite the high level of donor chimerism and IDUA activity, weekly laronidase infusions improved cardiopulmonary HSCT-related complications in a MPS-I patient[20].

In addition, in our study also plasma GAGs levels were strongly reduced after all three treatment approaches, as compared to MPS-I untreated mice. Particularly, the nBMT+ERT treatment was able to normalize HS-NS, Di-4S and mono-sulfated KS, the latter considered a biomarker of skeletal dysplasia[41-42], suggesting an improved outcome on the severe bone lesions typical of this disease.

Bone and brain are known to be difficult-to-treat organs, impacting patient's quality of life even after a successful treatment. Regarding the CNS, we observed a significant reduction of the number of Purkinje cells in the cerebellum of untreated MPS-I mice, in agreement with Visigalli *et al.*[43]. nBMT and nBMT+ERT seemed to restore Purkinje cells density, increasing their number to values that are only slightly reduced compared to WT.

In order to deeply investigate cerebellum alterations, we quantified vacuolated cells within the Purkinje cell layer. We demonstrated a significant vacuolization, indicative of GAGs accumulation, in the Purkinje cells of the cerebellum of untreated MPS-I mice, as reported also for MPS-I patients[44]. Nevertheless, treated mice displayed a similar storage, without an evident reduction of vacuolated cells. This result was in agreement with the measurement of IDUA activity in the brain of treated mice that was only barely detectable. As a matter of fact, Visigalli *et al.* proposed a threshold value for IDUA activity for CNS correction, that corresponded to 20nmol/mg/h, 30 fold the values reached in our study[43]. Regarding ERT administration to treat CNS lesions, it is considered quite challenging, due to the impermeable nature of the BBB. Nevertheless some studies demonstrated an amelioration at neurological level increasing the dose of ERT[45]. Baldo *et al.* hypothesized the mechanism at the basis of this process, suggesting that lysosomal enzymes, when found in high concentration in serum, may cross the BBB through pinocytosis[46]. The efficacy of transplantation in arresting CNS deterioration seems to be related to infiltration of myeloid cells secreting the enzyme. Nevertheless, the migration of blood cells into brain is a slow process and it takes several months to replace sufficient microglia, and there might be a delay in CNS amelioration[47]. A previous neonatal non-myeloablative HSCT approach to MPS-VII mice failed to eliminate storage in neurons, resulting in an enzyme level that was only 0.3% of normal in brain at 1 year after transplant[48]. Although it has been demonstrated that irradiation and chemotherapy-based conditioning regimen may alter the permeability of the BBB, enhancing donor microglia

engraftment[49-50-51], we were not able to observe an important recovery of IDUA activity attributable to the presence of donor cells in CNS, even after full intensity conditioning with busulfan.

As neuroinflammation is one of the main processes involved in brain pathology in MPS-I[52], we investigated the status of microglial cells, one of the well-known key player. Under quiescent conditions, microglia present a ramified morphology with a small cell body. Brain injuries or inflammatory stimuli trigger microglia activation, a process characterized by a rapid change in morphology, in particular increased body cell size and thickening of processes[53]. Thanks to this phenomenon we were able to differentiate between resting and activated microglia, using the specific marker Iba-1[26]. Untreated MPS-I mice exhibited an increased activated microglia as compared to WT mice, confirming an on-going neuroinflammatory process in the disease[54]. This up-regulation is partially relieved in MPS-I mice after the three treatments under evaluation, suggesting a modulation of the inflammation even in the case of MPS-I mice treated with ERT alone. Similarly, previous studies demonstrated improvements of brain inflammatory status after early ERT treatment in the MPS-I mouse model, with reduction of the protein GFAP, indicative of neuroinflammation, and a consequent amelioration in behavioural tests[11]. Furthermore, even if ERT treatment was started in adult life, Pasqualim *et al*. showed a reduced inflammation process in brain cortex, in the absence of GAGs reduction[55].

We then focused on skeletal deformities, and in particular we evaluated the effect of all the treatments under evaluation on long

bones thickness, which is clearly manifested in MPS-I mice at 37 weeks of age.

Interestingly, radiographs analysis displayed no improvement of bone thickness after ERT treatment, showing no difference in comparison with untreated MPS-I animals, with the exception of femur width, where a partial correction could be detected. The reduced ability of ERT to correct skeletal lesions could be due to its poor vascular supply[56], to the short half-life of lysosomal enzymes, and their rapid binding to M6PR in visceral organs[57]. However, familial case reports of affected siblings demonstrated that early initiation of ERT determined a better skeletal outcome in the younger sibling. Nevertheless, it is important to mention that these clinical improvements were demonstrated in patients with an attenuated MPS-I form[16-58]. With respect to experimental data, a better correction of skeletal abnormalities was demonstrated with higher dose of the infused enzyme in large animal models[34], or combining ERT with bone-targeting strategy in murine Morquio A syndrome[59] or with chemically modified enzymes which allowed prolonged half-life in a MPS-VII murine model[60]. Our findings, in agreement with Baldo et. al in which no improvement in joint abnormalities were found after neonatal ERT[11], suggested that conventional ERT, even started at birth, was not able to correct and/or prevent bone pathology. On the other hand, both groups of mice receiving transplantation or transplantation and ERT showed reduced thickness of long bones compared to untreated MPS-I mice with significant improvements of this parameter, approaching complete normalization.

We have previously demonstrated that neonatal transplantation was able to prevent skeletal dysplasia, using both BM and umbilical cord blood (UCB) stem cell sources[12-13].

The effectiveness of transplantation is strongly demonstrated in several case reports in which the typical skeletal deformities of MPS-I patients were significantly reduced even in the severe form of this disease[61-62]. Indeed, transplantation allows a continuous expression of the enzyme and importantly, donor monocytes may cross the capillary wall, differentiate into macrophages, and secrete the enzyme in peripheral tissues[6]. Moreover, bone marrow can contain also cells of mesenchymal lineage, which may migrate within the bone and differentiate in osteoblastic cells, contributing to bone repair.

Of note, hi-nBMT and hi-nBMT+ERT groups showed comparable efficacy regarding their capacity to reduce the width of the long bones, demonstrating a similar effect in modifying this parameter. On-going histopathologic evaluation will better characterize the skeletal phenotype, showing if number and vacuolization of osteocytes in the cortical bone are affected after treatments.

Besides radiographs analysis, we are currently performing micro-CT scans on the femurs of treated mice, to evaluate the cortical and trabecular structure of bones. Trabecular number and separation, cortical thickness and bone volume are some of the parameters that we are taking into account. We will assess if the treatments under evaluation are able to reduce trabecular density, known to be higher in affected mice, and the cortical bone, known to be thick and irregular.

Furthermore, a paper from Schinke's group recently demonstrated an alteration of bone remodelling status both in MPS-I mice and patients

after transplantation[23]. In particular, as they observed an increased and unexpected osteoclastogenesis after treatment, which can be reverted by the combination of BMT and ERT, we decided to investigate this particular aspect in treated mice, assessing the number of pre-osteoclasts and osteoclasts on sections of long bones and bone volume.

At present, the incomplete improvement of the skeletal phenotype obtained in patients may be explained by the fact that bone abnormalities could be irreversible at the time of transplantation. Indeed, as affected children appear normal at birth[63], the first months of life could represent the best time window to prevent bone disease. In 2016 the US Secretary of Health and Human Services added MPS-I to the recommended uniform screening panel (RUSP) for newborn screening[64], and dried blood spot analyses, measuring HS and DS by liquid chromatography tandem-mass spectrometry (LC-MS/MS), have been under development for this purpose[42]. In fact, an early diagnosis, which allows an early treatment with the restoration of the missing or defective enzyme may have a stronger impact on patients outcome.

In conclusion, we have assessed the efficacy of standard treatments, ERT and BMT, alone or in combination, in the neonatal period, which can be considered the best therapeutic window. We demonstrated an increased IDUA activity in visceral organs after treatments, with a consequent reduction of GAGs storage. In particular the combination therapy had a better efficacy in reducing GAGs accumulation in difficult-to-treat organs, such as kidney and heart. Furthermore, although the impact of the immune response on outcome remains unknown, the combination therapy determined immune tolerability,

avoiding anti-IDUA antibody development. With respect to bone phenotype, we confirmed the ability of neonatal transplantation in reducing bone thickness, also by the addition of ERT treatment. On the other hand, ERT administration alone, even if performed at birth, was not able to improve bone abnormalities. Nevertheless, other bone parameters must be evaluated in order to better understand treatments effects. Furthermore, a limited impact was noticed at brain level with all three treatments under investigation. We were able to observe a moderate improvement of inflammation without a reduction of vacuolated cells in the cerebellum. Enzyme supply by healthy donor transplantation and/or ERT do not seem to be sufficient for complete disease correction, even if administered at birth. In this sense, gene therapy (GT) could represent a fascinating therapeutic option for MPS-I and other monogenic metabolic disorders at birth. Transduction of autologous cells may provide supraphysiological enzyme activity levels, even if full donor chimerism has not achieved[65-66]. In these last years, the field of GT has expanded, and in 2016 the first ex vivo GT was approved for Adenosine deaminase-severe combined immunodeficiency (ADA-SCID)[67]. Indeed, the possibility of a neonatal GT approach to correct storage diseases is not so far from the clinical reality.

MATERIALS AND METHDOS

Mouse model

The MPS-I mouse model (Idua$^{-/-}$ mice, C57BL/6-CD45.2 background) was purchased from The Jackson Laboratory. A breeding colony was established from heterozygous mating pairs (Charles River) and genotyping was performed on tail clips or ear snips DNA, as previously described[24]. Pregnant dams obtained from the colony were housed in the animal facility of the University of Milano-Bicocca. 6- to 12-week old C57BL/6-CD45.1 donor mice were purchased from Charles River. Procedures involving animal handling and care conformed to institutional guidelines, in compliance with national laws and policies.

Experimental groups and treatment procedures

Treatment schedule was shown in *Figure 1*. There are three treatment groups: nBMT, ERT and nBMT + ERT. Control groups are untreated MPS-I and untreated or treated WT mice. Groups were sex balanced.

nBMT. 1-to 2-day old pups were conditioned with a single intraperitoneal injection of busulfan (20mg/kg; Busilvex, Pierre Fabre). 24 hours after conditioning, newborn mice were transplanted by intravenous (via temporal vein) injection of $2x10^6$ cells collected by flushing from the long bones of CD45.1 WT donor mice, as described in our previuos work[12].

ERT. 2-day old pups were treated with 0,58 mg/kg human alpha-L-iduronidase (Laronidase® Genzyme) diluted in PBS, once a week until sacrifice (total 36 times). The first injection was performed via

temporal vein, the second to fourth injections were intraperitoneal, and the following ones via tail vein. Mice were sacrified one week after last ERT administration.

nBMT+ERT. 1-to 2-day old pups were conditioned with busulfan (20mg/kg IP), and the next day received BM transplantation ($2x10^6$ cells) and alpha-L-iduronidase (0,58mg/kg), administered with a single injection via temporal vein. The subsequent ERT injections followed the scheme adopted for the second group.

Engraftment evaluation

At different time points (1, 2, 4, and 6 months after transplantion and at sacrifice) peripheral blood (PB) of transplanted mice was collected by tail bleeding. After lysis with ACK buffer, samples were stained with anti-mouse CD45.1 PE (clone A20) and anti-mouse CD45.2 APC (clone 104) (eBioscience). The levels of donor cell engraftment have been evaluated as: [donor $CD45.1^+$/ (donor $CD45.1^+$ + recipient $CD45.2^+$) x 100].

Multilineage engraftment was analysed at sacrifice on BM cells, collected by flushing of tibiae, and on splenocytes, collected by smashing the spleen on a 70µm cell strainer. The following antibodies (eBioscience) were used: anti-mouse CD45.1 APC (clone A20), anti-mouse CD45.2 PE (clone 104), anti-mouse CD3e PE (clone 145-2C11), anti-mouse CD45R (B220) PE (clone RA3-6B2), anti-mouse CD11b (Mac-1) PE (cloneM1/70), anti-mouse Ly-6G (Gr-1) FITC (clone RB6-8C5), anti-mouse CD45.1 PerCP-Cy5.5 (clone A20), anti-mouse Ly-6A/E (Sca-1) APC (clone D7), anti-mouse CD117 (c-Kit) PE (clone 2B8), and anti-mouse Haematopoietic Lineage eFluor 450

cocktail. FACSCanto™ II flow cytometer and FACS Diva software (BD Biosciences) were employed for acquisition and analyses.

Detection of anti-rhIDUA antibodies

Peripheral blood was harvested every month, just prior to ERT, to assess the presence of antibodies anti-rhIDUA in serum. After coagulation of blood at RT, samples were centrifuged (10 min 3000 rpm) and serum was collected and frozen until analysis. Briefely, 96-well ELISA plates were coated with 2 ug/ml of laronidase in 1M carbonate buffer overnight and blocked with 1% BSA+0.05% Tween-20. Diluted serum (1:50) was added in duplicates and incubated for 2 hours. The secondary antibody (Anti-mouse IgG 1:10000, Sigma-Aldrich) was incubated for 2 hours and revealed with o-phenylenediamine dihydrochloride (OPD) for 7 minutes. The reaction was stopped with H_2SO_4 1M and absorbance was read at 492 nm using a microplate reader Multiskan GO (Thermo Fisher).

IDUA activity assay

At sacrifice, organs (spleen, liver, heart, lungs, kidneys and brain) were collected, frozen on dry ice and stored at -80°C. Lysis was performed in 500 µL of 0.9% NaCl containing 0.2% Triton X-100 (Sigma-Aldrich) and a protease inhibitor cocktail (P8340, Sigma-Aldrich) for 1 hour on ice. Protein concentration in clarified supernatants of organ homogenates was determined by Pierce BCA assay (Thermo Scientific). IDUA activity was then measured using the fluorogenic substrate 4-methylumbelliferyl-alpha-L-iduronide (Glycosynth). 5 µg of protein were added to a solution of 0.1 M

sodium formate buffer, pH 3.2, containing 8 mM D-Saccharic acid 1,4-lactone and 0.4 mM 4-methylumbelliferyl-alpha-L-iduronide. After incubation (1 hour at 37°C), the reaction was stopped by adding 1 mL of 0.5 M carbonate buffer, pH 10.7. Fluorescence was read at 365 nm excitation and 488 nm emission wavelengths using a Tecan GENios microplate reader fluorometer (Tecan).

Glycosaminoglycans quantification in tissues

After overnight digestion of organs at 65°C with papain (Sigma-Aldrich), GAGs levels were measured in clarified supernatants using the Blyscan Sulfated Glycosaminoglycan colorimetric assay (Biocolor) according to the manufacturer's instructions. The absorbance at 620 nm was read using a Tecan GENios microplate reader fluorometer (Tecan), and GAG levels were expressed as µg GAGs/mg protein.

Glycosaminoglycans quantification in plasma

Peripheral blood was collected in EDTA from the tail vein before sacrifice, and plasma was obtained after centrifugation at 587 g for 10 min. Samples were stored at -80°C. Ten µl of plasma sample and 90 µl of 50 mM Tris–hydrochloric acid buffer (pH 7.0) were placed in wells of AcroPrep™ Advance 96-Well Filter Plates (OMEGA 10K, PALL Co). The filter plates were placed on the receiver and centrifuged at 2000 g for 15 min to remove free disaccharides. The membrane plates were transferred to a fresh receiver plate. Ten µl of IS solution (5 µg/ml), 20 µL of 50 mM Tris-HCl buffer, and 10 µL of chondroitinase B, heparitinase, and keratanase II (each 2 mU/10 µL of 50 mM Tris-

HCl buffer) were added onto each filter. After incubation (37°C for 5 hours) and centrifugation at 2000 g for 15 min, the receiver plate containing disaccharides was stored at -20°C until injection to liquid chromatography tandem mass spectrometry (LC-MS/MS).

The chromatographic system consisted of 1260 Infinity (Agilent Technologies) and Hypercarb column (2.0 mm i.d. 50 mm, 5 µm, Thermo Electron). The mobile phase was a gradient elution from 0.025% ammonia to 90% acetonitrile in 0.025% ammonia. The 6460 Triple Quad mass spectrometer (Agilent Technologies) was operated in the negative ion detection mode with thermal gradient focusing electrospray ionization (Agilent Technologies). A m/z 354.29 precursor ion and m/z 193.1 product ion was used to detect the IS (chondrosine). Peak areas for all components were integrated automatically using QQQ Quantitative Analysis software (Agilent Technologies). The concentration of each disaccharide was calculated using QQQ Quantitative Analysis software.

Histopathology

For the evaluation of organs (liver, spleen, kidney and cerebellum) morphology, samples were fixed with a solution of paraformaldehyde 4%+glutaraldehyde 2% in 0.12 M phosphate buffer and postfixed with 1% osmium tetroxide. After alcohol dehydration, samples were embedded in Epon (Sigma) and placed overnight in a 60°C oven. Transverse sections of 1 micron thick were cut by Ultramicrotome Leica, stained with toluidine blue and examined on light microscopy (Olimpus BX51) for morphological analysis. Images were acquired at 40X. An arbitrary score (from 0 to 4) was given by the pathologist on

the basis of the percentage of vacuoles observed in each field for liver, spleen and kidney. 3 images from 3 different animals per group were acquired.

For Purkinje cell quantification, at least 20 images from 4 different animals per group were acquired. Purkinje cell frequency was calculated by number of total cells/length of Purkinje cells layer, calculated by ImageJ software.

Immunofluorescence staining

Cerebellum samples were embedded in OCT (Miles) and snap frozen in liquid nitrogen for cryosections. Indirect immunofluorescence was performed on transverse criosections (10 um thick), fixed in cold acetone for 2 minutes and rinsed twice in PBS. Before staining with rabbit antibody anti Iba-1 (Wako 1:200) for 1 hour at room temperature, the slides were incubated with 2% bovine serum albumin (BSA) for 20 minutes. Sections were treated with FITC-conjugates secondary antibody (Southern Biotechnology Associates, Inc) diluited 1:100 in PBS and examined with fluorescence microscopy at 20X (Olimpus BX51). 10 images from 4 different animals per group were acquired.

Radiograph analysis

After fixation in 4% formaldehyde, long bones radiographs were obtained by Faxitron MX-20 Specimen Radiography System (Faxitron X-ray Corp.) at an energy of 30 kV for 90 seconds with Eastman X-OMAT TL film (Eastman Kodak Co.) and processed by an automated

X-ray film developer (Model M35A, Eastman Kodak Co.). Bone thickness was measured at mid-diaphysis using ImageJ software.

Statistical analysis

Statistical analyses were performed using STATA software. Continuous variables were contrasted between groups by the unpaired Wilcoxon test for equality of the medians. All tests were at 5% significance level and on a 2-sided alternative, except data on organs histopathology (spleen, liver and kidney) where a 1-sided alternative was considered. An ordinary regression model with binary regression was applied to assess the impact of combined treatment on bone thickness data.

SUPPLEMENTARY MATERIALS

Supplementary *Figure 1.*

Table S1. Effect of combined treatment on bone measurements.

	Variables		
	β1 coeff (p value)	β2 coeff (p value)	γ coeff (p value)
Femur width	-3.33 (0.143)	-25.09 (<0.0001)	5.33 (0.111)
Humerus width	-4.43 (0.244)	-27.59 (<0.0001)	5.92 (0.287)
Tibia width	-0.36 (0.911)	-15.70 (<0.0001)	2.60 (0.589)
Radio/Ulna width	-4.45 (0.182)	-18.51 (<0.0001)	3.62 (0.454)

Anova obtained through a regression model on categorical variables. β1 is the effect on the parameter considered due to ERT on MPS-I; β2 is the nBMT effect on MPS-I; γ is the differential effect of ERT+nBMT on MPS I.

ACKNOWLEDGMENTS

We thank Dr. Daniela Tomasoni for her technical support for ELISA assay.

AUTHOR CONTRIBUTIONS

L.S. performed research, analyzed the data and wrote the manuscript; G.D.P., G.D., A.C. and K.S. performed research and analyzed the data; L.A. performed statistical analysis; A.P, S.G, A.A and A.Q and S.T. analyzed the data; A.B. edited the manuscript; M.S. designed research, interpreted the data, and edited the manuscript.

REFERENCES

1. de Ru, M. H. De *et al.* Capturing phenotypic heterogeneity in MPS I: results of an international consensus procedure. *Orphanet J. Rare Dis.* 7: 22 (2012).
2. Aldenhoven, M., Sakkers, R. J. B., Boelens, J., Koning, T. J. De & Wulffraat, N. M. Musculoskeletal manifestations of lysosomal storage disorders. *Ann Rheum Dis.* 68:1659–1665 (2009).
3. Kakkis, E. D. *et al.* Enzyme-replacement therapy in Mucopolysaccharidosis I. *N Engl J Med*. 344:182–188 (2001).
4. Muenzer, J. Early initiation of enzyme replacement therapy for the mucopolysaccharidoses. *Mol. Genet. Metab.* 111, 63–72 (2014).
5. Pastores, G. M. Laronidase (Aldurazyme®): enzyme replacement therapy for mucopolysaccharidosis type I. *Expert Opin Biol Ther*. 8:1003–1010 (2008).
6. Aldenhoven, M., Boelens, J. & Koning, T. J. De. The Clinical Outcome of Hurler Syndrome after Stem Cell Transplantation. *Biology of Blood and Marrow Transplantation*. 14:485–498 (2008).
7. Tomatsu, S. *et al.* Neonatal cellular and gene therapies for mucopolysaccharidoses: the earlier the better? *J Inherit Metab Dis*. 39:189–202 (2016).
8. Schmidt, M. *et al.* Musculoskeletal manifestations in mucopolysaccharidosis type I (Hurler syndrome) following hematopoietic stem cell transplantation. *Orphanet J. Rare Dis.* 11:93 (2016).
9. Poe, M. D., Chagnon, S. L. & Escolar, M. L. Early Treatment is Associated with Improved Cognition in Hurler Syndrome. *Ann Neurol*. 76:747–753 (2014).
10. Tomatsu, S. *et al.* Enzyme replacement therapy in newborn mucopolysaccharidosis IVA mice: early treatment rescus bone lesions? *Mol Genet Metab.* 114:195–202 (2016).
11. Baldo, G. *et al.* Enzyme replacement therapy started at birth improves outcome in dif fi cult-to-treat organs in mucopolysaccharidosis I mice. *Molecular Genetics and Metabolism*. 109:33–40 (2013).
12. Pievani, A. *et al.* Neonatal bone marrow transplantation prevents bone pathology in a mouse model of mucopolysaccharidosis type I. *Blood.* 125:1662–1672 (2015).
13. Azario, I. *et al.* Neonatal umbilical cord blood transplantation halts skeletal disease progression in the murine model of MPS-I. *Scientific Reports.* 7:9473 (2017).
14. Aldenhoven, M. *et al.* Hematopoietic Cell Transplantation for Mucopolysaccharidosis Patients Is Safe and Effective : Results after Implementation of International Guidelines. *Biol. Blood Marrow Transplant.* 21, 1106–1109 (2015).
15. Boelens, J. J. *et al.* Outcomes of transplantation using various hematopoietic

cell sources in children with Hurler syndrome after myeloablative conditioning. *Blood*. 121:3981–3987 (2013).

16. Gabrielli, O. *et al.* 12 year follow up of enzyme-replacement therapy in two siblings with attenuated mucopolysaccharidosis I : the important role of early treatment. *BMC Med. Genet.* 17:19 (2016).
17. Grigull L. *et al.* Variable disease progression after successful stem cell transplantation: Prospective follow- up investigations in eight patients with Hurler syndrome. *Pediatr Transplantation*. 15:861–869 (2011).
18. Bijarnia, S. *et al.* Combined enzyme replacement and haematopoietic stem cell. *Journal of Pediatrics and Child Health*. 45:469–472 (2009).
19. Ghosh, A. *et al.* Enzyme replacement therapy prior to haematopoietic stem cell transplantation in Mucopolysaccharidosis Type I: 10 year combined experience of 2 centres. *Molecular Genetcis and Metabolism*. 1–5 (2016).
20. Valayannopoulos, V. *et al.* Laronidase for Cardiopulmonary Disease in Hurler Syndrome 12 Years After Bone Marrow Transplantation. *Pediatrics*. (2015).
21. Tolar, J. *et al.* Combination of enzyme replacement and hematopoietic stem cell transplantation as therapy for Hurler syndrome. *Bone Marrow Transplantation.* 41:531–535 (2008).
22. Saif, M. A. *et al.* Hematopoietic stem cell transplantation improves the high incidence of neutralizing allo-antibodies observed in Hurler's syndrome after pharmacological enzyme replacement therapy. Stem Cell Transplantation. 97:1320-8 (2012).
23. Kuehn, S. C. *et al.* Impaired bone remodeling and its correction by combination therapy in a mouse model of mucopolysaccharidosis-I. *Human Molecular Genetcis.* 24:7075–7086 (2015).
24. Clarke, L. A. *et al.* Murine mucopolysaccharidosis type I : targeted disruption of the murine α - L -iduronidase gene. *Human Molecular Genetcis* 6:503–511 (1997).
25. Rowan. Assessment of bone dysplasia by micro-CT and glycosaminoglycan levels in mouse models for mucopolysaccharidosis type I, IIIA, IVA, and VII. *J Inherit Metab Dis.* 36:235–246 (2014).
26. Ahmed, Z. *et al.* Actin-binding Proteins Coronin-1a and IBA-1 Are Effective Microglial Markers for Immunohistochemistry. *The Journal of Histochemistry & Cytochemistry*. 55:687–700 (2007).
27. Wraith, J. *et al.* Enzyme replacement therapy for Mucopolysaccharidosis I: a randomized double-blinded, placebo-controlled, multinational study of recombinant human a-L-iduronidase (Laronidase). *J Pediatr.* 144:581-588 (2004).
28. Prasad, V. K. & Kurtzberg, J. Transplant Outcomes in Mucopolysaccharidoses. *Seminars in Hematology.* 47:59–69 (2010).
29. Parini, R. *et al.* Open issues in Mucopolysaccharidosis type I-Hurler. *Orphanet Journal of Rare* Diseases.12:112 (2017).

30. Aldenhoven, M. *et al.* Long-term outcome of hurler syndrome after HCT. *Blood*. 125:2164-72 (2015).
31. Grewal, S. S., Wynn, R., Abdenur, J. E. & Burton, B. K. Safety and efficacy of enzyme replacement therapy in combination with hematopoietic stem cell transplantation in Hurler syndrome. *Genet Med.* 7:143–146 (2005).
32. Cox-Brinkman, J. *et al.* Haematopoietic cell transplantation (HCT) in combination with enzyme replacement therapy (ERT) in patients with Hurler syndrome. *Bone Marrow Transplantation.*38:17–21 (2006).
33. Watson H.A. *et al.* Heparan Sulfate Inhibits Hematopoietic Stem and Progenitor Cell Migration and Engraftment in Mucopolysaccharidosis I. *Journal of Biological Chemistry.* 289:36194–36203 (2014).
34. Dierenfeld, A. *et al.* Replacing the Enzyme α-L-iduronidase at Birth Ameliorates Symptoms in the Brain and Peripehery of Dogs with Mucopolysaccharidosis type I. *Sci Transl Med.* 2:60ra89 (2011).
35. Kim, K. H., Messinger, Y. H. & Burton, B. K. Successful reduction of high-sustained anti-idursulfase antibody titers by immune modulation therapy in a patient with severe mucopolysaccharidosis type II. *MGM Reports* 2:20–24 (2015).
36. Dickson, P. *et al.* Immune tolerance improves the efficacy of enzyme replacement therapy in canine mucopolysaccharidosis I. *The Journal of Clinical Investigation.* 118:2868-2876 (2008).
37. Ponder, K. P. Immune response hinders therapy for lysosomal storage diseases. *The Journal of Clinical Investigation* . 118:2686-9 (2008).
38. Turner, C. T., Hopwood, J. J. & Brooks, D. A. Enzyme Replacement Therapy in Mucopolysaccharidosis I: Altered Distribution and Targeting of α - L-Iduronidase in Immunized Rats. *Molecular Genetics and Metabolism.* 69:277-285 (2000).
39. Kakkis, E. D. *et al.* Enzyme Replacement Therapy in Feline Mucopolysaccharidosis I. *Molecular Genetics and Metabolism.* 72:199–208 (2001).
40. Akiyama, K. *et al.* Enzyme augmentation therapy enhances the therapeutic ef fi cacy of bone marrow transplantation in mucopolysaccharidosis type II mice. *Molecular Genetics and Metabolism* 111:139–146 (2014).
41. Tomatsu, S. *et al.* Development and Testing of New Screening Method for Keratan Sulfate in Mucopolysaccharidosis IVA. *Pediatric Research.* 55:592–597 (2004).
42. Tomatsu, S., Montaño, A. M., Oguma, T. & Dung, V. C. Dermatan sulfate and heparan sulfate as a biomarker for mucopolysaccharidosis I. *J Inherit Metab Dis.* 33:141–150 (2010).
43. Visigalli, I. *et al.* Gene therapy augments the efficacy of hematopoietic cell transplantation and fully corrects mucopolysaccharidosis type I phenotype in the mouse model. *Blood.* 116:5130–5139 (2013).

44. Bigger, B. W., Begley, D. J., Virgintino, D. & Pshezhetsky, A. V. Anatomical changes and pathophysiology of the brain in mucopolysaccharidosis disorders. *Molecular Genetics and Metabolism.* 125:322-331 (2018).
45. Ou, L. High-Dose Enzyme Replacement Therapy in Murine Hurler Syndrome. *Mol Genet Metab.* 111:116–122 (2015).
46. Baldo, G., Giugliani, R. & Matte, U. Lysosomal enzymes may cross the blood – brain-barrier by pinocytosis: Implications for Enzyme Replacement Therapy. *Medical Hypotheses.* 82:478–480 (2014).
47. Boelens, J. J. & Hasselt, P. M. Van. Neurodevelopmental Outcome after Hematopoietic Cell Transplantation in Inborn Errors of Metabolism: Current Considerations and Future Perspectives. *Neuropediatrics.* 47:285-92(2016).
48. Soper, B. W. *et al.* Nonablative neonatal marrow transplantation attenuates functional and physical defects of β-glucuronidase deficiency. *Blood*. 9:1498–1505 (2016).
49. Mildner, A. *et al.* Microglia in the adult brain arise from Ly-6C hi CCR2 + monocytes only under defined host conditions. *Nature Neuroscience*. 10:1544–1553 (2007).
50. Eisengart, J. B. *et al.* Enzyme replacement is associated with better cognitive outcomes after transplant in Hurler syndrome. *J Pediatr.* 162:375–380 (2014).
51. Capotondo, A. *et al.* Brain conditioning is instrumental for successful microglia reconstitution following hematopoietic stem cell transplantation. *PNAS*. 109:15018-15023 (2012).
52. Wilkinson, F. L. *et al.* Neuropathology in Mouse Models of Mucopolysaccharidosis Type I, IIIA and IIIB. *PLos ONE*. 7:e35787. (2012).
53. Ransohoff, R. M. & Perry, V. H. Microglial Physiology: Unique Stimuli, Specialized Responses. *Annu Rev Immunol*. 27:119-45 (2009).
54. Archer, L. D., Langford-smith, K. J., Bigger, B. W. & Fildes, J. E. Mucopolysaccharide diseases : A complex interplay between neuroinflammation , microglial activation and adaptive immunity. *J Inherit Metab Dis.* 37:1–12 (2014).
55. Pasqualim, G., Baldo, G., Carvalho, T. G. De & Maria, A. Effects of Enzyme Replacement Therapy Started Late in a Murine Model of Mucopolysaccharidosis Type I. *PLoS ONE. 10:e*0117271 (2015).
56. Concolino, D., Deodato, F. & Parini, R. Enzyme replacement therapy : efficacy and limitations. *Italian Journal of Pediatrics.* 44:120 (2018).
57. Tomatsu, S. *et al.* Therapies for the bone in mucopolysaccharidoses. *Mol Genet Metab.* 114:94–109 (2016).
58. Al-sannaa, N. A. *et al.* Early treatment with laronidase improves clinical outcomes in patients with attenuated MPS I: a retrospective case series analysis of nine sibships. *Orphanet J. Rare Dis.* 10:131 (2015).
59. Tomatsu, S. *et al.* Enhancement of Drug Delivery: Enzyme- replacement

Therapy for Murine Morquio A Syndrome. *The American Society of Gene & Cell Therapy.* 18:1094–1102 (2010).

60. Rowan, D. J., Oikawa, H., Sosa, C., Chen, A. & Sly, W. S. Long Circulating Enzyme Replacement Therapy Rescues Bone Pathology in Mucopolysaccharidosis VII Murine Model. *Mol Genet Metab.* 107:161–172 (2013).
61. Yasuda, E. *et al.* Long-term follow-up of post hematopoietic stem cell transplantation for Hurler syndrome: Clinical, biochemical, and pathological improvements. *MGM Reports.* 2:65–76 (2015).
62. Eisengart, J. B. *et al.* Long-term outcomes of systemic therapies for Hurler syndrome: an international multi-center comparison. *Genet Med.* 20:1423–1429 (2018).
63. Chakrapani, A., Cleary, M. A. & Wraith, J. E. Detection of inborn errors of metabolism in the newborn. *Arch Dis Child Fetal Neonatal Ed.* 84:F205-10 (2001).
64. Grosse, S. D., Lam, W. K. K., Wiggins, L. D. & Kemper, A. R. Cognitive outcomes and age of detection of severe mucopolysaccharidosis type 1. *Genetics in Medicine.* 19:975-982. (2017).
65. Mango, R. L. *et al.* Neonatal retroviral vector-mediated hepatic gene therapy reduces bone, joint, and cartilage disease in mucopolysaccharidosis VII mice and dogs. *Molecular genetics and Metabolism.* 82:4–19 (2004).
66. Liu, Y. *et al.* Liver-directed Neonatal Gene Therapy Prevents Cardiac, Bone, Ear, and Eye Disease in Mucopolysaccharidosis I Mice. *Molecular Therapy.* 11:35–47 (2005).
67. Stirnadel-farrant, H. *et al.* Gene therapy in rare diseases : the benefits and challenges of developing a patient- centric registry for Strimvelis in ADA-SCID. *Orphanet Journal of Rare Diseases.* 13:149 (2018).

CHAPTER 3

Neonatal umbilical cord blood transplantation halts skeletal disease progression in the murine model of MPS-I

Isabella Azario[a], Alice Pievani[a], Federica Del Priore[a], Laura Antolini[b], **Ludovica Santi[a]**, Alessandro Corsi[c], Lucia Cardinale[a], Kazuki Sawamoto[d], Francyne Kubaski[d,e], Bernhard Gentner[f], Maria Ester Bernardo[f], Maria Grazia Valsecchi[b], Mara Riminucci[c], Shunji Tomatsu[d], Alessandro Aiuti[f,g], Andrea Biondi[h], Marta Serafini [a]

[a] Dulbecco Telethon Institute, Centro Ricerca M. Tettamanti, Department of Pediatrics, University of Milano-Bicocca, Monza, 20900, Italy
[b] Centro di Biostatistica per l'epidemiologia clinica, Department of Health Sciences, University of Milano-Bicocca, Monza, 20900, Italy
[c] Department of Molecular Medicine, Sapienza University, Rome, 00161, Italy
[d] Department of Biomedical Research, Alfred I. duPont Hospital for Children, Wilmington, DE, 19803, USA
[e] Department of Biological Sciences, University of Delaware, Newark, DE,19716, USA
[f] San Raffaele Telethon Institute for Gene Therapy (SR-TIGET), San Raffaele Scientific Institute, Milan, 20132, Italy
[g] Vita Salute San Raffaele University, Milan, Italy
[h] Department of Pediatrics, University of Milano-Bicocca, Monza, 20900, Italy

Scientific Reports. 2017 August; 7 (1): 9473.

ABSTRACT

Umbilical cord blood (UCB) is a promising source of stem cells to use in early hematopoietic stem cell transplantation (HSCT) approaches for several genetic diseases that can be diagnosed at birth. Mucopolysaccharidosis type I (MPS-I) is a progressive multi-system disorder caused by deficiency of lysosomal enzyme α-L-iduronidase, and patients treated with allogeneic HSCT at the onset have improved outcome, suggesting to administer such therapy as early as possible. Given that the best characterized MPS-I murine model is an immunocompetent mouse, we here developed a transplantation system based on murine UCB. With the final aim of testing the therapeutic efficacy of UCB in MPS-I mice transplanted at birth, we first defined the features of murine UCB cells and demonstrated that they are capable of multi-lineage hematopoietic repopulation of myeloablated adult mice similarly to bone marrow cells. We then assessed the effectiveness of murine UCB cells transplantation in busulfan-conditioned newborn MPS-I mice. Twenty weeks after treatment, iduronidase activity was increased in visceral organs of MPS-I animals, glycosaminoglycans storage was reduced, and skeletal phenotype was ameliorated. This study explores a potential therapy for MPS-I at a very early stage in life and represents a novel model to test UCB-based transplantation approaches for various diseases.

INTRODUCTION

Hematopoietic stem cell transplantation (HSCT) can cure or greatly ameliorate a wide variety of genetic diseases, including defects of hematopoietic cell production or function and metabolic diseases mainly affecting solid organs[1]. In post-natal life, hematopoietic stem cells (HSCs) reside in the bone marrow (BM), so this was historically the first source of cells employed for HSCT. However, immediately after birth, HSCs can still be found in the fetal blood that flows in the umbilical cord vessels (umbilical cord blood, UCB). Unrelated donor UCB has several potential advantages over BM for HSCT, since it offers a relative ease of procurement, a greater degree of HLA (human leukocyte antigen)-mismatch, with increased probability to find a suitable donor and lower incidence of acute and chronic graft versus host disease (GVHD), and reduced risk of viral infections (like Epstein-Barr virus and Cytomegalovirus)[1-4]. Furthermore, in the specific case of transplantation for inborn errors of metabolism (IEMs), UCB transplantation (UCBT) shows two significant extra-advantages over BM transplantation (BMT)[3,5-7]. First, the availability of cells to transplant is more rapid, thanks to the augmented probability to find HLA-matched donors and the existence of cord blood banks where UCB units are stored frozen and ready to use. This factor is of primary importance because in many IEMs the timing of the treatment has a strong impact on patient outcome. Additionally, more patients transplanted with UCB achieve full donor chimerism and thus can obtain a normalization of the deficient enzyme levels in biological fluids, with consequent clinical benefits[3,6,8].

New strategies and novel developments are expected to improve engraftment and reconstitution, and to enable *in utero* or neonatal UCB-based transplantation for early therapy of these diseases[2,9]. Thus, convenient small animal models of these disorders are essential to investigate these developing strategies in the field of HSCT, including the use of alternative cellular sources and/or genetically modified HSCs.

Even though immunodeficient mouse models of many genetic disorders are available, in which the transplantation of human HSCs is feasible, many diseases lack an immunocompromised model that could fully recapitulate their clinical manifestations. In the case of Mucopolysaccharidosis type I-Hurler syndrome (MPS-IH), a lysosomal storage disease due to mutations in the α-L-iduronidase (*IDUA*) gene, immunocompetent mouse models have been deeply characterized for several features typical of this complicated disorder[10-13]. Recently, MPS-I immunocompromised models have been generated, but some aspects representative of the disease are not completely investigated yet[14,15]. In this disorder, the absence of IDUA activity causes the progressive accumulation of glycosaminoglycans (GAGs) in tissues, which leads to multiple organ dysfunction, with central nervous system involvement and various skeletal anomalies known overall as dysostosis multiplex[16,17]. The current first line therapy for MPS-IH is HSCT, which provides a constant reservoir of enzyme replacement through the engraftment of donor cells, and the use of UCB as stem cell source seems to guarantee the best results. However, transplantation is not completely effective in ameliorating bone abnormalities and neurocognitive dysfunctions, especially when

it is performed late in childhood[7,8,18,19]. Clinical and preclinical evidences attest that the precociousness of the treatment is critical to prevent long-term pathological consequences[20]. For this reason, we tested an UCBT approach at early age in MPS-I murine model[10], to investigate a novel and promising therapeutic strategy. Very few data are present in the literature about murine UCBCs and their transplantation. Attempts to mimic UCBT have been made with either fetal liver cells, blood or BM collected from mouse fetuses during the last third of pregnancy, or newborn blood[21-27], but, to our knowledge, no published data exist about the transplantation of murine UCB into newborn recipients, in particular in a mouse model of disease attesting a clinical correction.

Building upon the data from our previous study where we observed that the transplantion of normal BM into newborn MPS-I mice, soon after the placental protection, can prevent GAGs accumulation in multiple organs and the distinctive skeletal dysplasia[28], in this study we provide an extensive description of murine UCB cells (UCBCs) features, in comparison with adult BM cells (BMCs). We characterized UCBCs *in vitro*, by flow cytometry and colony forming cell (CFC)-assay, and assessed the repopulating ability of UCBCs in conditioned adult and newborn wild-type (WT) mice. Finally, we focused on the pathological setting and investigated a novel treatment strategy based on the transplantation of UCBCs in MPS-I mice at birth. We extensively evaluated the outcome of this therapy, regarding restoration of enzyme activity, reduction of GAG deposits in plasma and visceral organs, and correction of the skeletal phenotype.

RESULTS

Collection of UCBCs and their comparison with adult BMCs *in vitro*

We collected UCBCs at gestational day E18 from C57BL/6 pregnant dams, which carried a mean number of fetuses/dam of 6.97 (standard deviation [SD] 1.81; n=72 dams). The mean number of UCBCs collected from each dam was $1.38x10^6$ (SD $4.51x10^5$), and it varied proportionally with the number of fetuses/dam (data not shown). The mean number of cells obtained from each fetus was $19.8x10^4$ (SD $5.64x10^4$) (*Figure 1A*). Hematopoietic cells belonging to different lymphoid and myeloid lineages were found both in UCB and adult BM, as shown in the representative flow cytometry panels in *Figure 1B*. However, the proportion of lymphocytes (T cells and B cells) and of myeloid cells (monocytes/macrophages and granulocytes) was higher in BM than in UCB, suggesting that UCB could contain less mature cell populations (Supplementary Table S1). Interestingly, $Ter119^+$ erythrocytes were very few in BM after lysis but remained at a high percentage in UCB, probably because they are mostly immature and resistant to hypotonic shock (*Supplementary Figure S2*). Regarding the HSCs subset easily detectable within adult BMCs by $Lin^-Sca\text{-}1^+c\text{-}kit^+$ (LSK) staining, in UCBCs specimens there was a reduced proportion of LSK cells (*Figure 1B*). In the colony-forming cell (CFC) assay, performed to investigate the functionality of the hematopoietic progenitors, a similar frequency of colonies was found in UCB and BM (median 35.0 colonies/plate in UCB, range from 16 to 112, and 39.0 colonies/plate in BM, range from 18 to 78; p=1)

(*Figure 1C*). However, in UCB the majority of the colonies (93.2%) had a peculiar morphology, consisting of colonies containing large blast-like cells on a single layer (*Figure 1D-E*). These cells resemble the previously defined High Proliferative Potential-Colony-Forming Cells (HPP-CFC), primitive multipotent progenitor cells absent in BM-derived colonies[23]. Excluding HPP-CFCs, the relative distribution of the other colony subtypes (CFU-GEMM, BFU-E, CFU-GM) did not differ between UCB and BM (p=0.06, Chi-square test) (*Figure 1D*). The different subtypes of UCB and BM hematopoietic colonies were morphologically indistinguishable (*Figure 1E*).

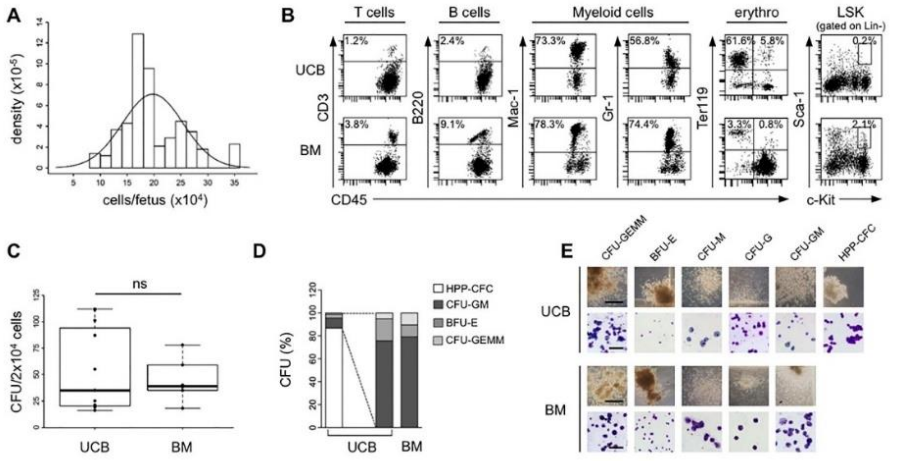

Figure 1. Murine UCBCs have unique features compared with BMCs.
A. *Number of UCBCs obtained at day E18 from each fetus (n=502 fetuses). The distribution of the medium number of cells per fetus was represented by density histogram with Gaussian approximation.* ***B.*** *Representative flow cytometry analysis of UCB and BM hematopoietic subpopulations: T cells ($CD45^+CD3^+$), B cells ($CD45^+B220^+$), myeloid cells ($CD45^+Mac\text{-}1^+$ and $CD45^+Gr\text{-}1^+$), erythroid cells ($TER\text{-}119^+$), and LSK cells ($lin^-Sca\text{-}1^+c\text{-}Kit^+$). Percentages of lymphocytes and myeloid cells were referred to $CD45^+$ leukocytes, percentage of $Ter119^+$ was referred to all cells (after hypertonic treatment), and percentage of LSK cells was referred to Lin^- leukocytes.*

C. *Absolute number of hematopoietic colonies detected on methylcellulose at day 14 after plating 2x10^4 UCB or BM cells/petri (n=11 UCB, n=6 BM). Data are represented by boxplot graphs, showing the exact data values by black dots. P=1 with 2-sided Wilcoxon unpaired test.* ***D.*** *Barplot with percentage of the different subtypes of HPP-CFC, CFU-GEMM, BFU-E and CFU-GM (CFU-M, CFU-G, and CFU-GM) among the total number of colonies obtained from UCB or BM.* ***E.*** *Representative photographs of the different subtypes of hematopoietic colonies in UCB and BM (10X magnification, bar: 400 μm) and of their cytospin preparations stained with May-Grumwald Giemsa (200X magnification, bar: 200 μm). CFU-GEMM = Colony-Forming Unit-Granulocyte, Erythroid, Macrophage, Megakaryocyte; BFU-E = Burst-Forming Unit-Erythroid; CFU-M = Colony-Forming Unit-Macrophage; CFU-G = Colony-Forming Unit-Granulocyte; CFU-GM = Colony-Forming Unit-Granulocyte, Macrophage; HPP-CFC = High Proliferative Potential-Colony-Forming Cell.*

UCB contains long-term multi-lineage repopulating hematopoietic stem cells

Before performing the transplantion of UCBCs into newborn MPS-I mice, we assessed whether they were able to rescue lethally-conditioned adult mice, to differentiate into cells of lymphoid and myeloid lineages, to persist long-term, and to repopulate in serial transplants. In an initial set of experiments, lethally-irradiated adult C57BL/6-CD45.1 mice were transplanted with 5x10^5 CD45.2$^+$ UCBCs (adult UCBT group, aUCBT) or with the same number of murine adult BMCs (adult BMT group, aBMT). At 1 month after transplantation, the short-term engraftment of donor cells was assayed in peripheral blood (PB), BM, spleen, and thymus of the recipients, by flow cytometric analysis of the leukocytes marked with anti-CD45.1 and anti-CD45.2 antibodies (*Figure 2A*). In the aUCBT group, median engraftment in PB was 71.7% (range from 66.9% to 74.3%), even higher than the one in the aBMT group that was 58.4% (range from

42.3% to 68.3%; p=0.03). In the BM, the median donor chimerism was 82.5% in the aUCBT group and 83.3% in the aBMT group, while it was, respectively, 62.7% and 69.3% in the spleen, and 22.8% and 23.2% in the thymus, without significant differences between UCBCs and BMCs (p=1, p=0.90, p=0.56, respectively). We next assessed if it was possible to use lower doses of UCBCs ($2.5x10^5$ and $1x10^5$cells/mouse) to establish long-term, stable chimerism. Rates of engraftment (number of surviving mice with ≥1% donor cells/total number of transplanted mice) were 100% for all the tested doses. While at 1 month after transplantation the level of donor cell engraftment in PB depended on the transplanted cell dose, beginning from 4 months after transplantation the engraftment reached values over 90% in all the experimental groups (*Figure 2B*). More importantly, UCBCs showed long-term repopulation ability, since PB engraftment was maintained up to 12 months after aUCBT. The engraftment in other hematopoietic organs was assayed at 4 months after transplantation, and it reached a median of 98.2% in BM, 93.5% in spleen, and 92.1% in thymus (data not shown). The presence of cells arisen from the original UCBCs ($CD45.2^+$ cells) in both lymphoid (T and B cells) and myeloid (monocytes/macrophages and granulocytes) lineages was attested in BM, spleen and thymus by flow cytometry (*Figure 2C*). $CD45.2^+$ LSK cells were also found in the BM of recipient mice, suggesting that, even if LSK cells were detected as a very rare population in UCB, UCBCs were able to repopulate also the HSCs pool in the recipients' BM (*Figure 2C*). To evaluate the functionality of UCB-derived hematopoietic progenitors, $CD45.2^+$ cells were sorted 4 months after aUCBT from the BM of recipients

and were tested in a CFC-assay, showing the differentiation in colonies belonging to all the different subtypes (*Figure 2 D-E*). Finally, a secondary transplantation assay into lethally-irradiated CD45.1 recipients was performed, to verify whether UCBCs contained long-term HSCs. The presence of sustained and durable levels of PB engraftment in secondary mice confirmed self-renewal and long-term repopulation capability of UCB-derived HSCs (*Figure 2F*). CD45.2^{+} mature subpopulations and LSK cells were also present in BM of secondary mice (data not shown).

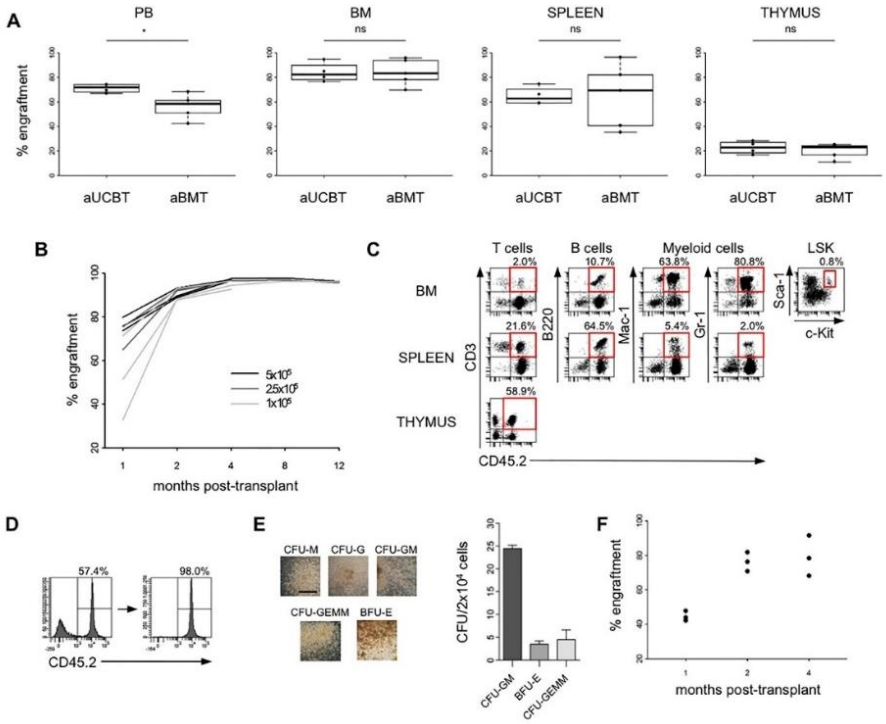

Figure 2. Murine UCBCs demonstrate long-term multi-lineage hematopoietic repopulating activity in adult transplantation setting.

A. *Levels of donor chimerism [donor CD45^{+} cells/(donor + host CD45^{+} cells) x 100] were determined by flow cytometry in the hematopoietic organs of adult lethally-irradiated recipients at 1 month after the transplantation of 5x10^{5} UCBCs (aUCBT) or BMCs (aBMT) (n=4 aUCBT, n=5 aBMT).**

$p \leq 0.05$ by Wilcoxon test. ***B.*** *Levels of chimerism analyzed serially in the PB of recipient mice between 1 and 12 months after the transplantation of $5x10^5$, $2.5x10^5$, or $1x10^5$ UCBCs/mouse (each line in the plot represents a single mouse).* ***C.*** *Representative lineage distribution of UCB-derived cells in the BM, spleen, and thymus of recipient mice at 4 months after aUCBT. Dot plots to determine donor-derived T cells ($CD45.2^+CD3^+$), B cells ($CD45.2^+B220^+$), myeloid cells ($CD45.2^+Mac\text{-}1^+$ and $CD45.2^+Gr\text{-}1^+$), and LSK cells ($CD45.2^+lineage^-Sca\text{-}1^+c\text{-}Kit^+$) are shown.* ***D.*** *FACS sorting of $CD45.2^+$ UCB-derived cells from the BM of a primary aUCBT recipient at 4 months after transplantation.* ***E.*** *Representative photographs and count of the different subtypes of hematopoietic colonies on methylcellulose formed by UCB-derived ($CD45.2^+$) BM sorted cells (10X magnification, bar: 400 μm).* ***F.*** *Donor chimerism in the PB of secondary mice after the transplantation of $3x10^6$ UCB-derived ($CD45.2^+$) BM sorted cells (n=3 recipient mice). Each black dot in the plot represent a single mouse, analyzed at 1, 2, and 4 months after transplant.*

Transplantation of UCBCs in the neonatal setting

For the transplantation of newborn mice, we adopted a previously established protocol with few modifications[28]. After conditioning with busulfan, CD45.2 newborn mice were intravenously transplanted with either $CD45.1^+$ UCBCs (neonatal UCBT group, nUCBT) or adult BMCs (neonatal BMT group, nBMT). The cell dose we defined to transplant ($2x10^5$ cells/mouse) was ideally comparable with the mean number of UCBCs harvested from a single fetus. At 1 month after transplantation, no difference in the PB engraftment was observed between nUCBT group (median: 18.5%, range from 1.0% to 71.8%) and nBMT group (median: 30.5%, range from 2.6% to 66.1%; p=0.10, including in our analysis only successfully transplanted mice with donor chimerism ≥1%) (*Figure 3A*). nUCBT mice with PB engraftment ≥50% at 1 month were analyzed serially at 2 and 4 months, and the levels of engraftment in PB increased over time,

approaching full donor chimerism (*Figure 3B*). The engraftment in BM, spleen, and thymus, the differentiation of transplanted UCBCs in lymphoid and myeloid lineages, and the retention of LSK cells were evaluated at 6 months post transplantation, and the results were comparable with the ones obtained in aUCBT mice (*Supplementary Figure S1* and data not shown). Thus, we could also confirm in the neonatal setting the hematopoietic repopulation ability of UCBCs.

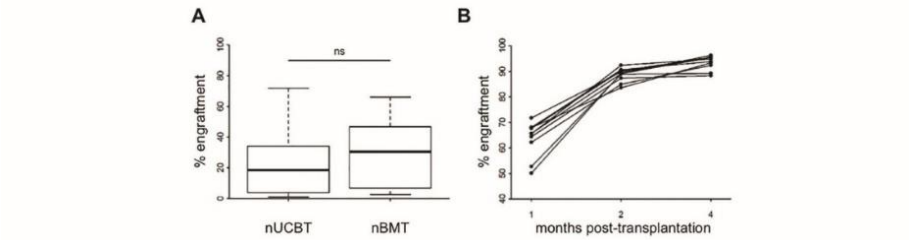

Figure 3. Murine UCBCs confirm long-term multi-lineage hematopoietic repopulating activity in neonatal transplantation setting.
A. *Levels of donor chimerism were determined by flow cytometry in the PB of busulfan-conditioned newborn mice at 1 month following the transplantation of 2x10^5 UCBCs (nUCBT) or BMCs (nBMT) cells (n=68 nUCBT, n=28 nBMT; p=0.10 by Wilcoxon test).* ***B.*** *Serial analysis of donor chimerism in the PB of nUCBT recipient mice performed at 1, 2, and 4 months after transplant (n=10, each line in the graph represents a single mouse).*

Engraftment and biochemical features of MPS-I mice receiving nUCBT

To investigate whether nUCBT could represent a curative treatment for metabolic diseases, we applied the settled protocol to the MPS-I mouse model. Newborn MPS-I and WT mice were transplanted with healthy UCBCs and evaluated at 20 weeks of age for their PB engraftment, IDUA activity in organs, GAGs accumulation in organs and plasma, and skeletal phenotype. PB engraftment did not differ

between MPS-I and WT mice at the time of sacrifice (median 38.7% in MPS-I, range from 1.6% to 96.2%; 9.8% in WT, range from 1.0% to 94.8%; p=0.24) (*Figure 4A*). Among MPS-I nUCBT mice, 5 of 12 mice presented a high hematopoietic chimerism, defined as more than 50% donor CD45.1^{+} cells in PB at 20 weeks after nUCBT (median engraftment: 93.3%, range from 55.7% to 96.2%). Hence, we included this subgroup of highly engrafted mice (named MPS-I nUCBT-hi) in all the studies reported hereafter. Five of 12 mice, instead, had a low hematopoietic chimerism, defined as less than 10% donor CD45.1^{+} cells in PB at 20 weeks after nUCBT, and were grouped as low engrafted mice (MPS-I nUCBT-lo). IDUA activity was evaluated in the spleen, liver, lung, kidney, and heart of MPS-I nUCBT mice compared with age-matched untreated WT and MPS-I mice. IDUA activity, which is absent in MPS-I mice and not restored in MPS-I nUCBT-lo mice, was partially increased in MPS-I nUCBT-hi mice in all the tissues analyzed, particularly in spleen, where the average values in MPS-I nUCBT-hi mice reached 40% of average WT values (*Figure 4B*). In the same harvested tissues, we quantified GAG levels, showing that MPS-I nUCBT-hi animals displayed a statistically significant reduction in GAGs storage material in all organs, in comparison with untreated MPS-I mice ($p \leq 0.03$ for all organs) (*Figure 4C*). The average reduction on MPS-I is over 50% for spleen, heart, lung and kidney. In particular, in spleen, liver, and lung of MPS-I nUCBThi animals GAG levels completely normalized (MPS-I nUCBThi *vs.* WT, p=0.76, p=1, and p=0.11, respectively) (*Figure 4C*). To further confirm the occurred correction, we measured the levels of plasma GAGs (HS-0S, HS-NS, DS, and mono-sulfated KS),

showing that the levels of these GAGs were significantly reduced in MPS-I nUCBT-hi compared to untreated MPS-I mice (*Figure 4D*). Of note, in MPS-I nUCBT-hi mice the level of mono-sulfated KS, which has been associated with severity of skeletal dysplasia in the mouse model of MPS-I, was similar to WT animals (MPS-I nUCBThi *vs.* WT; p=0.72) (*Figure 4D*). Instead, GAG levels in both peripheral organs and plasma were not consistently reduced in MPS-I nUCBT-lo mice (*Figure 4 C-D*). Taken together, these biochemical data prove that nUCBT greatly corrects the error of metabolism in these tissues in animals with high donor chimerism.

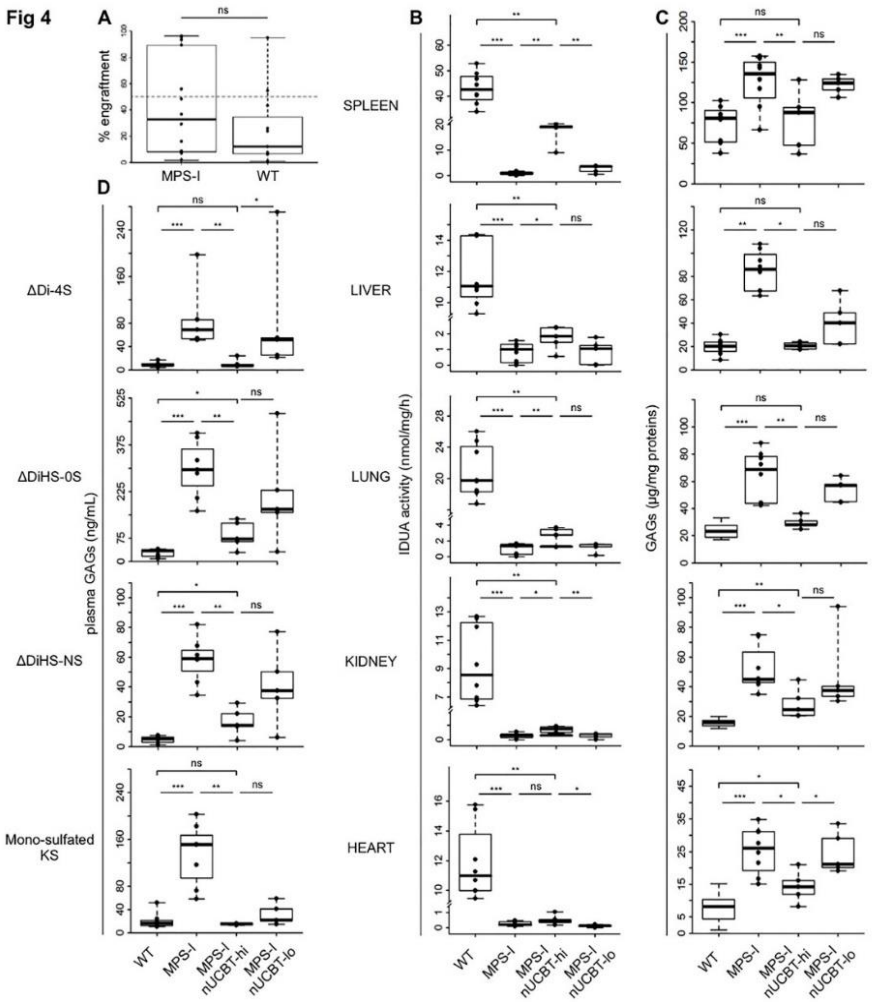

Figure 4. Neonatal UCBT prevents GAGs accumulation in MPS-I mice. A. *Donor chimerism (percentage of CD45.1$^+$ cells) determined by flow cytometry in the PB of recipient MPS-I and WT mice at 20 weeks (time of sacrifice) after nUCBT (n=12 for MPS-I, n=12 for WT; p=0.24 by Wilcoxon test). Dashed line indicates the level of 50% donor engraftment, and identifies the highly-engrafted mice group (with ≥50% donor cells in PB, nUCBT-hi).* ***B.*** *IDUA activity in spleen, liver, lung, kidney, and heart of WT (n=8), MPS-I (n=8), MPS-I nUCBT-hi (n=5), and MPS-I nUCBT-lo mice (n=5).* ***C.*** *GAG levels in the indicated organs of the same WT, MPS-I, MPS-I nUCBT-hi, and MPS-I nUCBT-lo mice.* ***D.*** *Levels of ΔDiHS-0S, ΔDiHS-NS, ΔDi-4S, and mono-sulfated KS in the plasma of the mice. *p≤0.05, **p≤0.01, ***p≤0.001 by Wilcoxon test.*

Prevention of dysostosis in MPS-I mice receiving nUCBT

Dysostosis multiplex is the well-known skeletal consequence of MPS-I in humans and mouse models. In particular, the MPS-I model adopted in this work shows abnormal craniofacial bone morphology and progressive thickening of the long bone segments. At the age of sacrifice (20 weeks) radiographic analyses confirmed a marked increase in the width of the skull and of the zygomatic arches in untreated MPS-I mice compared to WT animals (*Figure 5A*). Instead, in MPS-I nUCBT-hi mice, a significant reduction of these parameters was observed (skull width p=0.008; zygomatic arch width p=0.005, MPS-I nUCBT-hi *vs.* untreated MPS-I mice). A similar trend was observed in the femur and humerus, where the thickening and the meta-diaphyseal sclerosis of the skeletal bones of MPS-I mice revealed by radiographic analysis were prevented in MPS-I nUCBT-hi animals (*Figure 5B*). Considering that busulfan toxicity *per se* could cause a reduction in bone dimensions of treated mice regardless of their genotype, we adopted a regression model capable of separating

the adverse effect of busulfan treatment from the therapeutic effect of transplantation on MPS-I[28]. By this analysis, we obtained the confirmation of the differential effect of the treatment on MPS-I attributable to transplantation only (Supplementary Table S2). Moreover, considering the MPS-I nUCBT-lo group, the improvement in radiographic measurements was limited compared to MPS-I nUCBT-hi, confirming the importance of high donor chimerism for disease correction (*Figure 5A and B*). Micro-computed tomography (micro-CT) scans and histomorphometry performed on the femurs of male mice again highlighted the improvement of the skeletal phenotype in the MPS-I nUCBT-hi group. 2- and 3D micro-CT images revealed that the endocortical perimeter of MPS-I femurs appeared distinctly irregular at 20 weeks and returned to normal in MPS-I nUCBT-hi mice (*Figure 6A*). Specifically, all the examined parameters (total cortical area, cortical bone area, medullary area, and cortical thickness) were ameliorated in MPS-I nUCBT-hi mice, demonstrating the impact of the high donor engraftment on femoral architecture (*Figure 6B*). In addition, comparative histomorphometric analysis of the femur cortical thickness at mid-diaphysis and the area of the osteocytic lacunae confirmed the benefit of nUCBT on bone abnormalities in MPS-I mice (*Figure 6C* and data not shown). Considering the impact that osteoclastogenesis seems to have on MPS-I disease[29], we determined the effect of nUCBT on osteoclast numbers and function. There were no significant differences in the ability of BM cells derived from untreated WT and MPS-I mice to differentiate into TRAP-positive multinucleated osteoclasts *ex vivo* and in their resorptive capacity *in vitro* when cultured on

dentine slides (*Figure 6D*). Nonetheless, nUCBT treatment caused increased osteoclastogenesis regardless of the mice's genotype ($p \leq 0.05$, treated *vs.* untreated mice) (*Figure 6E*), although an effective reduction of bone mineral density could not be found *in vivo* (*Supplementary Figure S3*).

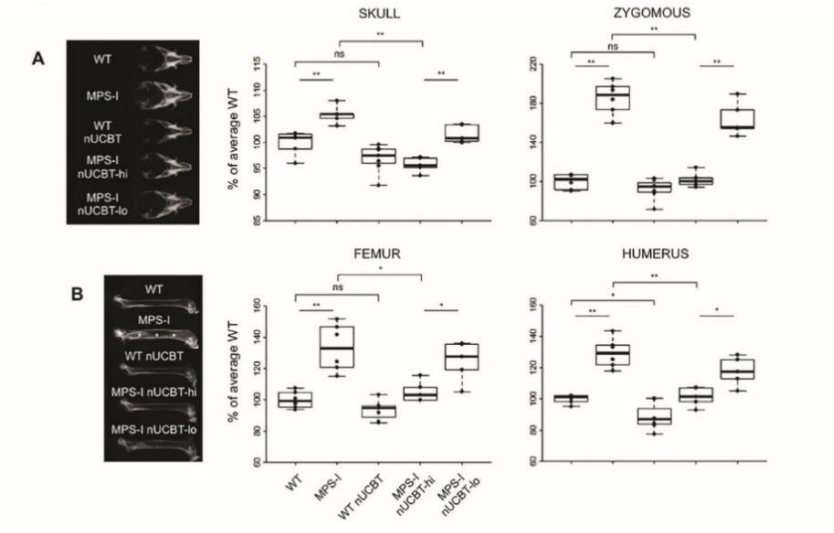

Figure 5. Neonatal UCBT prevents bone thickening in MPS-I mice.
A. *On the left, representative radiographs of the skull of 20-weeks-old WT, MPS-I, WT nUCBT, MPS-I nUCBT-hi, and MPS-I nUCBT-lo mice. On the right, measurements of the skull width and zygomous width, performed on radiographs of WT (n=6, 3 males and 3 females), MPS-I (n=6, 3 males and 3 females), WT nUCBT (n=7, 3 males and 4 females), MPS-I nUCBT-hi (n=5, 3 males and 2 females), and MPS-I nUCBT-lo mice (n=5, 3 males and 2 females).* ***B.*** *On the left, representative radiographs of the femur of 20-weeks-old WT, MPS-I, WT nUCBT, MPS-I nUCBT-hi, and MPS-I nUCBT-lo mice. The increase in meta-diaphyseal bone density observed in MPS-I (asterisks) is significantly prevented in MPS-I nUCBT-hi mice. On the right, measurements of the femur and humerus widths, performed on the radiographs of the same animals as in panel A. *p≤0.05, **p≤0.01, by Wilcoxon test.*

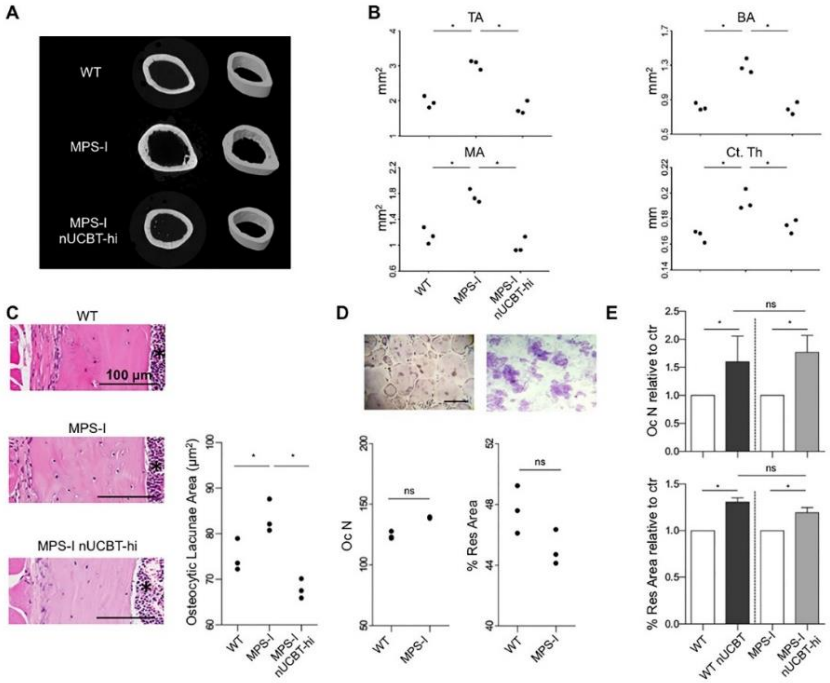

Figure 6. Neonatal UCBT improves cortical bone architecture in MPS-I mice.

*A. Representative 2D and 3D micro-CT images showing regions of femoral cortical bone in WT, MPS-I, and MPS-I nUCBT-hi 20-weeks-old male mice. B. Graphs representing the measurement of total area (TA/mm2), bone area (BA/mm2), medullary area (MA/mm2), and cortical thickness (Ct.Th/mm) of 3 mice per group (WT, MPS-I, and MPS-I nUCBT-hi). C. Representative hematoxylin and eosin stained histological sections of the femur cortical bone at the mid-diaphysis are shown in the panels on the left. The graph illustrates the measurement (mean ± SD) of the area of the osteocytic lacunae within the femur cortical bone of 3 mice per group (WT, MPS-I, and MPS-I nUCBT-hi). The BM cavity is indicated by an asterisk. Bar: 100 µm. D. Representative pictures of TRAP-positive multinucleated osteoclasts differentiated ex vivo (on the left, magnification 10X; bar: 300 µm) and their resorption plots on dentin slices (on the right, magnification 20X). Quantification of number and resoptive capacity of osteoclasts obtained by ex vivo differentiation of BM cells arised from untreated WT and MPS-I mice (n=3 male mice per group). E. Fold increase of the number and resoptive capacity of the osteoclasts obtained from treated mice, relative to control (untreated mice of the respective genotype) (mean ± SD). * p≤0.05 by Wilcoxon test.*

DISCUSSION

UCB is a clinically useful reservoir of HSCs and progenitor cells for the treatment of a wide variety of genetic diseases, particularly attractive for transplantation of infants and small children.

To fully realize the therapeutic potential of UCBT early after birth, it is fundamental to develop novel tools to test its efficacy in different defects. MPS-I offers an ideal model, since the relevance of UCBT in the treatment of this condition is well-known in clinic.

In this study, we demonstrate that the transplantation of murine UCBCs into lethally-irradiated congenic recipients long-term reconstitutes all blood cell lineages. Moreover, the BM of recipients contains cells capable of reconstituting the hematopoietic system of secondary hosts.

Furthermore, in the neonatal setting, MPS-I mice transplanted with UCBCs show high levels of chimerism with the donor healthy cells, that are both well tolerated and therapeutic. Indeed, the long-term engraftment results in the partial restoration of IDUA enzyme activity, clearance of GAGs storage, and significant improvement in altered bone architecture, with prevention of the skeletal phenotype.

In contrast to adult murine BM, the features of murine UCB have been poorly investigated. In a few studies, blood from late fetal and newborn mice has been employed, due to the similar hallmarks with UCB obtained at birth in human beings. In the current study, we used UCB collected from murine fetuses at embryonic day 18. Even if UCB contained few nucleated cells, the collected cell population

comprised the most representative committed lineages (T cells, B cells, and myeloid cells), although in different proportions if compared to BMCs. Notably, the majority of T cells are immature, with a double positive $CD4^+CD8^+$ phenotype and low levels of TCRα/β, as similarly reported for human UCB[27,30]. Both the low percentage of mature T cells and the weak reactivity of the numerous immature T cells can be responsible for the reduced incidence of GVHD in patients transplanted with UCB[31]. The almost complete absence of mature lymphocytes and the reduced number of innate immunity cells are allowed by the intra-uterine protection during fetal life[32]. Differently from murine adult BM, murine UCB is characterized by the presence of Ter119+ immature red blood cells resistant to hypotonic shock, including a population of nucleated red blood cells. These data are consistent with similar results reported for human UCB, which contains two distinct red cells populations, a minority of rapidly lysed cells and a majority of slowly disrupted cells[33].

Regarding the HSCs subset, the proportion of LSK cells, easily detectable within adult BM, was very low in UCB. This is consistent with the findings of Migishima et al., who stated that murine UCB virtually lacked cells with the LSK phenotype representative of adult BM-derived HSCs[24]. Considering that UCB cells successfully reconstituted lethally irradiated recipients, the authors conclude that some phenotypic differences between BM and UCB HSCs may exist. A possibility is that UCB HSCs do not express Sca-1, since they found a population of $Lin^-c\text{-}Kit^+$ cells among the side population. Another possibility is that UCB HSCs express Mac-1 similarly to fetal

liver HSCs, and consequently a LSK phenotype can be observed only if the anti-Mac-1 antibody is removed from the anti-lineage cocktail[33,34].

Furthermore, the majority of the colony progenitors was constituted by multipotent precursors that give rise to colonies with a peculiar blast-like morphology when cultured *in vitro*, resembling the previously-defined HPP-CFC[23]. As already reported, this population of hematopoietic cells demonstrating HPP-CFC activity begins to be present in the yolk sac and in the embryo and represents the earliest multi-potential precursors within the hematopoietic hierarchy than can be cultured without stromal support[35]. Similarly, human UCB cultures contain a higher proportion of immature, late developing, multi-potential colony-forming cells than adult BM cultures[36].

Even though these findings indicate that UCB has a different composition compared to BM, UCBCs can engraft with an extent similar to adult BM. In the congenic context, we do not observe any post-transplantation delay in hematopoietic recovery, differently than previously reported by Li *et al.* in an allogeneic UCBT model[26]. Notably, the persistence of donor-derived lymphoid and myeloid lineages over 4 month after transplantation demonstrates the long-term function of the HSCs contained in UCB, considering that most precursors and short-term HSCs that repopulate soon after transplantation are short-lived and disappear within 3 to 4 months after transplant in mice[37]. It has been further demonstrated that T and B cells derived from UCB-HSC are fully competent in immunological terms[25]. Long-term repopulating function of HSCs in UCB was definitively confirmed by the robust contribution to multi-lineage

engraftment in secondary irradiated recipients. Thus, HSCs from late fetal blood have a long-term multi-lineage repopulating ability similar to those from adult BM, in agreement with the similar competitive repopulation capacity previously demonstrated by Harrison *et al*[22].

Using a myelo-ablative conditioning regimen based on busulfan described in our previous work[28], we could demonstrate that also in the neonatal setting UCB has been able to repopulate the hematopoietic tissues, showing long-term multi-lineage reconstitution in mice transplanted at birth. Moreover, we showed that the number of cells derived from a single UCB sample can provide sufficient long-term repopulating ability to fully maintain a newborn recipient for at least 20 weeks.

To our knowledge, these are the first *in vivo* experiments carried out using UCBCs to perform a transplant at neonatal age. This new model of UCBT offers a potential tool to elucidate the biological features of the perinatal hematopoietic stem/progenitor cells and to develop early UCB-based therapies.

Notably, allogeneic murine late fetal or newborn blood has been transplanted in adult mouse models for prevention or treatment of autoimmune diseases such as type I diabetes and systemic lupus erythematosus[38,39], but never in models of genetic disorders at birth.

In Hurler disease, UCB has become in the most recent years the preferential stem cell source for affected infants and children because, in comparison with BM, this source demonstrated more immediate availability, higher donor chimerism, better enzyme recovery in blood, and superior engrafted-and-alive rates[8]. In our study, we provide evidence that neonatal UCBT in MPS-I mice allows efficient and

long-term hematopoietic engraftment. Twenty weeks after neonatal UCBT, MPS-I mice with more than 50% replacement by donor-derived hematopoiesis demonstrated near-complete normal values of biochemical parameters in visceral organs as compared with affected control mice. Indeed, the level of GAGs, which is an indicator of the disease progression, in the majority of the tissues investigated was completely normalized, confirming the efficacy of an early approach based on the infusion of UCBCs. Notably, the keratan sulfate (KS) level, which could be considered a biomarker of skeletal dysplasia in MPSs[40,41], was normalized after neonatal UCBT in MPS-I mice. We then focused our studies on skeletal disease, considering that it is one of the unmet clinical needs of utmost importance in transplanted MPS-I patients.

Definitely, the reconstitution of normal hematopoiesis in MPS-I mice was associated with a consistent amelioration of bone pathology, as revealed by radiographic skeletal examination. Micro-CT scans and histomorphometry remarked the impact of the high donor engraftment on the internal architecture of the femurs of transplanted mice. This could be due to enzyme delivery by hematopoietic cells close to the bone and also to tissue reconstitution by other donor-derived multipotent stem cells. Indeed, we recently demonstrated that a rare population of cells within the non-hematopoietic fraction of UCB, named cord blood-borne fibroblasts, shows *in vitro* and *in vivo* chondrogenic ability and the specific capacity of generating *in vivo* bone and a BM stroma that supports functional hematopoiesis[42,43]. Furthermore, Uchida *et al.* demonstrated that murine UCB transplantation could fully reconstruct not only hematopoietic cells,

but also mesenchymal cell lineages able to differentiate into osteoblastic cells in response to environmental specific cues[44,45].

Using a statistical model that separates the therapeutic effects of UCBT on MPS-I bones from the toxic effect of busulfan treatment on bones of transplanted MPS-I or WT mice[28], we could definitively demonstrate that neonatal UCBT reduced bone thickening in the skull, zygomatic arches, and long bone segments.

Another reported side-effect of the conditioning regimens with cyto-reductive chemotherapy agent such as busulfan is bone loss due to increased bone resorption[46]. In this sense, we observed a significant increase in the capacity of BM cells obtained from transplanted MPS-I mice to differentiate in TRAP-positive multinucleated osteoclasts *ex vivo*, but without achieving any actual reduction of femoral bone mineral density *in vivo*. A further assessment of bone turnover markers could be important to better elucidate the effect of conditioning on bone metabolism of MPS-I, in which the RANKL/OPG system is already altered[47].

UCB represents a promising source of stem cells for early HSCT therapeutic approaches for several diseases that can be diagnosed at birth and has several advantages such as easy and quick procurement, absence of risk to donors, immediate availability, low risk of transmitting infections, greater tolerance of HLA disparity, and lower incidence of severe GVHD[1,2,4]. Furthermore, UCB has unique composition and biological characteristics, due to the presence of HSCs as well as a mixture of multipotent stem cells such as unrestricted somatic stem cells, mesenchymal stem cells, and

endothelial colony-forming cells able to regenerate numerous tissue types with functional improvements[3,48]. For example, the administration of human UCB cells into MPS-III B mice decreased behavioral abnormalities and tissue pathology[50]. In particular, the neuroprotective effect of human UCBCs seems to be a function of enzyme delivery and anti-inflammatory effect mediated by donor cells found throughout the brain and can be enhanced by repeated administrations[49]. We do not know whether neonatal UCBT could be also effective at preventing or reverting brain pathology in MPS-I diseases. Although not investigated in our work, it is an important outstanding question that should be addressed in further studies.

Of note, UCB offers an alternative source of HSCs for gene therapy approaches, considering the possibility of collecting and storing autologous UCB at birth and reinfusing HSCs in the affected children after gene correction procedure. UCB-derived HSCs represent a particularly favorable target for gene therapy, given the reported higher gene transfer rates[50]. Moreover, a neonatal gene therapy approach could help to achieve supra-normal enzyme activity in transplanted mice before disease manifestation, even in the case of low levels of chimerism. Interestingly, a pioneering study published by Simonaro *et al.* showed evidence of transduction of hematopoietic neonatal blood stem cells derived from MPS-VI cats and long-term persistence of retrovirally transduced cells into adult recipients[51]. Further studies would be needed to identify the best preparatory regimen suitable for transplanting affected neonates or infants[52].

In conclusion, we demonstrated in an MPS-I mouse model the advantage of combining two factors that may allow for a better outcome in MPS-I patients: (1) early timing of the transplant and (2) the use of UCB, which is considered at the moment the best HSC source for this disease. This study serves as a proof of concept to develop early UCB transplantation strategies for newborns affected by genetic disorders, as well as an investigational platform for novel cell and gene therapy approaches for the treatment of genetic disorders diagnosed in the neonatal period.

MATERIALS AND METHODS

Animals. C57BL/6-CD45.2 and C57BL/6-CD45.1 mice were purchased from Charles River Laboratories (Calco, Italy). The MPS-I mouse model (Idua−/− mice, C57BL/6-CD45.2 background)[10] was purchased from The Jackson Laboratory (Bar Harbor, ME); a breeding colony was established and maintained from heterozygous mating pairs, and genotyping was performed on tail clips or ear snips DNA, as previously described[10]. Procedures involving animal handling and care conformed to institutional guidelines, in compliance with national laws and policies. Animals were used in accordance with a protocol approved by the Italian Ministry of Health (permit number 451/2015-PR).

UCB and BM cells collection. UCBCs were collected at E18 of pregnancy from C57BL/6 pregnant dams, as previously described[24]. Briefly, pregnant females were euthanized by CO_2 inhalation, the uterus was removed and cooled in ice-cold phosphate-buffered saline (PBS, Gibco). The fetuses were isolated, and the visceral yolk sac and amnion were removed. Then, the umbilical cord was cut, fetuses were transferred into warm heparinized PBS (10 U/mL), and blood was allowed to flow out. Fetuses were then euthanized. BMCs were collected from the long bones of 6 to 10-weeks-old C57BL/6 mice by flushing. UCBCs and BMCs were centrifuged at 670 g for 5 minutes, lysed using ACK (Ammonium-Chloride-Potassium) lysing buffer (StemCell Technologies) and counted in Bürker chamber with Turk solution.

Transplantation procedures. *Adult transplantation.* For transplantation in adult mice, 6 to 8-weeks-old C57BL/6-CD45.1 females were conditioned by lethal irradiation, administered in two doses of 4.25 Gy (tot 8.5 Gy), using the X-ray irradiator Radgil (Gilardoni S.p.A.). $CD45.2^+$ BMCs or UCBCs were transplanted by a single intravenous injection within 24 hours from conditioning.

Secondary mice. For secondary transplantation experiments, BMCs were harvested from primary mice at 4 months after transplantation and stained with anti-mouse CD45.2 PE antibody (clone 104, eBioscience). $CD45.2^+$ BMCs were sorted using a FACSAria cell sorter (BD Biosciences) and re-transplanted into congenic C57BL/6-CD45.1 recipients (3 × 106 cells/mouse) as described above.

Neonatal transplantation. UCBT in newborn mice was performed adjusting the scheme established by our group for the neonatal transplantation of murine BM[28]. 1 to 3-day-old pups from the MPS-I colony (CD45.2) were conditioned with a single intraperitoneal injection of 20 mg/kg busulfan (Busilvex, Pierre Fabre). 24 hours later, pups were transplanted by temporal vein injection of $CD45.1^+$ healthy donor-derived UCBCs (2 × 105 cells/mouse).

FACS analysis. For flow cytometry analysis of haematopoietic subpopulations, UCBCs and BMCs were collected and processed as specified above. For engraftment evaluation in transplanted mice, 50 μL of peripheral blood (PB) were collected in heparin by tail bleeding and lysed with ACK buffer. BM was collected by flushing long bones, while splenocytes and thymocytes were collected by smashing the respective organ on a 70 μm cell strainer (Greiner Bio-One).

Employed antibodies are listed in Supplementary Methods. Acquisition was performed on the FACSCanto™ II flow cytometer and the results were analyzed by FACS Diva software (BD Biosciences). The levels of donor cell engraftment have been evaluated as: [donor $CD45.1^+$/(donor $CD45.1^+$ recipient $CD45.2^+$) × 100], (or the opposite in the case of the transplant of $CD45.1^+$ mice with haematopoietic cells from $CD45.2^+$ donor).

Colony forming cell (CFC) assay. The CFC assay was performed in semi-solid medium supplemented with haematopoietic cytokines. Briefly, BMCs or UCBCs were resuspended in MethoCult GF M3434 (StemCell Technologies), plated in 35 mm low-adherence plastic dishes (Nunc) (20.000 cells/dish), and incubated at 37 °C and 5% CO2. Haematopoietic colonies were identified at day +14 by morphological observation on an inverted microscope. The nature of individual colonies was confirmed by picking them, cytospinning the cells on glass slides, and staining with May-Grünwald Giemsa.

IDUA activity assay. IDUA activity was measured fluorimetrically in organs at 20 weeks after transplantation, as previously described[28, 55]. See the Supplementary Methods for details.

Glycosaminoglycans quantification. GAGs were quantified in plasma and organs as described[28, 56]. See the Supplementary Methods for details.

Bone phenotyping. Radiographic images of each limb and cranium were obtained by Faxitron MX-20 Specimen Radiography System (Faxitron X-ray Corp.) at an energy of 30 kV for 90 seconds with Eastman X-OMAT TL film (Eastman Kodak Co.) and processed by an automated X-ray film developer (Model M35A, Eastman Kodak Co.). Bone thickness was measured between the outer edges of cortical bone at the mid-diaphysis using ImageJ software (free from the NIH website). Femurs from 20-weeks-old mice (n = 3 male mice/group) were scanned, using a SkyScan 1172 System (Bruker) with a source voltage and current of 65 kV and 153 μA, respectively. Following scanning, three-dimensional microstructural images were reconstructed using SkyScanNRecon software. SkyScan CT Analyzer software was used to calculate cortical micro-architectural parameters: cortical thickness (Ct.Th/mm), Total Area (TA/mm2), Bone Area (BA/mm2), and Medullary Area (MA/mm2).

Histopathology. For the evaluation of bone morphology, hind limbs were fixed in 4% formaldehyde in phosphate buffer, decalcified in 10% EDTA (Sigma-Aldrich), routinely processed for paraffin embedding and used for qualitative and quantitative histological analysis. Four μm sections were deparaffinized, rehydrated, and stained with haematoxylin and eosin by standard procedures. For quantitative analysis, a semiautomatic image analyser (IAS 2000, Delta System, Rome, Italy) was used to calculate the cortical thickness at the mid-diaphysis of the right femur and the area of the osteocytic lacuna within the same region of male WT, MPS-I, and MPS-I

nUCBThi mice (n = 3 for each group, at least 100 osteocytic lacunae/mouse).

In vitro **osteoclasts differentiation.** For osteoclastogenesis, mononuclear cells were isolated from the BM of 20-weeks-old mice as described above. Cells were plated at a density of 4 × 105 cells per well in 96 multiwell plates in the presence of 1 μM dexamethasone (Sigma-Aldrich), 5 ng/ml TGF-β1 (RandD Systems), 25 ng/ml M-CSF (Peprotech), and 100 ng/ml RANKL (Peprotech), and cultured for 10 days. Medium and factors were replaced every 3 days. Osteoclasts were detected 14 days after plating by cytochemical staining for TRAP (tartrate resistant acid phosphatase), using Leukocyte TRAP Kit 387-A (Sigma-Aldrich) according to the manufacturer's instructions. To determine the resorptive activity, cells were plated onto dentin discs (IDS) that were stained 21 days later by toluidine blue to quantify the resorbed area.

Statistical analysis. All statistical analyses were performed using R freeware software. Continuous variables were contrasted between groups by the nonparametric Wilcoxon test for equality of the medians. All tests were two-sided with a 5% significance level, except those on the micro-CT data, area of osteocytic lacunae, osteoclast number, and percentage of resorbed area where a 1-sided alternative was considered. Data on the distribution of haematopoietic colonies subtypes were analyzed using Chi-square test. An ordinary regression model with binary regressors was applied to assess the impact of both

disease and treatment. This enabled to separate the adverse effect of busulfan treatment from the therapeutic effect of UCBT on MPS-I.

SUPPLEMENTARY MATERIALS

Supplementary Methods

Antibodies

The following antibodies (eBioscience) were employed for flow cytometry analyses: anti-mouse CD45.1 PE (clone A20), anti-mouse CD45.1 APC (clone A20), anti-mouse CD45.2 PE (clone 104), anti-mouse CD45.2 APC (clone 104), anti-mouse CD45.2 PerCP-Cy5.5 (clone 104), anti-mouse CD3e PE (clone 145-2C11), anti-mouse CD45R (B220) PE (clone RA3-6B2), anti-mouse CD11b (Mac-1) PE (cloneM1/70), anti-mouse Ly-6G (Gr-1) FITC (clone RB6-8C5), anti-mouse TER-119 PE (clone TER-119), anti-mouse Ly-6A/E (Sca-1) APC (clone D7), anti-mouse CD117 (c-Kit) PE (clone 2B8), and anti-mouse Hematopoietic Lineage eFluor 450 cocktail.

IDUA activity assay

Organs (spleen, liver, heart, lungs, and kidneys) were harvested at sacrifice (20 weeks), frozen on dry ice and stored at -80°C. Portions of each organ were thawed and homogenized in 500 µL of 0.9% NaCl containing 0.2% Triton X-100 (Sigma-Aldrich) and a protease inhibitor cocktail (Sigma-Aldrich). The amount of protein in clarified supernatants of tissue homogenates was determined by Pierce BCA assay (Thermo Scientific). IDUA activity was then measured using the fluorogenic substrate 4-methylumbelliferyl-alpha-L-iduronide (Glycosynth). 5 µg of protein were added to a solution of 0.1 M sodium formate buffer, pH 3.2, containing 8 mM D-Saccharic acid

1,4-lactone and 0.4 mM 4-methylumbelliferyl-alpha-L-iduronide. Samples were incubated at 37°C for 1 hour, then the reaction was stopped by the addiction of 1 mL of 0.5 M carbonate buffer, pH 10.7. The fluorescence of the reaction product in the mix was read at 365 nm excitation and 488 nm emission wavelengths using a Tecan GENios microplate reader fluorometer (Tecan).

Glycosaminoglycans quantification in tissues

Portions of each organ collected at sacrifice were incubated overnight at 65°C with papain (Sigma-Aldrich), and then clarified for 10 min at 9391 g. GAG levels were measured using the Blyscan Sulfated Glycosaminoglycan colorimetric assay (Biocolor) according to the manufacturer's instructions. Chondroitin 4-sulfate was used as standard. Samples were read at 620 nm emission wavelength using a Tecan GENios microplate reader fluorometer (Tecan), and GAG levels were expressed as μg GAGs/mg protein in each sample.

Glycosaminoglycans quantification in plasma

At sacrifice, peripheral blood was collected in EDTA, and plasma was obtained by centrifugation at 587 g for 10 min and stored at -80°C. Ten μl of each plasma sample and 90 μl of 50 mM Tris–hydrochloric acid buffer (pH 7.0) were placed in wells of AcroPrep™ Advance 96-Well Filter Plates (OMEGA 10K, PALL Co). The filter plates were placed on the receiver and centrifuged at 2000 g for 15 min to remove free disaccharides. The membrane plates were transferred to a fresh receiver plate. Ten μl of IS solution (5 μg/ml), 20 μL of 50 mM Tris-HCl buffer, and 10 μL of chondroitinase B, heparitinase, and

keratanase II (each 2 mU/10 μL of 50 mM Tris-HCl buffer) were added onto each filter. The plate was incubated at 37°C for 5 hr and centrifuged at 2000 g for 15 min. The receiver plate containing disaccharides was stored at -20°C until injection to liquid chromatography tandem mass spectrometry (LC-MS/MS).

The chromatographic system consisted of 1260 Infinity (Agilent Technologies) and Hypercarb column (2.0 mm i.d. 50 mm, 5 μm, Thermo Electron). The mobile phase was a gradient elution from 0.025% ammonia to 90% acetonitrile in 0.025% ammonia. The 6460 Triple Quad mass spectrometer (Agilent Technologies) was operated in the negative ion detection mode with thermal gradient focusing electrospray ionization (Agilent Technologies). Specific precursor ion and product ion were used to detect and quantify each disaccharide. A m/z 354.29 precursor ion and m/z 193.1 product ion was used to detect the IS (chondrosine). Peak areas for all components were integrated automatically using QQQ Quantitative Analysis software (Agilent Technologies). The concentration of each disaccharide was calculated using QQQ Quantitative Analysis software.

Supplementary Figures and Tables

Table S1. Frequency of the different hematopoietic subpopulations in UCB and BM.

	UCB	BM	P value
T cells ($CD3^+$ in $CD45^+$)	2.5% (range from 1.4% tc 2.8%)	3.6% (range from 2.9% to 6.0%)	0.0147
B cells ($B220^+$ in $CD45^+$)	4.7% (range from 3.6% tc 8.7%)	10.6% (range from 7.9% to 13.2%)	0.0571
Myeloid cells ($Mac\text{-}1^+$ in $CD45^+$)	75.4% (range from 73.1% to 77.7%)	79.5% (range from 77.8% to 81.0%)	0.0286
Myeloid cells ($Gr\text{-}1^+$ in $CD45^+$)	54.3% (range from 48.6% to 56.8%)	76.0% (range from 71.6% to 78.5%)	0.0143
Erythrocytes ($Ter119^+$)	67.4% (range from 61.8% to 78.9%)	2.9% (range from 0.7% to 4.1%)	0.0500

The median percentages of the different hematopoietic subpopulations in UCB and BM are reported (n≥3 for UCB, n≥3 for BM). P values calculated by 1-sided Wilcoxon test.

Table S2. Effect of conditioning on bone measurements.

	Variables		
	β1 coeff (p value)	β2 coeff (p value)	γ coeff (p value)
Skull width	4.39 (0.0003)	-2.66 (0.0151)	-3.76 (0.0012)
Zygomous width	12.96 (<0.0001)	-1.23 (0.235)	-8.06 (<0.0001)
Femur width	6.25 (<0.0001)	-1.27 (0.2194)	-2.83 (0.0105)
Humerus width	6.96 (<0.0001)	-2.81 (0.0109)	-2.76 (0.0121)

Anova regression model on categorical variables. β1 is the effect on the parameter considered due to disease; β2 is the nUCBT effect on WT; γ is the differential effect of nUCBT on MPS I.

Figure S1. Multi-lineage UCB-derived reconstitution within BM, spleen, and thymus of a recipient mouse at 6 months after nUCBT

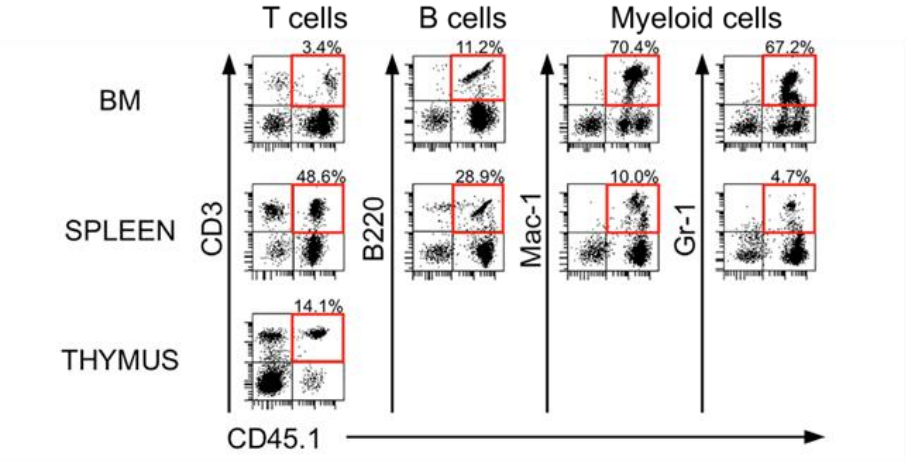

Representative lineage distribution of UCB-derived cells in the BM, spleen, and thymus of recipient mice at 6 months after nUCBT. Dot plots to determine donor-derived T cells (CD45.1$^+$CD3$^+$), B cells (CD45.1$^+$B220$^+$), and myeloid cells (CD45.1$^+$Mac-1$^+$ and CD45.1$^+$Gr-1$^+$) are shown. Percentages in total leukocytes are indicated.

Figure S2. Morphology of fetal red blood cells

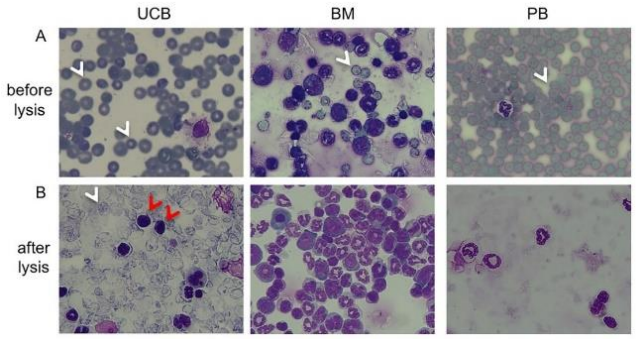

Smears of day 18-fetus UCB, adult BM, and PB. Red blood cells were indicated by white arrows. Note the heterogeneity in size and color of fetal red blood cells (Magnification 50x, May Grunwald-giemsa staining). B) Cytospin preparations of the same samples after lysis. Red blood cells resistant to hypotonic lysis (white arrow) and nucleated erithroblasts (red arrows) can be found in the umbelical cord blood sample (Magnification 50x, May Grunwald-giemsa staining).

Figure S3. Bone mineral density of the femurs of WT, MPS-I, and MPS-I nUCBT-hi mice.

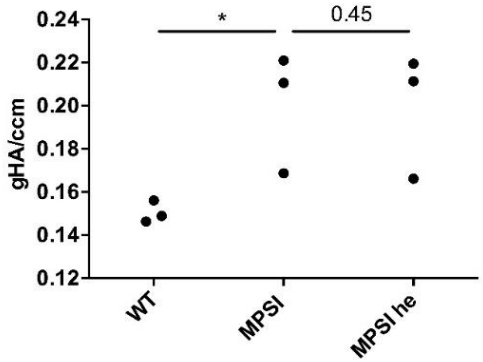

The graph represents the measurement of bone mineral density evaluated in the femurs of 20 weeks old WT, MPS-I, and MPS-I nUCBT-hi mice (n=3 for each group).

ACKNOWLEDGMENTS

This work was supported by Italian Telethon Foundation [TCP 07004 to M.S.]. L.S. is a recipient of a Ph.D. fellowship of the University of Milano-Bicocca supported by SANOFI GENZYME Italy. S.T. was supported by an Institutional Development Award (IDeA) from the National Institute of General Medical Sciences of NIH under grant number P30GM114736. F.K. was supported by Conselho Nacional de Desenvolvimento Científico e Tecnólogico (CNPq) and INAGEMP from Brazil.

We thank Dr. Massimiliano Cadamuro for his advice with microscopy, Dr. Elena Tassistro for her help with statistical analysis, Dr. Cristina Bugarin for having performed flow cytometry sorting, and Dr. Anna Villa for her support with osteoclast differentiation.

AUTHOR CONTRIBUTIONS

I.A., A.P. and A.C. performed research, analyzed the data and wrote the manuscript; F.D.P., L.S., L.C., K.S. and F.K. performed research and analyzed the data; L.A. performed statistical analysis; B.G., M.E.B., M.G.V., M.R. and S.T. interpreted the data and edited the manuscript; A.A. and A.B. edited the manuscript; M.S. designed research, interpreted the data, and wrote the manuscript.

REFERENCES

1. Prasad VK, Kurtzberg J. Cord blood and bone marrow transplantation in inherited metabolic diseases: scientific basis, current status and future directions. *Br J Haematol.* 2010;148(3):356-372.
2. Ballen KK, Gluckman E, Broxmeyer HE. Umbilical cord blood transplantation: the first 25 years and beyond. *Blood.* 2013;122(4):491-498.
3. Aldenhoven M, Kurtzberg J. Cord blood is the optimal graft source for the treatment of pediatric patients with lysosomal storage diseases: clinical outcomes and future directions. *Cytotherapy.* 2015;17(6):765-774.
4. Zhong XY, Zhang B, Asadollahi R, Low SH, Holzgreve W. Umbilical cord blood stem cells: what to expect. *Ann N Y Acad Sci.* 2010;1205:17-22.
5. Prasad VK, Kurtzberg J. Transplant outcomes in mucopolysaccharidoses. *Semin Hematol.* 2010;47(1):59-69.
6. Aldenhoven M, Jones SA, Bonney D, et al. Hematopoietic cell transplantation for mucopolysaccharidosis patients is safe and effective: results after implementation of international guidelines. *Biol Blood Marrow Transplant.* 2015;21(6):1106-1109.
7. Aldenhoven M, Wynn RF, Orchard PJ, et al. Long-term outcome of Hurler syndrome patients after hematopoietic cell transplantation: an international multicenter study. *Blood.* 2015;125(13):2164-2172.
8. Boelens JJ, Aldenhoven M, Purtill D, et al. Outcomes of transplantation using various hematopoietic cell sources in children with Hurler syndrome after myeloablative conditioning. *Blood.* 2013;121(19):3981-3987.
9. Broxmeyer HE, Farag S. Background and future considerations for human cord blood hematopoietic cell transplantation, including economic concerns. *Stem Cells Dev.* 2013;22 Suppl 1:103-110.
10. Clarke LA, Russell CS, Pownall S, et al. Murine mucopolysaccharidosis type I: targeted disruption of the murine alpha-L-iduronidase gene. *Hum Mol Genet.* 1997;6(4):503-511.
11. Ohmi K, Greenberg DS, Rajavel KS, Ryazantsev S, Li HH, Neufeld EF. Activated microglia in cortex of mouse models of mucopolysaccharidoses I and IIIB. *Proc Natl Acad Sci U S A.* 2003;100(4):1902-1907.
12. Rowan DJ, Tomatsu S, Grubb JH, Montaño AM, Sly WS. Assessment of bone dysplasia by micro-CT and glycosaminoglycan levels in mouse models for mucopolysaccharidosis type I, IIIA, IVA, and VII. *J Inherit Metab Dis.* 2013;36(2):235-246.
13. Wilkinson FL, Holley RJ, Langford-Smith KJ, et al. Neuropathology in mouse models of mucopolysaccharidosis type I, IIIA and IIIB. *PLoS One.* 2012;7(4):e35787.
14. Garcia-Rivera MF, Colvin-Wanshura LE, Nelson MS, et al. Characterization of an immunodeficient mouse model of

mucopolysaccharidosis type I suitable for preclinical testing of human stem cell and gene therapy. *Brain Res Bull.* 2007;74(6):429-438.

15. Mendez DC, Stover AE, Rangel AD, et al. A novel, long-lived, and highly engraftable immunodeficient mouse model of mucopolysaccharidosis type I. *Mol Ther Methods Clin Dev.* 2015;2:14068.
16. Clarke LA. The mucopolysaccharidoses: a success of molecular medicine. *Expert Rev Mol Med.* 2008;10:e1.
17. Beck M, Arn P, Giugliani R, et al. The natural history of MPS I: global perspectives from the MPS I Registry. *Genet Med.* 2014;16(10):759-765.
18. Staba SL, Escolar ML, Poe M, et al. Cord-blood transplants from unrelated donors in patients with Hurler's syndrome. *N Engl J Med.* 2004;350(19):1960-1969.
19. Schmidt M, Breyer S, Löbel U, et al. Musculoskeletal manifestations in mucopolysaccharidosis type I (Hurler syndrome) following hematopoietic stem cell transplantation. *Orphanet J Rare Dis.* 2016;11(1):93.
20. Tomatsu S, Azario I, Sawamoto K, Pievani AS, Biondi A, Serafini M. Neonatal cellular and gene therapies for mucopolysaccharidoses: the earlier the better? *J Inherit Metab Dis.* 2016;39(2):189-202.
21. Davenport C, Kumar V, Bennett M. Use of newborn liver cells as a murine model for cord blood cell transplantation. *J Immunol.* 1993;151(3):1597-1605.
22. Harrison DE, Astle CM. Short- and long-term multilineage repopulating hematopoietic stem cells in late fetal and newborn mice: models for human umbilical cord blood. *Blood.* 1997;90(1):174-181.
23. Scaradavou A, Isola L, Rubinstein P, et al. A murine model for human cord blood transplantation: near-term fetal and neonatal peripheral blood cells can achieve long-term bone marrow engraftment in sublethally irradiated adult recipients. *Blood.* 1997;89(3):1089-1099.
24. Migishima F, Oikawa A, Kondo S, et al. Full reconstitution of hematopoietic system by murine umbilical cord blood. *Transplantation.* 2003;75(11):1820-1826.
25. Oikawa A, Ito K, Seguchi H, et al. Development of immunocompetent lymphocytes in vivo from murine umbilical cord blood cells. *Transplantation.* 2007;84(1):23-30.
26. Li ZY, Wang CQ, Lu G, Pan XY, Xu KL. Effects of bone marrow mesenchymal stem cells on hematopoietic recovery and acute graft-versus-host disease in murine allogeneic umbilical cord blood transplantation model. *Cell Biochem Biophys.* 2014;70(1):115-122.
27. de La Selle V, Gluckman E, Bruley-Rosset M. Newborn blood can engraft adult mice without inducing graft-versus-host disease across non H-2 antigens. *Blood.* 1996;87(9):3977-3983.

28. Pievani A, Azario I, Antolini L, et al. Neonatal bone marrow transplantation prevents bone pathology in a mouse model of mucopolysaccharidosis type I. *Blood.* 2015;125(10):1662-1671.
29. Kuehn SC, Koehne T, Cornils K, et al. Impaired bone remodeling and its correction by combination therapy in a mouse model of mucopolysaccharidosis-I. *Hum Mol Genet.* 2015;24(24):7075-7086.
30. Harris DT, Schumacher MJ, Locascio J, et al. Phenotypic and functional immaturity of human umbilical cord blood T lymphocytes. *Proc Natl Acad Sci U S A.* 1992;89(21):10006-10010.
31. Risdon G, Gaddy J, Broxmeyer HE. Allogeneic responses of human umbilical cord blood. *Blood Cells.* 1994;20(2-3):566-570; discussion 571-562.
32. Levy O. Innate immunity of the newborn: basic mechanisms and clinical correlates. *Nat Rev Immunol.* 2007;7(5):379-390.
33. Morrison SJ, Hemmati HD, Wandycz AM, Weissman IL. The purification and characterization of fetal liver hematopoietic stem cells. *Proc Natl Acad Sci U S A.* 1995;92(22):10302-10306.
34. Coşkun S, Chao H, Vasavada H, et al. Development of the fetal bone marrow niche and regulation of HSC quiescence and homing ability by emerging osteolineage cells. *Cell Rep.* 2014;9(2):581-590.
35. Palis J, Chan RJ, Koniski A, Patel R, Starr M, Yoder MC. Spatial and temporal emergence of high proliferative potential hematopoietic precursors during murine embryogenesis. *Proc Natl Acad Sci U S A.* 2001;98(8):4528-4533.
36. Kim DK, Fujiki Y, Fukushima T, Ema H, Shibuya A, Nakauchi H. Comparison of hematopoietic activities of human bone marrow and umbilical cord blood CD34 positive and negative cells. *Stem Cells.* 1999;17(5):286-294.
37. Harrison DE, Zhong RK. The same exhaustible multilineage precursor produces both myeloid and lymphoid cells as early as 3-4 weeks after marrow transplantation. *Proc Natl Acad Sci U S A.* 1992;89(21):10134-10138.
38. Jayaraman S, Patel T, Patel V, et al. Transfusion of nonobese diabetic mice with allogeneic newborn blood ameliorates autoimmune diabetes and modifies the expression of selected immune response genes. *J Immunol.* 2010;184(6):3008-3015.
39. Chuan W, Wu-qing W, Zhu-wen Y, Zuo L. Effect of nonmyeloablative unrelated fetal and neonatal murine peripheral blood mononuclear cell infusion on MRL/lpr mice. *Lupus.* 2014;23(10):994-1005.
40. Tomatsu S, Okamura K, Taketani T, et al. Development and testing of new screening method for keratan sulfate in mucopolysaccharidosis IVA. *Pediatr Res.* 2004;55(4):592-597.

41. Tomatsu S, Montaño AM, Oguma T, et al. Dermatan sulfate and heparan sulfate as a biomarker for mucopolysaccharidosis I. *J Inherit Metab Dis.* 2010;33(2):141-150.
42. Sacchetti B, Funari A, Remoli C, et al. No Identical "Mesenchymal Stem Cells" at Different Times and Sites: Human Committed Progenitors of Distinct Origin and Differentiation Potential Are Incorporated as Adventitial Cells in Microvessels. *Stem Cell Reports.* 2016;6(6):897-913.
43. Pievani A, Sacchetti B, Corsi A, et al. Human umbilical cord blood-borne fibroblasts contain marrow niche precursors that form a bone/marrow organoid in vivo. *Development.* 2017;144(6):1035-1044.
44. Uchida K, Urabe K, Naruse K, Itoman M. Umbilical cord blood-derived mesenchymal cell fate after mouse umbilical cord blood transplantation. *Transplantation.* 2010;90(9):1037-1039.
45. Uchida K, Ueno M, Naruse K, et al. Bone marrow-engrafted cells after mice umbilical cord blood transplantation differentiate into osteoblastic cells in response to fracture and placement of titanium screws. *Exp Anim.* 2012;61(4):427-433.
46. Schulte C, Beelen DW, Schaefer UW, Mann K. Bone loss in long-term survivors after transplantation of hematopoietic stem cells: a prospective study. *Osteoporos Int.* 2000;11(4):344-353.
47. Gatto F, Redaelli D, Salvadè A, et al. Hurler disease bone marrow stromal cells exhibit altered ability to support osteoclast formation. *Stem Cells Dev.* 2012;21(9):1466-1477.
48. Aldenhoven M, Boelens JJ, de Koning TJ. The clinical outcome of Hurler syndrome after stem cell transplantation. *Biol Blood Marrow Transplant.* 2008;14(5):485-498.
49. Willing AE, Garbuzova-Davis SN, Zayko O, et al. Repeated administrations of human umbilical cord blood cells improve disease outcomes in a mouse model of Sanfilippo syndrome type III B. *Cell Transplant.* 2014;23(12):1613-1630.
50. Lu L, Xiao M, Clapp DW, Li ZH, Broxmeyer HE. High efficiency retroviral mediated gene transduction into single isolated immature and replatable CD34(3+) hematopoietic stem/progenitor cells from human umbilical cord blood. *J Exp Med.* 1993;178(6):2089-2096.
51. Simonaro CM, Haskins ME, Abkowitz JL, et al. Autologous transplantation of retrovirally transduced bone marrow or neonatal blood cells into cats can lead to long-term engraftment in the absence of myeloablation. *Gene Ther.* 1999;6(1):107-113.
52. Bernardo ME, Aiuti A. The role of conditioning in hematopoietic stem cell gene therapy. *Hum Gene Ther.* 2016.

CHAPTER 4

Summary, conclusions, future perspectives

Mucopolysaccharidosis type I (MPS-I) is a recessive lysosomal storage disorder due to the deficient activity of alpha-L-iduronidase (IDUA) enzyme. It results in the progressive accumulation of glycosaminoglycans (GAGs) heparan and dermatan sulphate in multiple tissues. From a clinical point of view, MPS-I patients present multiorgan morbidity, and in particular hepatosplenomegaly, airway disease, cardiac failure, cognitive impairment and skeletal abnormalities known as *dysostosis multiplex*[1]. Hematopoietic stem cell transplantation (HSCT) and enzyme replacement therapy (ERT) are the currently available treatments for MPS-I patients. Nevertheless, both treatments do not provide a complete resolution. In fact the clinical outcome could be variable, with persisting residual disease burden. In particular, muscoloskeletal deformities and neurocognitive defects still impact patient's quality of life even after treatment[2]. It has been widely demonstrated that the time of intervention is crucial to obtain a better outcome[3]. Indeed, evidences coming from both experimental[4] and clinical[5] data showed a higher successful rate in correcting disease abnormalities, if treatment is performed early in

life. Moreover, in our previous study, we could confirm the efficacy of neonatal bone marrow transplantation in correcting and preventing skeletal disease in a mouse model of MPS-I[6].

In the first part of this PhD project, we investigated the efficacy of ERT, nBMT and the combination of both, in a murine model of MPS-I, given in an early period of life. We decided to focus our studies in particular on brain and bone outcome, being two of the main aspects hardly corrected. First, we demonstrated a higher increase of IDUA activity in liver and spleen in mice treated with the combination of nBMT and ERT. Then, we were able to show a significant reduction of GAGs storage in visceral organs of mice treated with all the three treatments under evaluation. However, only the combination treatment determined a better decrease of GAGs accumulation in kidney and heart, known as difficult-to-treat organs, having an additive effect with respect to transplantation alone. Evaluating brain disease, we observed a slight improvement of the parameters analysed, with no difference between the three therapeutic approaches. We observed a moderate reduction of neuroinflammation, without an evident decrease of storage in Purkinje cells, after treatments. Further histological and behavioural studies will better determine whether these standard approaches administered during the best therapeutic window may have a significant benefit for brain alterations. With respect to the skeletal phenotype, we evaluated the effect of the three treatments in reducing long bone thickness. Even if ERT was started at birth, it did not provide any amelioration, whereas nBMT and the combination treatment determined a significant reduction of bone width, without any differences between each other. We confirmed that

transplantation performed during neonatal period is effective in delivering to the skeleton adequate levels of IDUA enzyme able to correct the metabolic defect. To deeply investigate the skeletal outcome, we are currently performing other studies. In particular micro-CT and histopathologic analyses will better clarify the bone remodelling status after treatment. Indeed, a recent publication has evidenced an alteration of osteoclastogenesis in MPS-I mice and patients after transplantation suggesting that the combination of ERT with transplantation could ameliorate this complication[7].

The second part of this PhD project was focused on umbilical cord blood (UCB), as a promising stem cells source for transplantation. Indeed, UCB presented some advantages over BM: it is easier to procure, it permits a greater degree of human leukocyte antigen (HLA)-mismatch, lower incidence of graft versus host disease (GVHD), and achievement of full donor chimerism[8-9]. In our recently published paper, we have characterized murine UCB cells and demonstrated their long-term and multilineage ability to engraft. We then performed neonatal UCB transplantation in a murine model of MPS-I, in order to demonstrate its therapeutic efficacy. We observed a significant amelioration of biochemical parameters, such as restoration of IDUA activity and reduction of GAGs accumulation in organs and plasma, and of the skeletal phenotype. Therefore, performing UCB transplantation at birth could confer a greater efficacy, offering a better clinical outcome in MPS-I patients.

With respect to the future perspectives of this part of the project, we plan to perform a neonatal HSCT-gene therapy (GT) approach at San

Raffaele-Telethon Institute for Gene Therapy (SR-Tiget) in Milan, in collaboration with Professor A. Aiuti. In HSCT-GT, modified cells express and secrete supranormal levels of the functional IDUA enzyme, allowing a better correction in particular in organs that are refractory to correct by other therapeutic approaches. Indeed, transplantation and/or ERT may deliver an amount of the missing enzyme that could not be sufficient to obtain a correction of the metabolic defect, in particular at brain level. Indeed, HSCT-GT could provide a greater efficacy in ameliorating some disease aspects. In this on-going study, we will perform neonatal transplantation of autologous UCB cells, previously modified by lentiviral-IDUA vectors, in the MPS-I mouse model. We will test the ability of HSCT-GT approach at birth to correct the currently disease manifestations, unsolved by the present-day therapies.

REFERENCES

1. Campos, D., Monaga, M. Mucopolysaccharidosis type I: current knowledge on its pathophysiological mechanisms. *Metab Brain Dis.* 27:121–129 (2012).
2. Tomatsu, S. *et al.* Neonatal cellular and gene therapies for mucopolysaccharidoses: the earlier the better? *J Inherit Metab Dis*. 39:189–202 (2016).
3. Boelens, J. J. *et al.* Outcomes of transplantation using various hematopoietic cell sources in children with Hurler syndrome after myeloablative conditioning Outcomes of transplantation using various hematopoietic cell sources in children with Hurler syndrome after myeloablative conditioning. *Blood*. 121:3981–3987 (2013).
4. Tomatsu, S. *et al.* Enzyme replacement therapy in newborn mucopolysaccharidosis IVA mice: early treatment rescus bone lesions? *Mol Genet Metab*. 114:195–202 (2016).
5. Aldenhoven, M. *et al.* Hematopoietic Cell Transplantation for Mucopolysaccharidosis Patients Is Safe and Effective : Results after Implementation of International Guidelines. *Biol. Blood Marrow Transplant.* 21:1106–1109 (2015).
6. Pievani, A. *et al.* Neonatal bone marrow transplantation prevents bone pathology in a mouse model of mucopolysaccharidosis type I. *Blood.* 125:1662–1672 (2015).
7. Kuehn, S. C. *et al.* Impaired bone remodeling and its correction by combination therapy in a mouse model of mucopolysaccharidosis-I. *Human Molecular Genetics*. 24:7075–7086 (2015).
8. Prasad, V. K. & Kurtzberg, J. Cord blood and bone marrow transplantation in inherited metabolic diseases: scientific basis, current status and future directions. *British Journal of Haematology*. 148:356–372 (2009).
9. Aldenhoven, M. & Kurtzberg, J. Cord blood is the optimal graft source for the treatment of pediatric patients with lysosomal storage diseases: clinical outcomes and future directions. *Cytotherapy*. 17:765-774 (2015).

PUBLICATIONS

- Azario I, Pievani A, Del Priore F, Antolini L, **Santi L**, Corsi A, Cardinale L, Sawamoto K, Kubaski F, Gentner B, Bernardo ME, Valsecchi MG, Riminucci M, Tomatsu S, Aiuti A, Biondi A, Serafini M. *Neonatal umbilical cord blood transplantation halts skeletal disease progression in the murine model of MPS-I*. Scientific Reports, 2017.

Meetings and conferences

- Montagna A, **Santi L**, Gatto F, Cardinale L, Mazzara PG, Cancellieri C, Verfaillie CM, Broccoli V, Biondi A, Serafini M. "*Osteogenic differentiation capability of induced pluripotent stem cells isolated from mucopolysaccharidosis type I patients (Hurler syndrome) through the generation of mesenchymal stromal cell"* Poster presentation. Tri-retreat meeting Telethon, May 26th-28th 2016, Rome, Italy.
- Azario I, Pievani A, Del Priore F, Antolini L**, Santi L**, Corsi A, Cardinale L, Sawamoto K, Kubaski F, Gentner B, Bernardo ME, Valsecchi MG, Riminucci M, Tomatsu S, Aiuti A, Biondi A, Serafini M. *Neonatal umbilical cord blood transplantation halts disease progression in the murine model of MPS-I*. Poster presentation. Convegno dell'Associazione Italiana per le Scienze degli Animali da Laboratorio (AISAL), October 26th-27th 2017, Milano, Italy.